DISSERTATIONES NEUROSCIENTIAE UNIVERSITATIS TARTUENSIS
13

DISSERTATIONES NEUROSCIENTIAE UNIVERSITATIS TARTUENSIS
13

MARI-ANNE PHILIPS

Characterization of Myg1 gene and protein: expression patterns, subcellular localization, gene deficient mouse and functional polymorphisms in human

TARTU UNIVERSITY
PRESS

Department of Physiology, University of Tartu, Tartu, Estonia

Dissertation is accepted for the commencement of the degree of *Doctor Philosophiae* in neurosciences on April 8, 2010, by the Council of the Commencement of Doctoral Degree in Neuroscience

Supervisiors: Eero Vasar, MD, PhD, Professor, Department of Physiology, University of Tartu

Sulev Kõks, MD, PhD, Professor, Department of Physiology, University of Tartu

Reviewers: Allen Kaasik, PhD, Professor, Department of Pharmacology, University of Tartu

Pärt Peterson, PhD, Professor, Department of Molecular Pathology, University of Tartu

Opponent: Scott F. Gilbert, PhD, Professor, Swarthmore College, USA

Commencement: June 21, 2010

This research was supported by the European Regional Development Fund.

Publication of this dissertation is granted by the University of Tartu.

ISSN 1736–2792
ISBN 978–9949–19–362–2 (trükis)
ISBN 978–9949–19–363–9 (PDF)

Tartu Ülikooli Kirjastus
www.tyk.ee
Tellimuse nr. 236

CONTENTS

LIST OF ORIGINAL PUBLICATIONS

I. **Philips MA**, Vikeså J, Luuk H, Jønson L, Lilleväli K, Rehfeld JF, Vasar E, Kõks S, Nielsen FC (2009). Characterization of *MYG1* gene and protein: subcellular distribution and function. *Biology of the Cell*; **101**(6):361–73.

II. **Philips MA**, Abramov U, Lilleväli K, Luuk H, Kurrikoff K, Raud S, Plaas M, Innos J, Puussaar T, Kõks S, Vasar E (2010). *Myg1*-deficent mice display alterations in stress-induced responses and reduction of sex-dependent behavioral differences. *Behavioural Brain Research*; **207**(1):182–95.

III. Kingo K, **Philips MA**, Aunin E, Luuk H, Karelson M, Rätsep R, Silm H, Vasar E, Kõks S (2006). *MYG1*, novel melanocyte related gene, has elevated expression in vitiligo. *Journal of Dermatological Science*; **44**(2):119–22.

IV. **Philips MA,** Kingo K, Karelson M, Rätsep R, Aunin E, Reimann E, Reemann P, Porosaar O, Vikeså J, Nielsen FC, Vasar E, Silm H, Kõks S (2010). Promoter polymorphism -119C/G in *MYG1* (C12orf10) gene is related to vitiligo susceptibility and Arg4Gln affects mitochondrial entrance of Myg1. *BMC Medical Genetics*, **11**(1):56.

Contribution of the author:

I. The author designed and conducted most of the experiments, designed and performed cloning for all DNA constructs, performed most of the cell culture experiments, expression analysis, wrote the manuscript and handled correspondence.

II. The author designed and performed genotyping of electroporated embryonic stem cells and chimeras during generation of *Myg1*-deficent mice; designed multiplex-genotyping assay, participated in the design of phenotyping schema; handled breeding and performed genotyping of all mice after behavioural studies; designed and prepared *in situ* hybridization probe; performed *Myg1* expression analysis after restraint stress experiment, wrote the manuscript together with U. Abramov and handled correspondence.

III. The author was involved in interpreting the data, collected most of the background information for the manuscript and participated in writing and correspondence.

IV. The author designed and cloned all DNA constructs, designed and performed most of the cell culture experiments, part of the expression analysis, all sequencing, wrote the manuscript and handled correspondence.

ABBREVIATIONS

3'-UTR	the three prime untranslated region
5'-UTR	the five prime untranslated region
Arg	arginine
ATP	adenosine triphosphate
bp	base pair
C12orf10	chromosome 12 open reading frame 10
cDNA	complementary DNA
CI	confidence interval
CMV	cytomegalovirus
C-terminal	carboxyl-terminal
CT	cycle threshold (in qRT-PCR)
DNA	deoxyribonucleic acid
E	embryonic day
ESC	embryonic stem cells
FRAP	fluorescence recovery after photobleaching
Gln	glutamine
GO	Gene Ontology
HEK293	human embryonic kidney 293 cell line
HMVEC	human microvascular endothelial cell culture
HPA-axis	hypothalamic-pituitary-adrenal axis
Hprt1	*Hypoxanthine guanine phosphoribosyl transferase 1* gene
HRP	horseradish peroxidase
Hsp90	*Heat shock protein of 90 kDa*
IP	immunoprecipitation
kb	kilobase(s); one thousand nucleotide bases or base pairs
kDa	kilodalton (molecular size)
LD	linkage disequilibrium
LPS	lipopolysaccharide
lx	lux (unit of illuminance)
Mb	megabase(s); one million nucleotide bases or base pairs
MHC	major histocompatibility complex
mRNA	messenger ribonucleic acid
MTS	mitochondrial targeting signal
Myg1	*Melanocyte proliferating gene 1* gene in any species other than human
MYG1	*Melanocyte proliferating gene 1* gene in human
Myg1	protein encoded by *Melanocyte proliferating gene 1* gene
NK	natural killer
NLS	nuclear localization signal
N-terminal	amino-terminal
OR	odds ratio
P	post-natal day
p	the short arm of the chromosome

q	the long arm of the chromosome
qRT-PCR	quantitative real-time polymerase chain reaction
RER	respiratory exchange rate (formula CO_2/O_2)
RMA	robust multiarray average
RNA	ribonucleic acid
siRNA	short interfering RNA
SNP	single nucleotide polymorphism
Th	T helper
UPF	uncharacterized protein family
WD-repeat	tryptophan-aspartate repeat
YFP	yellow fluorescent protein
YPD	yeast extract-peptone-dextrose (rich media for growing yeast)
YPE	yeast extract-peptone-ethanol medium

INTRODUCTION

This study characterizes *Myg1* (*Melanocyte proliferating gene 1*) gene and provides data about this novel gene and protein. Approximately 9,334 (37%) of human genes have no publications, documenting their function. Furthermore, for reasons not clear, the entry of new gene names into the literature has slowed down in recent years (Wren, 2009). Basic studies elucidating the functions of the remaining one-third of the genes that have unknown function are important for better understanding of human/mammalian biology and completing of the catalog of human gene function.

Our research team first identified *Myg1* as a most extensively up-regulated gene in the amygdaloid area of rats after cat odour-induced anxiety (Kõks *et al*, 2004). Studies linked to the current dissertation were designed to shed light on the function of the *Myg1* gene that had previously been cited in only one scientific abstract (Smicun, 2000) describing *Myg1* as a highly expressed gene in freely proliferating melanocytes and downregulated in malignant melanoma cells.

Our initial hypothesis was that *Myg1* could be a melanocyte specific gene as suggested by Smicun (2000). Therefore one of the aims of the present study was to study *Myg1* in relation with vitiligo, an acquired pigmentary disorder characterized by areas of depigmented skin resulting from loss of epidermal melanocytes (Zhang *et al*, 2005). Vitiligo involves complex interaction of environmental and genetic factors that ultimately contribute to melanocyte destruction, resulting in characteristic depigmented lesions (Spritz, 2007). First we showed an elevated expression of *MYG1* mRNA in both uninvolved and involved skin of vitiligo patients. Our later studies, however, have indicated that *Myg1* is not a melanocyte or skin-specific gene, but has a rather ubiquitous and homogenous expression and serves a more general function in the organism level. Therefore we propose that elevated expression of *MYG1* in the skin of vitiligo patients is rather indicative of systemic deviations in immune response or cellular metabolism.

The purpose of our studies was to considerably extend the existing knowledge about the functional role of *Myg1* gene and protein. Although our theories about the real functions of Myg1 in the cell and organism are still merely hypothetical, the data presented here shed light on the role of Myg1 in the complicated cellular machinery as we now know its expression patterns in adult and developing tissues, subcellular location, the effect of knock-down in cell culture and the impact of gene knock-out in *in vivo* mouse model.

REVIEW OF LITERATURE

1. Phylogenesis of Myg1 gene

Myg1 (*Melanocyte proliferating gene 1*, also known as C12orf10 in human and Gamm1 in plants) is a recently identified gene. Myg1 is the only member of an uncharacterized protein family UPF0160 (PF03690) with no described paralogues in any organism. According to sequence homology, UPF0160 domain contains a number of metal binding residues and is predicted to possess metal-dependent protein hydrolase activity. Myg1 protein is highly conserved and present in all eukaryotes from yeast to human (Nepomuceno-Silva *et al*, 2004). Orthologues have even been found in plants (Heazlewood *et al*, 2004) and in protozoan parasites. For example, *Trypanosoma cruzi* orthologue shares 56% similarity with human Myg1 on a 359 amino acid stretch (Nepomuceno-Silva *et al*, 2004).

The high conservation rate of *Myg1* throughout evolution has been confirmed by a study that identified 398 genes that are conserved at least in all 17 species out of 18 that were studied and *Myg1* orthologue was missing only in *P. falciparum* (Lee *et al*, 2008). However; *P. falciparum* is a parasite whose lifestyle and biological processes deviate from those of other organisms: less than 20% of the genes from *P. falciparum* can be grouped with genes from other species; various ATP synthases, many mitochondria-related genes and members of proteasome are missing in *P. falciparum* (Lee *et al*, 2008). Therefore *Myg1* is present in all studied species with conventional biological processes and metabolism. Figure 1 represents multiple sequence alignment between six eukaryotic organisms: human (*Homo sapiens*), chimpanzee (*Pan troglodytes*), mouse (*Mus musculus*), frog (*Xenopus tropicalis*), thale cress (a model organism in plant genetics, *Arabidopsis thaliana*) and baker's yeast (*Saccharomyces cerevisiae*). The conservation in amino acid level is high between human and chimpanzee (99.2%) and mouse (85.6%); somewhat lower between human and frog (60.9%) and moderate between human and *Arabidopsis thaliana* (43%) and *Saccharomyces cerevisiae* (39%). Nevertheless, there are several areas in the Myg1 protein that are conserved from human to plant and yeast (columns with black shading on Figure 1), indicating crucial domains for Myg1 function. Red shading in Figure 1 points to the conserved DHH (Asp-His-His) motif around amino acids 106–108 suggesting putative phosphoesterase activity (Aravind & Koonin, 1998). Despite high conservation, *Myg1* gene still seems to be under selection: *Myg1* is found to be among 154 genes that underwent positive selection in human evolution compared to chimpanzee evolution (Bakewell *et al*, 2007). Therefore *Myg1* can be one of the genes that are responsible for the differences between humans and chimpanzees.

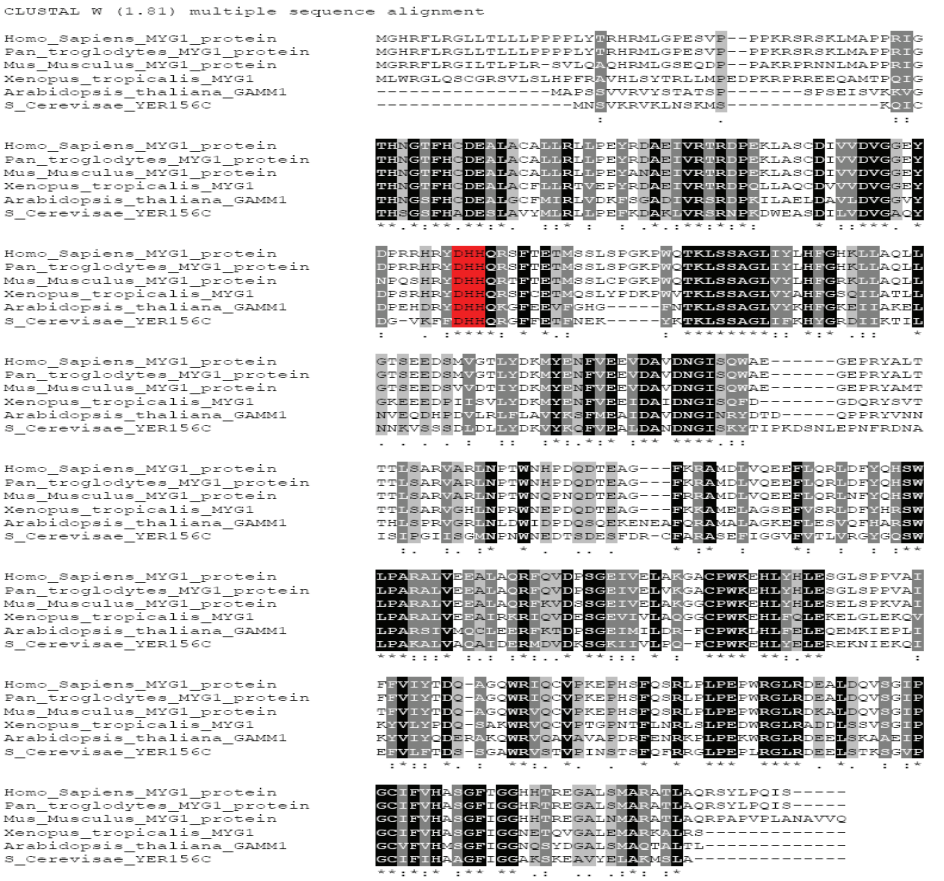

Figure 1. Multiple sequence alignment of Myg1 orthologues in different eukaryotic organisms. Sequences have been obtained from ncbi.org database and aligned by Crustal W program (1.81). A star (*) and black shading indicates an entirely conserved column; a colon (:) and dark grey shading indicates columns where all the residues have roughly the same size and the same hydropathy; and period (.) with light gray shading indicates columns where the size or the hydropathy has been preserved in the course of evolution. Red shading points to the conserved DHH motif suggesting putative phosphoesterase activity.

2. Conserved genomic neighbourhood of *Myg1* gene

In most vertebrates with sequenced genomes, *Myg1* gene is comprised of seven exons that span 7.5, 6.4 and 6.7 kb of genomic DNA in human, mouse and *Xenopus tropicalis*, respectively. The *Myg1* locus reveals a high degree of conservation with respect to the neighboring genes *Prefoldin5* (*PFDN5*, NM_002624 in human) and *AAAS* (NM_015665 in human), that lie upstream and downstream, respectively, of *Myg1* in all primates, most mammals and *Xenopus tropicalis* (Figure 2). The closest neighbours of *Myg1* are of interest, because it is likely that genes that lie in close

proximity may be co-regulated due to enhancer sharing or open chromatin conformation (Little, 2005). The closest upstream neighbour *PFDN5* is separated from *Myg1* only by 248 bp in human and by 222 bp in mouse genome. *PFDN5* is enoding subunit 5 for heterohexameric chaperone protein, Prefoldin (Vainberg *et al*, 1998); alternatively *PFDN5* is known as MM-1 or c-Myc-binding protein that is found to be a candidate for a tumor suppressor in leukemia/lymphoma and tongue cancer (Kimura *et al*, 2007). The intergenic area between *Myg1* and closest downstream neighbour *AAAS* is 281 bp in human and only 118 bp in mouse genome. *AAAS* gene encodes WD-repeat protein ALADIN that localizes to nuclear pore complex (Huebner *et al*, 2006). Mutations in *AAAS* are linked with triple A syndrome (OMIM #231550) that is a rare human autosomal recessive disorder characterized by the clinical triad of achalasia of the cardia (increased tone of the lower esophagus sphincter), alacrima (deficiency of tear production), and adrenocorticotropic hormone (ACTH)-resistant adrenal insufficiency. In addition to the three main symptoms, patients suffer from a variety of progressive neurological symptoms that indicate an involvement of the central, peripheral, and autonomic nervous systems (Huebner *et al*, 2006, Koehler *et al*, 2008). The conserved region around *Myg1* gene is wider: according to MSOAR database (http://msoar.cs.ucr.edu) human *MYG1* in chromosome 12 is located inside 19.54 Mb syntenic chromosome block that corresponds to 13.43 Mb conserved block in the mouse chromosome 15 F1–F3. This conserved chromosomal fragment includes full type II keratin cluster that is lying in 12q13.3 in human (Rogers *et al*, 2005), 346 kb upstream from *MYG1* and *HOX C* locus located 631 kb downstream of *MYG1*. The *HOX* genes constitute a network of homeobox transcription factors controlling embryonic development and play an important role in crucial adult eukaryotic cell functions (Cantile *et al*, 2003). Taken together, in human, mouse and several other vertebrates, *Myg1* gene is tightly surrounded by its closest neighbours and is located in a highly conserved chromosomal region between type II keratin cluster and *HOX C* locus.

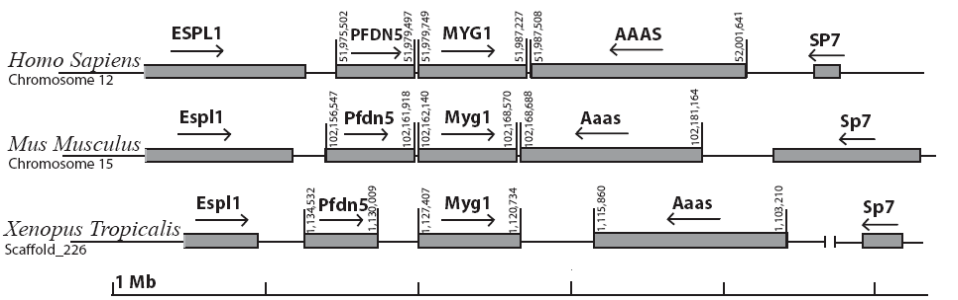

Figure 2. Schematic structure of *Myg1* genomic neighbourhood in human, mouse and *Xenopus tropicalis*. The *Myg1* locus reveals a high degree of conservation with respect to the neighbouring genes *Espl1* (*Extra spindle poles-like 1*), *Prefoldin5* (*PFDN5*), *AAAS* (achalasia, adrenocortical insufficiency, alacrimia; triple-A), Sp7 (zinc finger transcription factor of the SP gene family) that lie upstream and downstream of *Myg1* in all primates, most mammals and *Xenopus tropicalis*.

3. Dynamic expression of *Myg1* transcript during development

Developmentally dynamic expression of *Myg1* has been detected in various species from human (Chan *et al*, 2006), rat (Weng *et al*, 2006) mouse (Dorrell *et al*, 2004) to zebrafish (Mathavan *et al*, 2005). According to global expression analyses, *Myg1* tends to be up-regulated in undifferentiated and pluripotent cells. *Myg1* is specifically upregulated in mouse two- to four-cell embryos (Sharov *et al*, 2003). In E (embryonic day) 3.5 blastocyst, *Myg1* expression is higher in pluripotent inner cell mass than in differentiated trophectoderm (Tanaka *et al*, 2002). Similarly, *MYG1* expression is significantly higher in embryonic and hematopoietic stem cells compared with differentiated hematopoietic cells (Golan-Mashiach *et al*, 2005). Additionally, *Myg1* has fluctuating expression level in both prenatal and postnatal development in various tissues and organ types: during spermatogenesis (Chan *et al*, 2006), myogenesis (Tomczak *et al*, 2004), adipogenesis (Hackl *et al*, 2005), and during development of fetal lung (Weng *et al*, 2006) and postnatal retina (Dorrell *et al*, 2004). There are some functional hints of how Myg1 is involved in pluripotency: based on genomic sequence analysis or mouse embryonic stem cell (ESC) chromatin immunoprecipitation (ChIP) data, Myg1 has a putative Oct4 binding site (Loh *et al*, 2006) suggesting that *Myg1* is a candidate target gene of Oct4 (Octamer-4, also Pou5f1, NM_013633.2). Oct4 is an ESC pluripotency regulator and is often used as a marker for undifferentiated cells. Furthermore, *Myg1* is down-regulated in *Oct4* knockdown embryos (Foygel *et al*, 2008). Moreover, *Myg1* can also be implicated in adult stem cells: expression of *Myg1* is down-regulated 60 minutes after conditional knockout of *TLX* (also Nr2e1, NM_152229) gene that regulates adult neural stem proliferation by controlling cell proliferation and growth (Zhang *et al*, 2008). Myg1 involvement in the cellular pathways related with Oct4 and TLX can explain dynamic expression of *Myg1* during prenatal and postnatal development; however, the precise function of Myg1 in developing cells needs further research.

4. Expression changes of *Myg1* transcript induced by stress and immune response

Myg1 expression in adult tissues is rather homogenous and ubiquitous (Su *et al*, 2004) and seems to be regulated mainly as a response to stress. A screen for genes involved in the anxiety response identified an upregulation of *Myg1* in the amygdaloid area of rats after exposure to cat odour (Kõks *et al*, 2004). Other studies have reported alterations in *Myg1* mRNA expression in response to stress/illness conditions in human (Hawse *et al*, 2003; Liang *et al*, 2008; Sääf *et al*, 2008), rodent tissues (Rickhag *et al*, 2006) and in cell culture experiments (Lü *et al*, 2009). Certain cellular stress conditions such as cytotoxicity,

starvation and degeneration tend to induce down-regulation of *Myg1*. In yeast, the expression of *Myg1* orthologue decreases in response to oxidative stress, heavy metal stress, heat shock, osmotic stress and DNA damage (Chen *et al*, 2003). Similarly, *Myg1* expression is down-regulated in cytotoxicity induced by nickel ions (Lü *et al*, 2009). Stress-repressed genes are generally involved in energy-consumption and -balance, oxidative stress, RNA processing, transcription, translation, protein folding, biosynthesis of ribosomal subunits and nucleotides, membrane transport, cellular structure, and cell cycle control (Chen *et al*, 2003; Hawse *et al*, 2003). There is additional data suggesting that *Myg1* is repressed in restricted energy conditions and degeneration: *Myg1* is rapidly degraded during starvation-induced autophagy (Kristensen *et al*, 2008) and the expression level of *MYG1* is 6-fold decreased in human age-related cataract lenses relative to clear lenses (Hawse *et al*, 2003). Additionally, Myg1 is down-regulated in the entorhinal cortex and hippocampus of Alzheimer patients (Liang *et al*, 2008). Taken together, *Myg1* expression can be increased or decreased depending on the nature of cellular stress, but restricted cellular metabolism seems to correlate with decreased expression of *Myg1* transcript.

In some studies *Myg1* transcript has been reported to change specifically after immune system activation or repression. *Myg1* expression has been associated with immunological response in several cell culture and mouse models: *MYG1* expression is 2.78-fold decreased 24 hours after human microvascular endothelial cell culture (HMVEC) was infected with *Trypanosoma cruzi* parasite (Costales *et al*, 2009). Additionally, *Myg1* expression is up-regulated in lungs of mice infected with *Mycobacterium tuberculosis* and treated with genetic vaccine immunotherapy that was able to boost T helper (Th)1 immune response (Zárate-Bladés *et al*, 2009). Furthermore, *Myg1* mRNA expression is decreased in $CD8^+$ cytotoxic T-lymphocytes after interleukin-12 induced activation in a mouse mammary carcinoma model (Cao *et al*, 2004) and in response to *in vitro* treatment of peripheral blood cells with IFN-alpha (Taylor *et al*, 2004). IFN-alpha and IL-12 are macrophage-derived immunostimulatory cytokines that enhance innate and cell-mediated (Th1-type) immune responses (Lehtonen *et al*, 2003). Finally, up-regulation of *Myg1* mRNA has been reported in a methylcholanthrene-induced sarcoma tumour model following treatment with anti-inflammatory COX-inhibitor indomethacin (Axelsson *et al*, 2007).

5. Myg1 in cell cycle and cancer

There is no data that Myg1 could be directly involved in the regulation of cell cycle. On the contrary, a genome-wide study in *Schizosaccharomyces pombe* demonstrates that *Myg1* orthologue is not periodically expressed during cell cycle (Rustici *et al*, 2004), suggesting that the function of Myg1 is not related to cell cycle. Still, as Myg1 seems to be involved in basic cellular functions, it is not suprising that there are global expression reports that link Myg1 with cancer-related cellular alterations. As cited above, *Myg1* has been found to

change in response to immune therapies in cancer models: *Myg1* is induced in response to interleukin-12 treatment in mammary carcinoma (Cao *et al*, 2004) and reduced in response to COX-inhibitor in sarcoma tumour model (Axelsson *et al*, 2007). As cancer cells are highly reactive to changes in the immune system and several cancer therapies directly manipulate immune reactions, it is most probable that these changes in *Myg1* transcript are related with influence on immune reaction. Furthermore, *MYG1* is upregulated in oncocytomas that are large cell tumours characterized by an abnormal proliferation of mitochondria (Baris *et al*, 2004). Baris *et al* (2004) also found coordinated up-regulation of oxidative metabolism genes in thyroid oncocytic tumors; here again *Myg1* transcript can be induced by other cellular changes and not by malignancy. However, some evidence suggests that Myg1 can be directly involved in the cellular malignancy: *Myg1* is upregulated after knockdown of both DNMT1 and DNMT3b DNA methyltransferases in malignant glioma cell line. DNA methyltransferases regulate and maintain promoter methylation and are overexpressed in human cancer (Foltz *et al*, 2009), therefore Myg1 can be suppressed in malignant tumours by methylation. Another paper reports that *MYG1* is downregulated in metastatic prostate tumours compared with primary prostate tumours (Chandran *et al*, 2007). Finally, the first scientific abstract about Myg1 (Smicun, 2000) showed that *Myg1* mRNA is downregulated in mouse melanoma cells compared with normal melanocytes. In conclusion, changes of *Myg1* transcript in tumour cells can be related with changes in cell's immune response or metabolism, but there is evidence that Myg1 tends to be down-regulated in malignant tumours.

6. Vitiligo genetics and candidate genes

We have been interested in *MYG1* as a putative candidate gene in vitiligo genetics, because according to our initial hypothesis *Myg1* was a melanocyte specific gene or have specific functions in melanocytes as suggested by Smicun (2000) who initially named the gene as *Melanocyte proliferating gene 1* or *Myg1*. Vitiligo is an acquired pigmentary disorder characterized by areas of depigmented skin resulting from loss of epidermal melanocytes (Zhang *et al*, 2005). Considered the most common pigmentary disorder, vitiligo occurs with a frequency of 0.1–2.0% in various populations (Alkhateeb *et al*, 2003). Vitiligo involves complex interaction of environmental and genetic factors that ultimately contribute to melanocyte destruction, resulting in characteristic depigmented lesions (Spritz *et al*, 2007). Strong evidence from twin and family studies indicates the importance of genetic factors in the development of vitiligo (Zhang *et al*, 2005). Nevertheless, the concordance of vitiligo in monozygotic twins has been reported to be only 23%, indicating that a non-genetic component also plays an important role (Alkhateeb *et al*, 2003). Attempts to identify genes involved in susceptibility to generalized vitiligo have involved gene expression studies, genetic association studies of candidate genes, and genome-

wide linkage analyses to discover new genes (Spritz *et al*, 2007). However, the search is complicated, because the genetics of vitiligo is characterized by incomplete penetrance, non-Mendelian pattern, multiple susceptibility loci and genetic heterogeneity (Zhang *et al*, 2005).

For at least three decades, separate investigators have been defending their favourite theory – such as the autoimmune theory, the cytotoxic metabolites theory, the neural theory and the genetic theory. Recently, some other theories have been added, e.g. the hydrogen peroxide theory, the growth factor theory and the chronic pressure theory (Schallreuter *et al*, 2008). Besides immunological approach, the study of the metabolic deregulations leading to toxic damage of the melanocytes appears to be more and more relevant (Dell'Anna & Picardo, 2006). Among these hypotheses about vitiligo pathogenesis, only autoimmune theory has gained support from repeatable association studies. In general, there are not many genes, which involvement has been proved in replication studies. Namely, the involvement of PTPN22 (1p13), MHC gene cluster (6p21.3) and NALP (SLEV1; 17p13) have been repeatedly associated with vitiligo according to two most comprehensive reviews about vitiligo genetics in recent years (Zhang *et al*, 2005 and Spritz *et al*, 2007). These genes are directly related with the regulation of immune response. PTPN22 encodes lymphoid protein tyrosine phosphatase, which is important in the negative control of T lymphocyte activation (Canton *et al*, 2005); *NALP1* encodes NACHT leucine-rich-repeat protein 1, a regulator of the innate immune system (Jin *et al*, 2007). Finally, the major histocompatibility complex (MHC) is a dense region of immune genes, which variation is a key determinant of susceptibility and resistance to a large number of infectious, autoimmune and other diseases (Traherne, 2008).

Vitiligo is indeed strongly related with autoimmune disorders: overall, about 30% patients with generalized vitiligo have been reported to be affected with at least one additional autoimmune disease (Alkhateeb *et al*, 2003). However, there is evidence that autoimmunity related loci are separable from other loci that are not related with autoimmunity. Spritz *et al* (2004) found evidence for linkage at most loci: AIS1 (1p31), AIS2 (7q) and SLEV1, was mainly from the autoimmunity-associated families, on the other hand, the linkage effect of AIS3 locus (8p) was primarily from the families with no autoimmune diseases, suggesting that vitiligo might be divided into at least two distinct phenotypic subcategories that involve different disease loci or alleles. Moreover, there is other evidence that vitiligo can be divided into different genetic subgroups: for example, there is little overlap between the linkage findings of Chinese and Caucasian populations (Chen *et al*, 2005) suggesting that vitiligo is associated with a strong genetic heterogeneity and might involve different genetic risk factors in different ethnic populations. Taken together, vitiligo is a highly heterogenous disease and many genetic factors that mediate pathogenesis of vitiligo are currently unknown. Therefore studies investigating new gene candidates are important to provide new targets for understanding, preventing and treatment of vitiligo.

CONCLUDING REMARKS

Myg1 is one of the most conserved genes that have been evolutionarily crucial to maintain from protozoans to humans. Despite that, Myg1 has not been associated with any remarkable disease conditions or fundamental cellular processes. Global expression analysis suggests that Myg1 is altered in diverse cellular conditions: development, cell cycle and various stress responses. The purpose of the present study was to perform a comprehensive investigation about Myg1 in DNA, mRNA, protein, cell culture and organism level in order to get more information about the function of this highly conserved gene and protein. We investigated *Myg1* transcript, expression dynamics during development and adulthood and subcellular location of Myg1 protein. Additionally we performed *in vitro Myg1* knockdown experiment followed by global expression profiling and created a mouse line with targeted deletion of *Myg1* gene followed by comprehensive phenotyping that covered a multitude of behavioural, cognitive, neurological, physiological and stress-related functions. Finally, we explored functional polymorphisms of human *MYG1* gene and studied *MYG1* expression and polymorphisms in relation to an acquired pigmentary disorder – vitiligo.

AIMS OF THE STUDY

The general goal of present study was to collect comprehensive experimental data about the function of Myg1 gene and protein. More specific aims of the present study were as follows:

1. To characterize the expression pattern of *Myg1* mRNA in human and mouse tissues using real-time quantitative PCR, northern blotting and *in situ* RNA hybridization (Studies I, II, III).
2. To identify subcellular distribution of Myg1, to find possible interaction partners and cellular pathways of Myg1 (Studies I and IV).
3. To create a *Myg1*-deficient mouse model and to characterize behavioural, cognitive, neurological, physiological and stress-related responses in *Myg1*-deficient mice (Study II).
4. To confirm a possible involvement of Myg1 in the acquired pigmentary disorder – vitiligo. To characterize functional *MYG1* SNPs and *MYG1* mRNA levels in the skin biopsies of vitiligo patients (Studies III and IV).

MATERIALS AND METHODS

1. Expression of *Myg1* mRNA

1.1. Northern blot analysis (Study I)

Ten micrograms of human total RNA from ten different tissues (BD Bioscience Clontech, Palo Alto, CA) was denatured in glyoxal-dimethyl sulfoxide and separated in 1.5% agarose gel, transferred to Hybond-XL membrane (Amersham), and hybridized with *MYG1* full length cDNA probe labeled with [α-32P]dCTP. Washed membrane was exposed to autoradiographic screen, and hybridization signals were visualized with a Starion bioimager.

1.2. Affymetrix Genechip analysis of *MYG1* mRNA expression in human total RNA samples (Study I)

MYG1 mRNA levels in human total RNA samples (Clontech) from fetal brain, adult brain, cerebellum, thymus, spleen, stomach, ileum, colon, kidney, prostate, heart, liver, lung, testis, skeletal muscle, thyroid and salivary gland were determined by Human Affymetrix Genechip (HG-U133plus2) analysis.

1.3. qRT-PCR analysis of *Myg1* expression in mouse tissues (Studies I and II)

Myg1 mRNA level was determined by quantitative real-time PCR (qRT-PCR) in 10 brain regions and 9 non-neural tissues from 3 wild-type mice from 129Sv strain. All reactions were performed by using qPCR™ Core Kit for SYBR® Green I Master Mix (Eurogentec, Belgium). RNA extraction, cDNA synthesis, qRT-PCR and data analysis was performed as described earlier (Areda *et al*, 2006). Embryonic cDNAs from MTC™ PanelI (Clontech) that provide a cDNA pool of 200 mouse embryos were used for analyzing E7, E11, E15 and E17 embryonic stages. Two primer-pairs were used for detecting *Myg1* mRNA: primers 1 and 2 (see Table 1 for primer sequences) specific to exons 2 and 3 of *Myg1* mRNA; and primers 3 and 4 specific to exons 3 and 4 of *Myg1* mRNA. Hypoxanthine guanine phosphoribosyl transferase (*Hprt1*) was used as endogenous reference gene (primers 7 and 8). Specific primers were designed to detect the short splice variant of mouse *Myg1* mRNA that was incidentially cloned from mouse testis mRNA pool. As short variant lacks exons 5 and 6 (Figure 6C), a reverse primer was designed on the junction of exons 4 and 7 (primer 5). Primers 5 and 6 were used to generate a 100 bp amplicon for quantitative measurements of *Myg1* short splice variant. To confirm that primer 5 is annealing the unique junction site of exons 4 and 7, we used primer 5 with

different forward primers from *Myg1* cDNA (Figure 6A) to achieve 207 bp amplicon (primers 3 and 5) and 341 bp amplicon (primers 1 and 5) (Figure 6D). qRT-PCR data in Figure 5C and 5D and 20A–20C is presented on a linear scale, calculated as $2^{-\Delta CT}$, where ΔCT is the difference in cycle threshold (CT) between the target gene (*Myg1*) and housekeeper gene (*Hprt1*).

1.4. qRT-PCR analysis of *MYG1* expression in human skin biopsies (Studies III and IV)

Gene expression level of *MYG1* was detected applying TaqMan Assay-On-Demand (Hs000222208_m1, FAM-labelled MGB-probe) gene expression assay mix (20X, Applied Biosystems, Foster City, CA, USA) and TaqMan® Universal PCR Master Mix (Applied Biosystems, Foster City, CA, USA) in the ABI Prism 7900HT Sequence Detection System (Applied Biosystems, Foster City, CA, USA). Reactions were carried out in 10 µl reaction volumes in four replicates. Data is presented as $2^{-\Delta CT}$ calculated in relation to the *HPRT1* (primers 9 and 10 and VIC-TAMRA-labelled probe were used) (Kingo *et al*, 2008) and unpaired Student's t-test and one-way ANOVA were used to test for differences between the groups.

1.5. *In situ* RNA hybridization analysis (Studies I and II)

Mouse *Myg1* full-length cDNA was cloned from a cDNA pool from wild-type mice testis using primers 15 and 16 and inserted into *pGEM7*-Zf(+) vector (Promega) for creating an *in situ* probe. *Gad1* RZPD cDNA clone (accession: BC027059) was used to synthesize positive control RNA probe. Whole mouse embryos were hybridized with digoxigenin-UTP (Roche) labeled RNA probes according to Wilkinson (1993), recorded, and cut into 45 µm slices with vibratome. The embryos were dissected from timed matings and the stages were confirmed according to Kaufman (1995). RNA *in situ* hybridization on free-floating PFA-fixed 40 µm mouse brain cryosections using digoxigenin-UTP (Roche) labelled *Myg1* sense and antisense RNA probes was performed according to Braissant & Wahli (1998). As a major modification, active DEPC treatment was avoided and 0.25% TritonX-100 was added into PBS to improve probe penetration. The stained sections were transferred onto slides in 0.5% gelatine and air dried, mounted with Pertex (Histolab, Malmö, Sweden).

Table 1. Primer sequences. Restriction sites within primer sequences are given in lowercase letters.

	No	Name	Sequence
Expression primers	1.	Mouse Myg1 Ex2 Fw	5'-GATGTGGGCGGTGAGTACAAC-3'
	2.	Mouse Myg1 Ex2-3Rev	5'-GAACTCATGGTTTCTGTAAAAGTCCTC-3'
	3.	Mouse Myg1 Ex3 Fw	5'-GCACTTCGGACGTAAGCTCCT-3'
	4.	Mouse Myg1 Ex3-4Rev	5'-TCTTCCACAAAGTTCTCATACATCTTG-3'
	5.	Mouse Myg1 junction 4-7Rev	5'-TCTCGAGTGTGGTGCCG-3'
	6.	Mouse Myg1 Ex4 Fw	5'- ATGCGGTGGACAATGGGA-3'
	7.	Mouse Hprt1 Fw	5'-GCAGTACAGCCCCAAAATGG -3'
	8.	Mouse Hprt1 Rev	5'-AACAAAGTCTGGCCTGTATCCAA-3'
	9.	Human HPRT1 exon 6	5'-GACTTTGCTTTCCTTGGTCAGG-3'
	10.	Human HPRT1 exon 7	5'-AGTCTGGCTTATATCCAACACTTCG-3'
	11.	Human Myg1 Ex2 Fw	5'-CACCGATATGACCATCACCA-3'
	12.	Human Myg1 Ex3-4 Rev	5'-TCCTCCACAAAGTTCTCATACATCTTG-3'
	13.	Beta-actin Fw	5'-ACTGGGACGACATGGAGAAG-3'
	14.	Beta-actin Rev	5'-GGGGTGTTGAAGGTCTCAAA-3'
Cloning primers	15.	Mouse Myg1 ATG Fw	5'-ATGGGTAGACGTTTCCTGCGTGG-3'
	16.	Mouse Myg1 nostop Rev	5'-TTGGACTACAGCATTTGCAAGAGGC-3'
	17.	Human Myg1 YFPNheIATG	5'-ATATgctagcCATGGGACACCGCTTCCTGCGCG-3'
	18.	Human Myg1 YFPSacIInostop	5'-ATATccgcggGGAGATTTGTGGGAGGTATGAG-3'
	19.	NoMitoMygKzNheIF	5'-TATAgctagcCATGGGAACCCGGCACCGCATGCTCG-3'
	20.	NoNLSMygHindIIIFw	5'-ATATaagcttAGCAAACTCATGGCACCGCC-3'
	21.	NoNLSMygHindIIIRew	5'-ATATaagcttGACGGACTCTGGACCGAGCA-3'
	22.	NoSignalMygKzNheIF	5'-ATATgctagcCCATGGGAAGCAAACTCATGGCACCGC-3'
	23.	Human Myg1 4Arg ATG Fw	5'-ATATgctagcCATGGGACACCGCTTCCTGCGCG-3'
	24.	Human Myg1 4Gln ATG Fw	5'-ATATgctagcCATGGGACACCAATTCCTGCGCG-3'
	25.	MYG1-300KpnIF	5'-TATAggtaccAGAATGTTGGTCTTTTCTTGGATTAAGC-3'
	26.	MYG1-1kbKpnIF	5'-TATAggtaccGAGAAGAGTCTCATTCTCACC-3'
	27.	MYG15utrHindIIIR	5'-ATATaagcttAAGCAGCTCCCTGCAGGGAG-3'
Genotyping primers	28.	Mouse Myg1_-2 kbFw	5'-GCCCAGCGAGATGATCTTTAG-3'
	29.	LacZRev	5'-GTGCTGCAAGGCGATTAAGTTG-3'
	30.	Mouse Myg1+740 Rev	5'-ATCCTTGAACTAGAAGGATCCAGC-3'
	31.	Mouse Myg1-255 Fw	5'-CAAATGGGGTGGTCTATTCTTGC-3'

2. Cell culture experiments

2.1. Cell culture, immunocytochemistry and fluorescence microscopy (Studies I and IV)

All cell culture experiments were performed with HeLa cells. *MYG1* cDNA constructs were transfected into HeLa cells using FuGENE 6 Transfection Reagent (Roche, USA). For immunocytochemistry, cells expressing FLAG-tagged constructs were fixed with 4% paraformaldehyde for 15 min at room temperature and permeabilized with 0.1% Triton X-100 in PBS for 3 min. After blocking with 1% bovine serum albumin (BSA) in PBS for 1 h at room temperature, cells were incubated with primary anti-FLAG antibody (Sigma-Aldrich, Denmark, diluted 1:5,000) in 1% BSA PBS overnight at 4°C, washed 3x5 min in PBS and incubated with Alexa Fluor 488-conjugated anti-mouse secondary antibody (Molecular Probes, USA, diluted 1:1,000). Mitochondria were visualized by using MitoTracker Red CMXRos (Molecular Probes, USA). MitoTracker (final concentration 100 nm) was applied to the cells 45 min before examination. Prior to photo-bleaching (FRAP) experiments, cells were incubated 2 hours with cyclohexamide (40 µg/ml) to block protein synthesis. In a FRAP experiment a region (mitochondria or nucleus) of the YFP-Myg1 transfected cell was briefly illuminated with a high-intensity laser beam with a wavelength near the excitation peak of a fluorophore. Consequently, most of the YFP-Myg1 molecules inside that region lost their fluorescence irreversibly, a phenomenon known as photobleaching. Recovery of fluorescence inside the bleached region was considered to reflect the mobility of YFP-Myg1 fusion-molecules. Images were aquired with a Zeiss LSM 510 confocal laser-scanning microscope.

2.2. Mutant and wild-type *MYG1* cDNA constructs for subcellular localization (Studies I and IV)

Human *MYG1* full-length cDNA was cloned from HeLa cell line using primers 17 and 18 and inserted into pEYFP-N1 and pEYFP-C1 vectors (Clontech, Palo Alto, USA) for N- and C-terminal fluorescent tagging, and into pQM-FLAGCTag (Quattromed, Estonia) vector for C-terminal affinity tagging. Myg1 signal-sequence deletion constructs were generated by deletion of cDNA fragments corresponding to aminoacids 1-20 (Figure 9B; NoMTS Myg1, primers 18 and 19), aminoacids 33-39 (Figure 9B; NoNLS Myg1, primers 17, 18, 20, 21) or aminoacids 1-39 (Figure 9B; NoSignal Myg1, primers 18 and 22) of Myg1 protein. All deletion mutants were inserted into pEYP-N1 and pQM-FLAGCTag vectors. Full-length human *MYG1* cDNA with both variants for Myg1 Arg4Gln polymorphism were inserted into pEYFP-N1 vector (Clontech, Palo Alto, USA) by using NheI and SacII restriction sites. Myg1 4Arg cDNA was cloned by using primers 18 and 23 and Myg1 4Gln cDNA with primers 18 and 24.

2.3. Preparation of FLAG-transfected cells for Western Blot analysis (unpublished data)

Four million HeLa cells in 4 ml cell culture dishes were transfected with 6 µg Myg1-FLAG DNA plasmids (wild-type, NoMTS or NoNLS). Cells were washed 48 hours after transfections (2x with PBS) and collected by suspending in 350 µl 2x SDS buffer. Cell samples and biotinylated protein ladder (#7727; Cell Signaling Technology) were separated in 10% SDS-polyacrylamide gel and transferred to Hybond-P membranes (Amersham Biosciences). Membrane was incubated overnight with primary mouse monoclonal anti-FLAG antibody (Sigma-Aldrich, Denmark, diluted 1:20,000) followed by horseradish peroxidase (HRP)-conjugated horse anti-mouse IgG antibody (#7076; Cell Signaling Technology; diluted 1:3,000) and anti-biotin HRP-linked antibody (1:1,000). Immunoreactive proteins were detected with SuperSignal chemiluminescence reagents (Pierce) and captured with LAS-1000 luminescence imager (Fuji) using Image Gauge 4.0 software (Fuji).

2.4. Human *MYG1* promoter DNA constructs (Study IV)

For *MYG1* promoter analysis, fragments from *MYG1* promoter area were cloned into pGL3-Basic Vector (Promega) by using KpnI and HindIII restriction sites. Genomic DNA from two control subjects was used to make reporter gene constructs and all fragments were sequenced to verify genotype and lack of additional mutations in the constructs. Short promoter fragment that includes a 291 bp genomic sequence before *MYG1* coding ATG was amplified by using primers 25 and 27. Long, 1 kb promoter fragment was amplified with primers 26 and 27. Both long and short promoter fragments were created in two variants with respect of *MYG1* promoter polymorphism C/G -119bp. Two different lengths of promoter fragments were used because of lack of information how long promoter area is needed to trigger maximum promoter activity for *MYG1* gene. 291 bp fragment was used, because it is the maximum *MYG1* unique promoter area that is not overlapped with 3'-UTR of closest neighbour gene *PFDN5*.

2.5. Luciferase assay (Study IV)

For luciferase assay 200,000 cells per well were plated into six-well cell-culture dishes 24 h prior transfections and five replicas were created for each plasmid, with two different DNA preparations of the same clone. For each well 1 µg of the construct was transfected along with 1µg of pRLO renilla luciferase reporter vector as the control for transfection efficiency. Luciferase gene with CMV promoter was used as positive control and empty pGL3-Basic vector as negative control. The cells were harvested 24 h after transfection, and the activity of firefly and renilla luciferase was measured with GloMax 96 Luminometer (Promega).

The normalized luciferase data (renilla/firefly) were used to perform statistical analysis (t-test) and are expressed relative to empty pGL3-Basic vector.

2.6. RNAi-mediated knockdown of *MYG1* mRNA in HeLa cells and Affymetrix Genechip analysis (Study I)

We tested 3 predesigned short interfering RNAs (siRNAs) from Qiagen: siRNA 1 (target sequence CACCCTCTATGACAAGATGTA around junction of exons 3 and 4) and siRNA 3 (target sequence CCCACAAATCTCCTAGTCTAA in the end of exon 7). Different siRNAs were used in order to control for off-target effects. siRNA 2 was excluded from the experiment because of deviant appearance of treated cells that was not related with more effective knockdown of *MYG1* mRNA. siRNA-induced effect on *MYG1* mRNA expression in HeLa cells was determined by quantitative RT-PCR using primers 11 and 12 and beta-actin as an endogenous reference (primers 13 and 14). Six million HeLa cells in 10 ml cell culture dishes were either mock-treated or transfected with siRNA 1 or siRNA 3 by using Oligofectamine reagent (Invitrogen, USA). All three treatments were carried out in six replicas. The cells were harvested 72 h after transfection, RNA was extracted with Trizol reagent (Invitrogen) and pooled in a set of two. siRNA-mediated down-regulation of *MYG1* mRNA was confirmed by qRT-PCR. Nine samples of cRNA (all three treatments in three replicas) were hybridized to Affymetrix human HG-U133plus2 arrays (Affymetrix, USA) containing 54,613 probe sets. The arrays were processed according to the manufacturer's protocol.

2.7. Analysis of Genechip data (Study I)

The .CEL files were obtained using the Affymetrix GCOS v1.4 software and analyzed by use of BioConductor (version 1.8) (www.bioconductor.org) for the statistical software R (version 2.3) (www.r-project.org) (http://www.r-project.org). The gcrma package (version 2.4.1) and the affy package (version 1.10.0) were used to correct for optical noise and nonspecific binding, for normalization between arrays, and to summarize multiple probes into a single expression value. The default settings for gcrma modeling was used, i.e. 'background correction', quantile normalization' 'PM-only modeling', and 'median polish summarization'.

Expression values (natural scale) were read into dChip (build date Sep 12, 2008) (www.dChip.org) for downstream analyses and clustering (Supplementary file 3). The compare samples function was used to compute fold-changes and corresponding p-values. The p-values were calculated by Welch' modified two-sample t-test. Differentially expressed transcripts between Mock and siRNA treated cells were filtered using the following criteria: fold-changes > than 1.5 using, differences of means > 25, and p-values < 0.01. Significantly changed genes were grouped based on their biological function using the Gene

Ontology (GO) database (www.geneontology.org), the categorization principle was to cover all transcripts with a minimum number of clusters.

2.8. Immunoprecipitation (IP) (Study I)

C-terminally FLAG-tagged *MYG1* cDNA construct was used for immunoprecipitation experiments. FLAG-*Erg1* construct was used as a negative control. 3.5 million HeLa cells were seeded on fibronectin-coated 12.5 cm^2 flasks 24 h prior to transfection. FLAG-tagged *MYG1* cDNA construct was transfected using FuGENE 6 Transfection Reagent (Roche). Cells were harvested 48 h after transfection at 90% confluency. 120 million cells were used for each purification. Immunoprecipitations were performed as previously described (Jønson *et al*, 2007). Specifically, the proteins were extracted by resuspending the cells in lysis buffer consisting of 50 mM tris-HCl pH 7.4, 150 mM NaCl, 1% Triton X-100, 0.5 mM phenylmethanesulphonylfluoride (PMSF) and 5 µl/ml Inhibitor cocktail (Sigma), followed by sonication. The lysis buffer was used both for extraction and IP. Protein extraction from 120 million HeLa cells in 3 ml lysis buffer, followed by removal of the post-mitochondrial fraction by centrifugation yielded approximately 20 µg protein per µl lysis buffer, based on quantification of total protein content using BCA protein assay kit (Pierce). After IP, the IP proteins were washed in wash buffer (50 mM tris-HCl pH 7.4, 150 mM NaCl, 0.5 mM phenylmethanesulphonylfluoride (PMSF) and 5 µl/ml Inhibitor cocktail (Sigma)). Immunoprecipitated samples were separated on a 10% SDS-polyacrylamide gel and silver-stained using Silverquest (Invitrogen) according to manufacturer`s instructions. Western blot analysis (see section 2.3. for technical details) was performed to detect possible Hsp90 immunoreactivity in different phases of IP experiment (in cell lysate, in fraction that is not bound to anti-FLAG beads, in the solution of FLAG binding beads and in the eluate of beads) by using mouse monoclonal antibody (ab1429, Abcam).

3. Generation and phenotyping of *Myg1*-deficient mice (Study II)

3.1. Generation, breeding and genotyping of mice lacking *Myg1* (-/-)

Myg1 knockout targeting construct was created by PCR amplification genomic arms from wild-type 129/SvEvTACfBr mouse genomic DNA. The 5' genomic arm (1.6 kb) included a sequence from the upstream neighbour gene *Pfdn5* *Myg1* promoter sequence, and the 3' genomic arm (3.6 kb) included a sequence from the downstream neighbour gene *Aaas*. A LacZ-NEO cassette was inserted immediately after the *Myg1* promoter; as a result of homologous recombination,

LacZ transgene replaced all seven exons of *Myg1* gene spanning in genomic area of 6.1 kb (Figure 3A). pGEM-11Zf(+) cloning plasmid (Promega) was used as a backbone during cloning, and a pgk-TK negative selection cassette was cloned upstream of the 5' genomic arm. NotI-linearized targeting construct was electroporated into W4/129S6 embryonic stem (ES) cells (Taconic) which were selected for resistance to Neomycin and Gancyclovir. ES cell colonies were tested for homologous recombination by PCR using recombination-specific primer pair (primers 28 and 29) 2.3 kb PCR-product was sequenced to verify the integration site. ES cell clone 8A1 was injected into C57/Bl6 blastocysts. *Myg1* F1 (+/-) founder animals were produced by mating male chimeras with C57/Bl6 female mice. F2 generation *Myg1* (+/+) and their (-/-) littermates were obtained by mating heterozygous (+/-) founder animals. Multiplex genotyping reaction (primers 29, 30 and 31) was used for all tree genotypes (+/+, +/-, -/-) (Figure 3B).

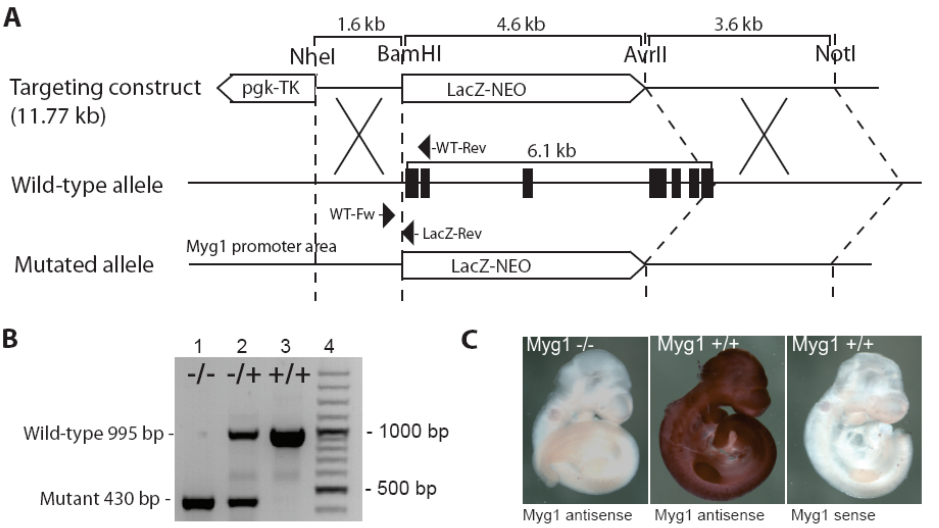

Figure 3. Targeted disruption of the *Myg1* gene. (**A**) Restriction enzyme recognition site map surrounding *Myg1* wild-type allele indicates the region of homology selected for construction of the targeting vector and location of targeted homologous recombination event that replaced all seven exons of *Myg1* gene with LacZ-NEO transgene. Arrowheads represent locations and directions of genotyping primers (WT-Rev, WT-Fw and LacZ-Rev). (**B**) A multiplex-PCR-based genotyping assay (primer locations shown in (**A**)) amplifies 995-bp fragment from the endogenous allele and a 430-bp fragment from the targeted allele and is used for genotyping mice with all three genotypes: *Myg1* -/- (lane1), *Myg1* +/- (lane 2) and *Myg1* +/+ (lane 3). GeneRuler 100bp DNA Ladder Plus (Fermentas) was used as a fragment size marker (lane 4) (**C**) Whole mount *in situ* hybridisation analysis with full-length *Myg1* antisense probe revealed lack of *Myg1* mRNA in *Myg1* (-/-) embryo in contrast to *Myg1* (+/+) embryo. *Myg1* sense probe was used as a negative control to verify the specificity of *Myg1* antisense probe staining.

3.2. Animals

Female and male wild-type (+/+) and homozygous *Myg1*-deficient (-/-) mice were used in the present study (F2 hybrid). F2 hybrid *Myg1* (-/-) mice are vital, fertile and lack visible abnormalities. Mice were separately housed by genotype and sex in standard laboratory cages (425 × 266 × 155 mm) 6–9 animals per cage. Mice were kept in the animal house at 22±1 C under a 12:12 h light/dark cycle (lights off at 19:00 h). Tap water and food pellets were available *ad libitum*. Unless stated otherwise, testing was carried out between 13:00 and 19:00 of the light phase. All animal procedures in this study were performed in accordance with the European Communities Directive (86/609/EEC) and permit (No. 74, March 16, 2007) from the Estonian National Board of Animal Experiments.

3.3. Phenotyping strategy

For the present study a total of 10 batches of mice were reared, each batch comprising 4 cages (2 genotypes × 2 sexes). The phenotyping of mutant mice was carried out in two different testing batteries with the addition of a few tests requiring naïve animals (summarised in Table 2). The aim of the first battery was to characterise a large variety of behavioral and physiological functions, whereas the second battery was constructed to specifically target anxiety- and stress-related phenotypic alterations. The testing order was chosen according to Võikar *et al* (2004) with less stressful and invasive tests preceding the more stressful tests. Testing began at age 60 days (2 months).

Table 2. Phenotyping strategy in mice lacking *Myg1* (-/-) and their wild-type (+/+) littermates. The number of batches enrolled, the list and order of tests in two phenotyping batteries, and additional tests have been given.

Battery I (3 batches)	**Battery II (3 batches)**	**Additional tests (2 × 2 batches)**
Plus-maze test	Light-dark exploration	General description (body weight, blood glucose, rectal temperature)
Locomotor activity and habituation	Marble burying test	Restraint-induced corticosterone and *Myg1* gene expression
Hot plate test	Stress-induced hyperthermia	
Social interaction test	Hyponeophagia test	
Forced swim test	Restraint-induced analgesia	
Rota-rod	LPS-induced weight loss	
Indirect calorimetry		
Water maze		
Sensory-motor descripiton		

The first battery of tests comprised plus-maze test (day 0), locomotor activity and habituation (days 3–4), hot plate test (day 7), social interaction test (day 10), forced swim test (day 13), rota-rod (day 16), indirect calorimetry (days 19–20), water maze (days 23–26) and general sensory-motor description (days 29–30). Three batches of mice were used to carry out the first testing battery (*Myg1* +/+ male n=21, *Myg1* +/+ female n=25, *Myg1* -/- male n=24, *Myg1* -/- female n=26). Due to the lack of available standard opponents, however, social interaction test was performed with only two batches of mice.

The second battery of tests comprised light-dark exploration (day 0), marble burying (day 7), stress-induced hyperthermia (day 14), hyponeophagia test (day 21), restraint-induced analgesia (day 28) and lipopolysaccharide (LPS)-induced weight loss (day 35). For the second battery of tests another 3 batches of naïve mice were used (*Myg1* +/+ male n=21, *Myg1* +/+ female n=21, *Myg1* -/- male n=20, *Myg1* -/- female n=21).

A separate group of mice (2 batches: *Myg1* +/+ male n=17, *Myg1* +/+ female n=17, *Myg1* -/- male n=16, *Myg1* -/- female n=17) was used to measure body weight, rectal temperature and blood glucose at 2 months of age. Mice from this group were later used as standard opponents in the social interaction test (the first phenotyping battery). Another separate group of naïve mice (2 batches: *Myg1* +/+ male n=17, *Myg1* +/+ female n=14, *Myg1* -/- male n=15, *Myg1* -/- female n=17) was subjected to 30 min restraint only, followed by immediate sacrifice to determine plasma corticosterone concentrations and *Myg1* gene expression in various brain structures.

3.4. First phenotyping battery

3.4.1. Elevated plus-maze test. The plus-maze test was carried out as described earlier (Abramov *et al*, 2008) with some modifications. The apparatus consists of two opposite open (17.5 × 5 cm) arms without sidewalls and two enclosed arms of the same size with 14 cm high sidewalls and an end wall. The entire plus-maze apparatus was elevated to a height of 30 cm and placed in a brightly lit room (450 lx in open arms). Pre-experimental social separation for 15 min was employed in order to increase exploratory activity. Testing began by placing a mouse on the central platform facing an open arm. Standard 5 min test duration was used, and the maze was thoroughly cleaned with damp and dry towels between the subjects. Test sessions were video-recorded and the videotapes were analysed by a trained observer unaware of testing conditions. The following parameters were observed: number of total entries on open and closed arms; entries on the open arms expressed as % of total entries on open and closed arms; time spent on the open arms expressed as % of total time spent on open and closed arms; number of stretched-attend postures (SAPs); total number of head-dippings; number of unprotected head-dippings defined as head-dippings made on open arms and expressed as % of total head-dippings. A

male *Myg1* (-/-) mouse fell off the apparatus during testing and was consequently excluded from analysis.

3.4.2. Locomotor activity and habituation. For the study of locomotor activity the animals were placed singly into soundproof photoelectric motility boxes (448 × 448 × 450 mm) connected to a computer (TSE, Technical & Scientific Equipment GmbH, Germany) for 60 min on 2 consecutive days. The illumination level of the transparent test boxes was ~400 lx. After removing the mouse from the box, the floor was cleaned with damp towels and dried thoroughly. Distance travelled (m), number of rearings, number of corner entries and distance travelled in the central area of the apparatus expressed as % of total distance were registered. In order to characterise within-trial habituation distance travelled during the first period (0–30 min) of the first exposure to the apparatus on day 1 was compared to distance travelled during the second period (30–60 min) of the first exposure. To analyse between-trial habituation distance travelled on day 1 was compared to distance travelled on day 2.

3.4.3. Hot plate test. The plate was heated to 52ºC and the mouse was confined there by Plexiglass cylinder (diameter 15 cm, height 20 cm). Latency (s) to show hind paw response (licking or shaking) and latency (s) to jump from the plate were measured. The cut-off time was set at 120 s.

3.4.4. Social interaction test. Social interaction test was carried out as described previously (Shi *et al*, 2003) with slight modifications. Two unfamiliar mice of the same sex and genotype were simultaneously placed in an empty housing cage (267 × 207 × 140 mm) with cover made of transparent plexiglass. Subjects were matched for age and body weight, and their behavior was videotaped for 10 min. Illumination level on test arena was ~400 lx. Active social interaction (s) but not passive body contact was registered. No aggressive encounters were observed in any pairs of mice.

3.4.5. Forced swim test. The mouse was placed for 6 min in the glass cylinder (diameter 12 cm, height 24 cm, water depth 15 cm) filled with water at 25±0.5 ºC. Test sessions were video-recorded and the videotapes were subsequently analysed by a trained observer unaware of testing conditions. The time (s) of immobility (passive floating, when the animal was motionless or doing only slight movements with tail or one hind limb) was measured during the last 4 min of the test.

3.4.6. Rota-rod. The equipment consisted of a motor-driven drum (3 cm in diameter) rotating at fixed speed (11 rpm). Rota-rod is one of the standard tests to measure coordination and balance, but also procedural learning in rodents. Every mouse was given three trials on rota-rod with 2 h inter-trial intervals. The time of maximal performance for each trial was set at 120 s. Due to the problems encountered in previous studies (Abramov *et al*, 2008), the latency (s)

to either fall from the drum or to make first complete revolution was recorded (see also McIlwain *et al*, 2001). Also, the total number of falls and revolutions was registered for each trial.

3.4.7. Indirect calorimetry. Open-circuit indirect calorimetry was carried out using TSE LabMaster Calorimetry Module supplied with 3D motility frame (TSE, Technical & Scientific Equipment GmbH, Germany). The standard protocol was shortened in order to adapt it for high-throughput testing. This protocol is suitable for screening for robust alterations in RER or energy expenditure. This approach enables characterisation of metabolism in highly active animals (the first 30 min of exposure) as well as almost inactive (habituated) animals (the last 30 min of exposure). Calibration of oxygen (O_2) and carbon dioxide (CO_2) sensors was performed before each set of experiments. Measurements were carried out between 09:00 and 19:00 of the light phase. Airflow rate was 0.5 l/min and ambient room temperature was 22°C. Mice were individually placed in hermetically closed plexiglasss cages (250 × 150 × 240 mm) for 2 hours. Food and water were not provided during the study period. O_2 consumption (ml/kg/h), CO_2 production (ml/kg/h) and locomotor activity (counts) of subjects were recorded every 15 min for 3 min per cage. LabMaster software was used to calculate respiratory exchange rate (RER; formula CO_2/O_2) and heat production (kcal/kg/h; formula $(3.941\times O_2+1.106\times CO_2)/1000$).

3.4.8. Water maze. The water maze (TSE, Technical & Scientific Equipment GmbH, Germany) consisted of a circular pool (150 cm in diameter), escape platform (16 cm in diameter), video camera and computer. The pool was filled with tap water (22°C) to a depth of 38 cm. The water was made opaque with the addition of a small amount of non-toxic white putty. The escape platform, positioned in the center of the Southwest quadrant (Q2), 20 cm from the wall, remained in a fixed position. The water level was 1 cm above the platform, making it invisible. Each trial, the animals were put into the water, facing the wall, at pseudo-randomly assigned starting positions (East, North, South or West). The acquisition phase of the experiment consisted of a series of 20 training trials, lasting up to 60 s each (5 trials per day for 4 consecutive days, inter-trial interval 1 hour). Mice were allowed to search for the platform for a maximum of 60 s at which time the mice were gently guided to the platform by means of a metal sieve. Mice remained on the platform for 15 s. Posters and furniture around the maze served as visual cues. During testing, the room was dimly lit with diffuse white light (20 lx). The distance (m) travelled during each trial, the latency (s) to find the submerged platform and swim velocity (cm/s) were registered. The average value per day obtained by collapsing data on 5 trials for each animal was used. On day 4, one hour after the last training trial, the platform was removed for a probe trial. Mice were put into the water in the Northeast position (Q4) and were allowed to swim for 60 s. The time (s) spent in all 4 quadrants (Q1, Q2, Q3, Q4) was measured, with time spent in target quadrant (Q2) where the platform had been located serving as indicator of

spatial memory. Data on one animal (*Myg1* +/+ female) were expelled from the water maze analysis as the animal was subsequently found to be blind (sensory-motor description).

3.4.9. Sensory-motor testing. The methodology was derived from Crawley (2007). The aim of sensory-motor testing was to rule out robust deficits in sensory or motor functions of *Myg1* (-/-) mice. Before sensory testing, mice were deprived of food for 24 h in order to increase their motivation to search for food pellets. Testing of motor abilities followed that of sensory abilities 24 h later (food provided *ad lib*, again). Time to find a visible (visual cue) or coffee-impregnated hidden food pellet (olfactory cue), forepaw reach, pupillary reflex, ear twitch to pen click, eye blink to air-puff, facial reaction (whisker twitch, grimace) to light touch with von Frey filament (0.4 g), righting reflex, wirehang and vertical pole performance were estimated by an experienced observer.

3.5. Second phenotyping battery

3.5.1. Light-dark exploration. The plexiglass box (45 × 20 × 20 cm) was divided into two parts: two-thirds was brightly illuminated (~600 lx) by 60 W light bulb fixed 30 cm above the floor, one-third was painted dark green, covered by the lid and separated from the white compartment with a partition containing an opening (13 × 5 cm) at the floor level. Mice were kept under reduced light conditions (~20 lx) for at least 60 min before the testing (Võikar *et al*, 2004). The animal was placed in the center of the light compartment facing away from the opening, and the latency to move to the dark, the time spent in the light compartment and the number of transitions between the two compartments were measured. The duration of the test was 5 min beginning from the first entry to the dark (the test was terminated if this time was more than 300 seconds).

3.5.2. Marble burying test. The test was adopted from Njung'e & Handley (1991). Mice were placed individually in clear plexiglass boxes (267 × 207 × 140 mm) containing clean sawdust (depth 50 mm) and 20 glass marbles (diameter 15 mm), which were evenly spaced along the perimeter of the cage. For the assessment of general locomotor activity motility frame (TSE, Technical & Scientific Equipment GmbH, Germany) adjusted to the height of sawdust was used. Illumination level was ~400 lx. The number of marbles buried to at least two-thirds of the depth and distance travelled (m) were registered during 30 min.

3.5.3. Stress-induced hyperthermia. The test was carried out as described by Tasan *et al* (2009). Mice were transferred to experimental room and put individually into holding cages (267 × 207 × 140 mm). After an adaptation period of 90 min basal temperature was obtained with a rectal mouse probe (TSE, Technical & Scientific Equipment GmbH, Germany). The tip of the

probe was 1.7 mm in diameter and inserted 19 mm into the mouse rectum, while the animal was gently restrained manually. Before insertion the probe was dipped into vaseline and maintained in the rectum until stable values were obtained. Temperature was measured to the nearest 0.1°C. After 10 min the second value was determined to calculate the stress-induced hyperthermia ($\Delta T=T2-T1$).

3.5.4. Hyponeophagia test. Mice were deprived of food for 24 h prior to testing (Võikar *et al*, 2005). The test was performed in a square plexiglass box (448 × 448 × 450 mm) with clear walls. Illumination level was ~400 lx. The animal was placed in the center of the arena facing a standard food pellet. Maximum duration of the test was 6 min. The latency to start eating (s) was registered.

3.5.5. Restraint-induced analgesia. Restraint stress was induced by placing a mouse in 50 ml plastic tube for 30 min (Abramov *et al*, 2008). Adequate ventilation was provided by means of holes on the tip and the sides of the tube. Remaining space in the tube was filled with soft clean paper towel swab to restrict animal's movements. Every effort was made to spare animals of any stress but restraint itself. The nociceptive threshold was determined using radiant heat tail flick system (Ugo Basile, Italy) immediately after termination of the procedure. Unstressed control group comprised undisturbed animals taken from their home cage immediately before tail-flick measurement. Cut-off time was set at 15 s to avoid tissue damage.

3.5.6. Lipopolysaccharide (LPS)-induced weight loss. Animals from each genotype and sex were randomly assigned to receive lipopolysaccharide (LPS; *Escherichia coli* serotype 0111:B4, Sigma-Aldrich, Finland) diluted in sterile saline at dose 50 μg/kg (i.p.) or an equal volume of sterile saline. Animals were weighed immediately before injection, marked with non-toxic marker and weighed again 24 h later. Weight loss was expressed as % change of the initial weight (weight2-weight1/weight1×100%).

3.6. Additional tests

3.6.1. Body weight, rectal temperature and blood glucose determination. A group of naïve mice was used to determine body weight, rectal temperature and tail-vein blood glucose concentration at 2 months of age. Rectal temperature was measured using a TSE thermometer (TSE Technical & Scientific Equipment GmbH, Germany) to the nearest 0.1ºC in hand-held mice by inserting lubricated rectal probe (tip diameter 1.7 mm) 19 mm into the rectum. For the measurement of blood glucose mice were restrained shortly and blood was collected from a small incision to the right lateral tail vein. Glucose concentrations were determined using Accu-Check GO portable glucometer (Roche, Mannheim, Germany).

3.6.2. Restraint-induced corticosterone elevation and *Myg1* expression in brain structures of wild-type (+/+) mice. Another group of naïve mice was used for this experiment. 30 min restraint was carried out as described in the restraint-induced analgesia section. Undisturbed animals from home cage served as unstressed controls. Immediately after restraint animals were decapitated, brains were quickly dissected into three parts (the prefrontal cortex, mesolimbic area and temporal lobe) and frozen in liquid nitrogen. Blood from the trunk of the body (mixed arterial and venous blood) was collected into heparinized tubes and centrifuged for 10 min at 1500 × *g*. Sera were stored at -20°C until the assay using corticosterone HS ELISA kit Octeia from Immunodiagnostic Systems (U.K.) according to manufacturer's instructions (described in detail in Luuk *et al*, 2009). Changes in *Myg1* gene expression in response to restraint-stress were determined in wild-type (+/+) animals by means of qRT-PCR (see section 1.3).

3.7. Statistical analysis for behavioural studies

Results are expressed as mean values ± S.E.M. Statistica for Windows 7.0 software was used for statistical analysis. The results of the plus-maze, locomotor activity, hot plate, social interaction, forced swim test, visible and hidden food finding, body weight, blood glucose, rectal temperature, light-dark exploration, marble burying, stress-induced hyperthermia and hyponeophagia were analysed using two-way independent-groups ANOVA (genotype × sex). The probe trial of the water maze, restraint-induced analgesia, restraint-induced corticosterone elevation and LPS-induced weight loss were analysed using three-way independent-groups ANOVA (genotype × sex × quadrant or restraint or LPS). Within-trial and between-trial habituation to the locomotor activity cages, rota-rod, indirect calorimetry measurements and the acquisition phase of the water maze were analysed using mixed design three-way ANOVA with 2 between-subjects variables (genotype × sex) and 1 within-subjects variable (period, day, trial, 15 min time period and day, respectively). Data on *Myg1* gene expression in response to restraint-stress in wild-type (+/+) mice were analysed by two-way independent-groups ANOVA (sex × stress). *Post hoc* comparisons between individual groups were performed by means of Newman-Keuls test.

4. Human *MYG1* gene polymorphisms and *MYG1* expression levels in healthy controls and vitiligo patients (Studies III and IV)

4.1. Characteristics of study participants

Unrelated Caucasian patients living in Estonia with a clear clinical diagnosis of vitiligo were enrolled at the Department of Dermatology, University of Tartu, Estonia. The control group consisted of healthy unrelated Caucasians without a personal or family history of vitiligo. The total number of individuals, sex distribution, age range and mean age of onset of vitiligo are shown in Table 3.

Table 3. Characteristics of study participants in *MYG1* expression and association studies.

		Total number of individuals	Females	Males	Age range (years)	Mean age of onset of vitiligo
***MYG1* expression (Study III)**	Vitiligo patients	32	22	10	22–75	30.4 years
	Healthy controls	27	17	10	21–67	
***MYG1* association (Study IV)**	Vitiligo patients	124	88	36	18–82	27.8 years
	Healthy controls	325	180	145	18–71	

The diagnosis of vitiligo was based on such clinical signs as characteristic skin depigmentation with typical localization and white colour on the skin lesions under Woods lamp. Two skin biopsies (Ø 4 mm) were obtained from the central part of involved and from non sun-exposed uninvolved skin from patients with vitiligo. One skin biopsy (Ø 4 mm) from non sun-exposed skin was taken from healthy control subjects. Based on the stage of progression of the disorder, patients were divided into two subgroups: patients with progressive vitiligo (active vitiligo) in which new areas of depigmentation or enlargement of depigmentation were observed during the previous 3 months (n=86 in association study; n=23 in expression study) and patients with stable vitiligo (inactive vitiligo) in which no new depigmentation or enlargement of depigmentation had been observed for more than 3 months (n=38 in association study; n=9 in expression study). Patients were also divided into four subgroups based on the extent of the skin lesion: less than 10% (n=65); 10–50% (n=37); 51–90% (n=15) and more than 90% (n=3). The Ethics Review Committee on Human Research of the University of Tartu approved the study and written informed consent was obtained from all participants.

4.2. Selection of *MYG1* polymorphisms

In human, *MYG1* gene (also known as C12orf10) is composed of seven exons that span 7.5 kb of genomic DNA in chromosomal region 12q13. According to NCBI's dbSNP database (www.ncbi.nlm.nih.gov/SNP/) *MYG1* gene contains 10 polymorphisms that are defined as single nucleotide polymorphisms (SNPs). None of the *MYG1* polymorphisms have been previously studied in association analysis, but two polymorphisms are potentially functional. SNP rs1465073 is located 119 bp upstream of *MYG1* translation start site (ATG) and we hereafter designate this SNP as *MYG1* promoter polymorphism (-119C/G). Another polymorphism involves nucleotides 11–12 (rs1534284–rs1534283) downstream from translation start ATG. As it becomes evident from EST and genomic DNA sequence analysis, these polymorphisms are not real SNPs because they always appear as couple AA or GC (Table 4) in human populations. These nucleotides are coding second and third position of amino acid four in the N-terminus of Myg1 protein (CAA and CGC, respectively) and the polymorphism is potentially functional, since it changes basic amino acid into polar and uncharged. CGC that is common in Caucasians codes for basic amino acid arginine (Arg); CAA that according to HapMap database (www.hapmap.org) is highly prevalent in Nigerian population is coding for polar and uncharged amino acid glutamine (Gln). We hereafter refer to rs1534283–rs1534284 polymorphism as Myg1 Arg4Gln.

Table 4. Analysis of rs1534283 and rs1534284 variants (Myg1 Arg4Gln) in human EST (mRNA) and genomic DNA sequences from NCBI and UCSC databases. First (ATG) and fourth (CAA or CGC) amino acids are underlined.

	Fourth amino acid	Accession	Sequence coding eight first amino acids from *MYG1* initial ATG	Source of mRNA
mRNA sequences	Gln	NM_021640	atgggacaccaattcctgcgcggc	
	Gln	CR626228.1	atgggacaccaattcctgcgcggc	fetal brain
	Gln	CR614390.1	atgggacaccaattcctgcgcggc	neuroblastoma
	Arg	BC051871	atgggacaccgcttcctgcgcggc	
	Arg	BC013956	ccgcttcctgcgcggc	
	Arg	AF289485	atgggacaccgcttcctgcgcggc	melanocytes
Genomic DNA	Gln	NT_029419	ATGGGACACCAATTCCTGCGCGGC	
	Gln	NC_000012	ATGGGACACCAATTCCTGCGCGGC	
	Gln	UCSC database	ATGGGACACCAATTCCTGCGCGGC	
	Arg	NW_925395.1	ATGGGACACCGCTTCCTGCGCGGC	

4.3. Detection and statistical analysis of human *MYG1* gene polymorphisms

DNA was extracted from blood samples by standard salting-out method. A panel of nine SNPs located inside and also up- and downstream of the *MYG1* gene was investigated. The ID numbers from NCBI's dbSNP database of *MYG1* SNPs that were examined in this study are listed on Figure 4. For the SNPs rs2694861, rs1465073, rs1534284, rs4759054, rs4325348, rs2279025, rs1545650, and 4759281 the Applied Biosystems (Foster City, California) SNPlex assay pool was used. The ZipCode probes were detected with an Applied Biosystems 3730 DNA Analyzer, and data interpretation was performed with the Applied Biosystems Genemapper v4.0 software (De La Vega *et al*, 2005). SNPbrowser version 3.5 was used for SNP selection and SNPlex assay pool design. Single marker association analysis was performed using the Haploview program (Barrett *et al*, 2005). Allele frequencies were investigated using the chi-square test. To evaluate deviation from the Hardy-Weinberg equilibrium, observed and expected genotype frequencies were compared by Fisher's exact test in the examined groups (cases and controls). Pairwise linkage disequilibrium (LD) between markers was estimated by a log-linear model and standardized D' characteristics were used to demonstrate the extent of disequilibrium. Since SNPlex assay was not functional for detecting rs1534284, we used direct sequencing for rs153484 and neighbour SNP rs1534283 in 54 subjects (24 vitiligo patients and 30 healthy controls) using ABI Genetic Analyzer 310 (Applied Biosystems, Foster City, CA, USA). The direct sequencing of incidental DNA samples was also performed for rs1465073 for verification of the SNPlex results.

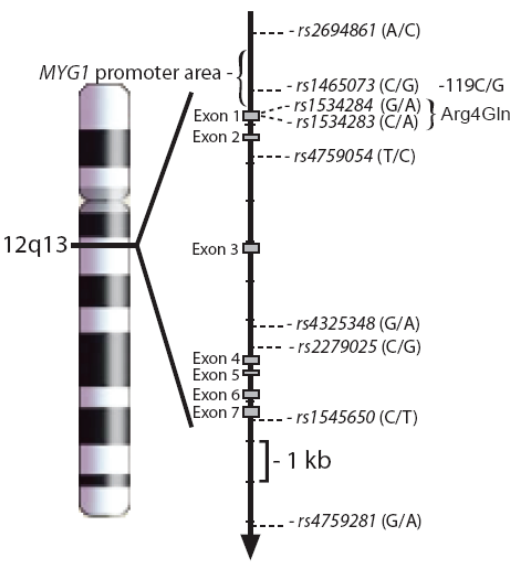

Figure 4. Genomic localization of single nucleotide polymorphisms (SNPs) in *MYG1* gene that were examined in this study. Relative positions of selected SNPs are represented by their ID number from NCBI's dbSNP database. Grey boxes are representing exons and arrow indicates the direction of transcription of *MYG1* gene.

For analysis of functional significance of promoter genotype in the regulation of gene expression, we used subjects (n=52) from whom both genomic DNA and skin biopsy was available. *MYG1* expression was measured from skin biopsy of 24 normal control subjects (15 female, 9 male) and 28 vitiligo patients (20 female, 8 male). The distribution of control group according to sex is shown in Table 5.

Table 5. Distribution of male and female control subjects divided according to the -119C/G promoter genotype.

Promoter genotype	**C/C** (low activity)	**C/G**	**G/G** (high activity)	**Total number of individuals**
Number of males	0	6	3	9
Number of females	5	9	1	15
Total	5	15	4	24

RESULTS

1. Expression of *Myg1*/*MYG1* mRNA

1.1. *Myg1*/*MYG1* mRNA expression in human and mouse tissues

We examined human *MYG1* and mouse *Myg1* expression in different tissues. The Northern analysis of human total RNA samples showed that all tissues express a 1.3 kb transcript corresponding to full length *MYG1* mRNA (Figure 5A). Both Northern and Affymetrix Genechip analyses of human tissue samples (Figure 5B) and quantitative real-time PCR (qRT-PCR) analysis of mouse tissues revealed persistently highest *MYG1* expression in testis. Above-average expression in human adult brain led to a more detailed analysis of mouse brain (Figure 5D) but *Myg1* expression measured in ten different brain areas of mouse appeared to be at the same level as in non-neural tissues. No significant inter-mouse differences were detected.

While the full-length transcript of *Myg1* is approximately 1.3 kb long, we also detected a short (693 bp) splice variant that is consistently expressed in all mouse tissues investigated (see Figure 6D, where 9 tissues are shown), albeit at an approximately 50-fold lower level (data not shown). This short splice variant lacks partly exon 4, completely exons 5 and 6 and partly the beginning of exon 9, but the reading frame is maintained. Another alternative mRNA variant was found in human testis. According to Northern hybridization there is around 1.5 kb strongly expressed alternative transcript present in the human testis besides 1.3 kb mRNA that is present in all tissues (Figure 6B). Expression of FLAG-tagged full length Myg1 in cell culture consistently resulted in two separate FLAG-immunoreactive bands on the Western blot membrane (Figure 6A). We hypothesized that the lower band could be a mitochondrial protein variant resulting from the cleavage of the mitochondrial signal after the protein has been transported into mitochondria (Cameron *et al*, 2005). However, it seems not to be the case because the size of the Myg1 protein without the mitochondrial signal (NoMito Myg1-FLAG) on the Western membrane does not correspond to the smaller fragment obtained after expressing the full length Myg1.

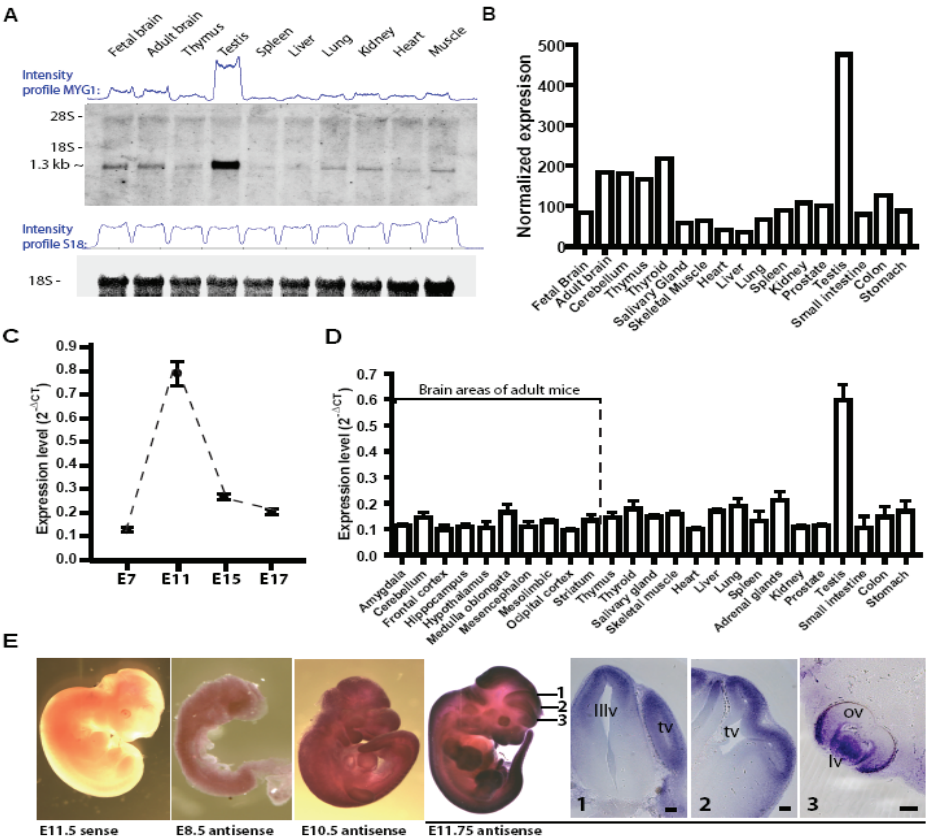

Figure 5. Human and mouse *MYG1*/*Myg1* mRNA expression levels in different tissues. (**A**) Northern blot analysis with *MYG1* cDNA probe in human total RNA samples identified a 1.3 kb target sequence. (**B**) *MYG1* mRNA expression level in human tissues according to Affymetrix GeneChip analysis. (**C**) *Myg1* mRNA level in mouse embryonic cDNA pool according to qRT-PCR analysis. (**D**) *Myg1* mRNA level in mouse tissues according to qRT-PCR analysis. (**E**) Whole mount RNA in situ hybridization analysis on mouse embryos. "E11.5 sense" represents negative control, hybridized with *Myg1* sense probe. Embryos E8.5, E10.5 and E11.75, hybridized with *Myg1* antisense probe, are illustrating gradual changes in *Myg1* expression. Levels of the transverse vibratome sections 1, 2 and 3, are shown on the E11.75 embryo, sectioning was performed from the same specimen. Abbreviations: IIIv: third ventricle; lv: lens vesicle; ov: optic vesicle; tv: telencephalic vesicle. Scale bars 100 µm.

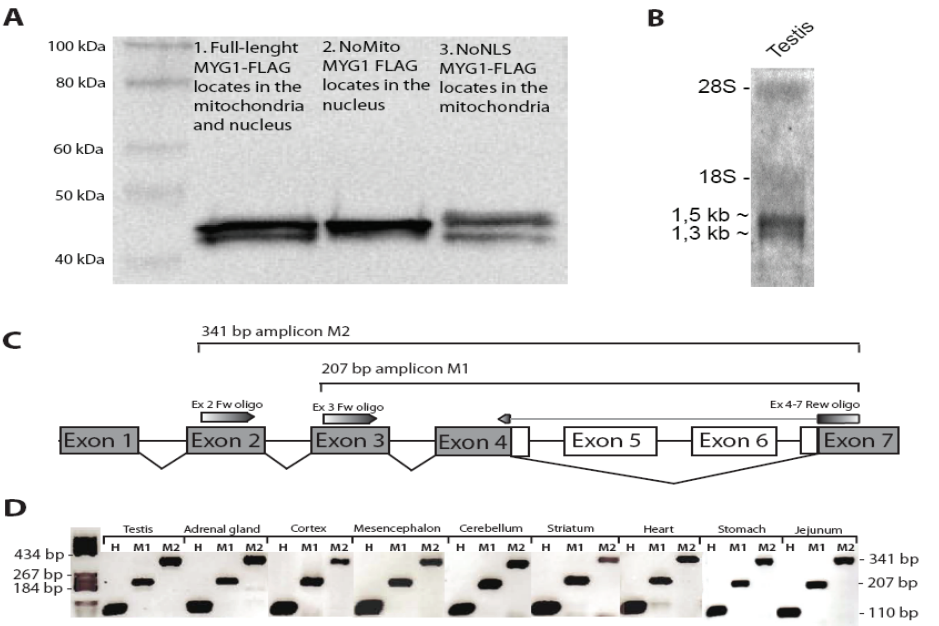

Figure 6. Alternative forms of Myg1 mRNA and protein. (**A**) Expression of FLAG-tagged full length Myg1 and FLAG-tagged Myg1 with either only nuclear or only mitochondrial localization resulted in different FLAG-immunoreactive bands on western blot. (**B**) Northern blot reveals alternative 1.5 kb *MYG1* transcript in human testis besides 1.3 kb *MYG1* mRNA that is present in all tissues. (**C**) Schematic structure of the short alternative splice variant and location of primers that were used for its detection. (**D**) A short (693 bp) alternative splice variant was consistently expressed in all mouse tissues investigated.

1.2. *Myg1* expression during embryonic development

During development we found a more than five-fold upregulation of *Myg1* during a period from E7 to E11. By embryonic stages E15 and E17 expression level had decreased but remained higher than in stage E7 (Figure 5C). Whole mount *in situ* RNA hybridization showed that at E8.5 (Figure 5E; E8.5 antisense) *Myg1* expression is widespread whereas from E10.5 (Figure 5E; E10.5 antisense) a more differential expression pattern begins to appear. Further analysis revealed that upregulation of *Myg1* around E11.75 is related to a specific expression pattern that is the most intensive in the developing forebrain, midbrain, limb buds and tail region. Vibratome sectioning of E11.75 embryo demonstrated that *Myg1* expression was the strongest in the ectoderm-derived areas as illustrated by pictures of the developing neuroepithelium (Figure 5E; sections 1 and 2). Strong expression was also detected in the developing eye, both in the lens vesicle as well as in the outermost region of the optic vesicle (Figure 5E; section 3).

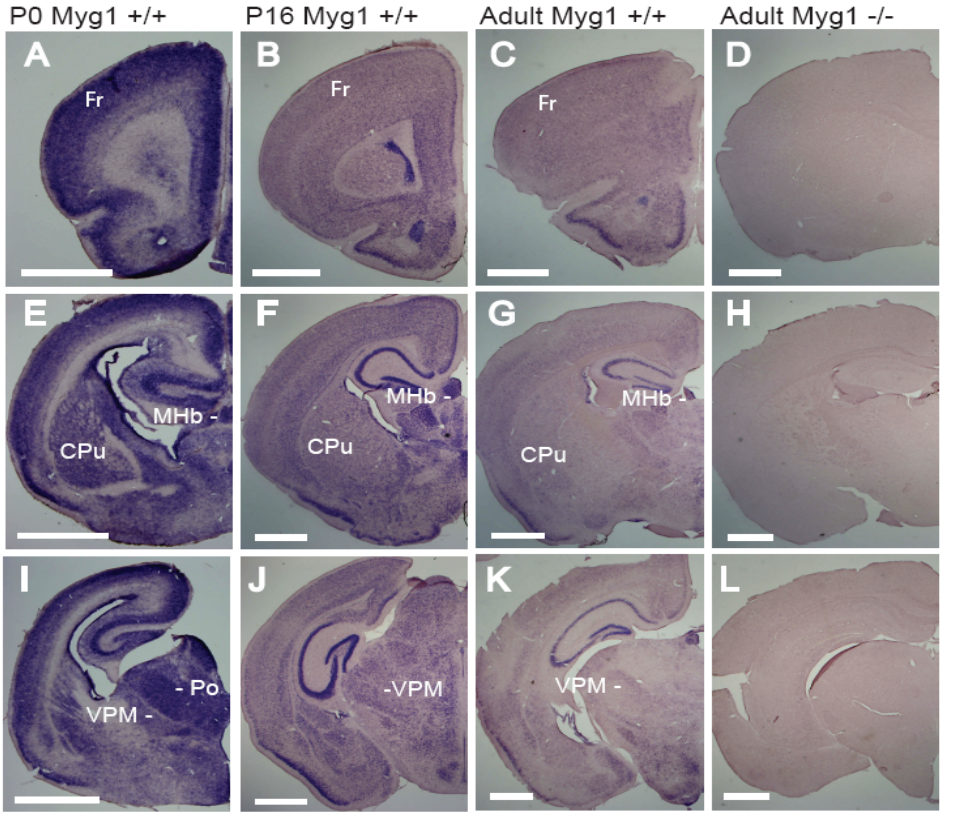

Figure 7. Developmental decline of *Myg1* expression in the mouse brain and lack of *Myg1* transcript in the brain of adult *Myg1* (-/-) mouse. *In situ* RNA hybridisation with full-length *Myg1* antisense riboprobe on 40 µm coronal cryoslices from forebrain (**A-D**) at the level of rostral hippocampus and caudate putamen (striatum) (**E-H**) and at the level of posterior thalamic nuclei (**I-L**) in mice at three different developmental stages (P0, P16, and adult P60). Comparable brain slices from adult *Myg* (-/-) mouse (**D**, **H**, **L**) indicate absence of *Myg1* transcript in adult *Myg1* (-/-) brain. Abbreviations: Fr: frontal cortex; CPu: caudate putamen; MHb: medial habenular nucleus; VPM: ventral posteromedial thalamic nucleus; Po: Posterior thalamic nuclear group. Scale bars represent 1 mm.

1.3. *Myg1* expression in postnatal and adult mouse brain

In the postnatal brain the expression of *Myg1* was ubiquitous (Figures 7, 8). While the spatial expression of *Myg1* was similar both in the developing and adult brain, remarkable difference was observed in its expression level. Namely, the signal of the expression of *Myg1* was stronger at birth (Figures 7A, 7E, 7I), fading gradually at subsequent stages (compare with Figures 7B, 7F, 7J), and achieving relatively moderate adult level (Figures 7C, 7G, 7K) by the third postnatal week (not shown). We confirmed these results also by RT-PCR,

which revealed 2.7-fold mRNA level differences between newborn forebrain and adult forebrain structures (data not shown). In order to confirm the specificity of the broad hybridization signal of *Myg1* antisense RNA probe, the *Myg1* mutant (-/-) brain sections were used as negative control; as expected, no signal was seen in the mutant brain (Figures 7D, 7H, 7L). In the adult brain, the hybridisation signal appeared strongest in the ependymal layer of the ventricular system (Figures 7B, 8), in the hippocampal formation, medial habenular nucleus, subfornical organ, hypothalamic nuclei, nucleus arcuatus and cerebellum (Figures 7F, 7G, 7J, 7K, 8, and data not shown).

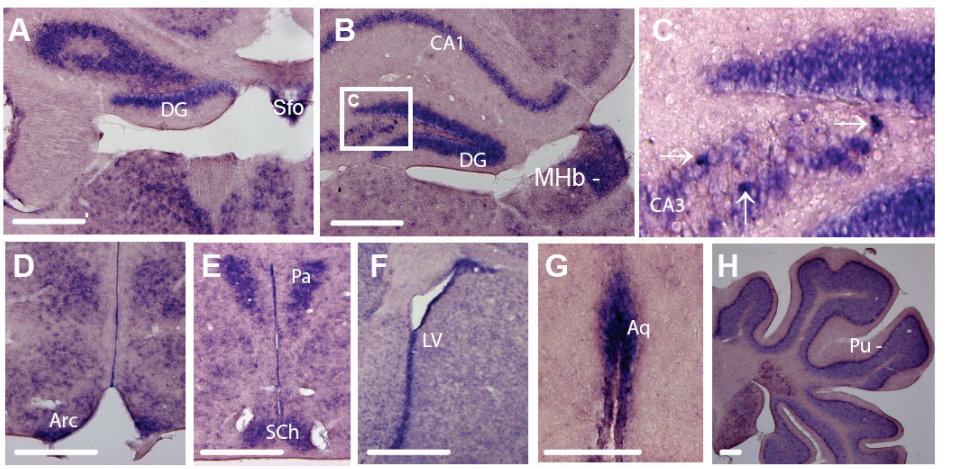

Figure 8. *Myg1* expression in adult mouse brain by *in situ* RNA hybridization. *In situ* RNA hybridisation with full-length *Myg1* antisense riboprobe on 40 µm coronal cryoslices from (**A**-**B**) adult rostral hippocampal area; (**C**) magnification of distinct cells with intensive Myg1 signal from B; (**D**) arcuate hypothalamic nucleus; (**E**) paraventricular and suprachiasmatic hypothalamic nuclei; (**F**) lateral ventricle; (**G**) aqueduct and (**H**) cerebellum. Abbreviations: DG: dentate gyrus; Sfo: subfornical organ; MHb: medial habenular nucleus; Arc: arcuate hypothalamic nucleus; Pa: paraventricular hypothelemic nucleus; SCh: suprachiasmatic nucleus; LV: lateral ventricle; Aq: aqueduct; Pu: purkinje cell layer of cerebellum. Scale bars represent 0.5 mm.

2. Cell culture experiments

2.1. Subcellular localization of Myg1 protein

To characterize the subcellular localization of Myg1, we expressed FLAG- and YFP-tagged Myg1 in HeLa cells. Preliminary experiments indicated that N-terminal fusion of Myg1 protein with YFP resulted in exclusively nuclear localization, whereas C-terminal fusion produced a more widespread distribution. We hypothesized that this discrepancy resulted from the masking of endogenous N-terminal signal sequences by the N-terminal tag and, therefore, all consequent experiments were carried out with C-terminally tagged Myg1 constructs.

Both C-terminally FLAG- and YFP-tagged Myg1 localized to the nucleus and mitochondria (Figure 9C, Full-length Myg1). To predict putative signal peptides in Myg1, we used PSORT II software (Nakai & Horton, 1999), which identified a conserved Pat7 type nuclear localization signal (NLS) around amino acid 35 and a possible cleavage site between aminoacids 20 and 21 in several mammalian species (Figure 9A). We hypothesized, that the putative cleavage site could designate the presence of an N-terminal leader sequence, characteristic for proteins destined to the mitochondria (Cameron *et al*, 2005). Consistent with our expectation, deletion of the first 20 amino acids of Myg1 protein (Figure 9B, NoMTS Myg1) produced exclusively nuclear localization pattern (Figure 9C, NoMTS Myg1), deletion of seven amino acids from position 33–39 (Figure 9B, NoNLS Myg1) produced exclusively mitochondrial localization (Figure 9C, NoNLS Myg1), and deletion of the first 39 amino acids (Figure 9B, NoSignal Myg1) produced a homogenous distribution characteristic of cytoplasmic localization (Figure 9C, NoSignal Myg1). Based on the above results, we concluded that Myg1 protein harbors a mitochondrial targeting sequence in the region between amino acids 1–20 and a nuclear localization signal in the region between amino acids 33–39 with no other subcellular localization signals being detectable. We also tested the possibility that Myg1 localization is dependent on the cell cycle. HeLa cells, arrested in S-phase by double-thymidine method, were released into a synchronous cell cycle and sampled every 2 hours during the whole cell cycle. Both in case of YFP- and FLAG-tagged Myg1 protein, Myg1 distribution in the nucleus and mitochondria was not dependent on the phase of the cell cycle. Comparison of subcellular localization signals of five mammalian species is shown in Figure 9A. Expressing mouse Myg1 protein in human HeLa cells revealed that mouse Myg1 is also distributed in the nucleus and mitochondria (Figure 10), which indicates high functional conservation of these signals.

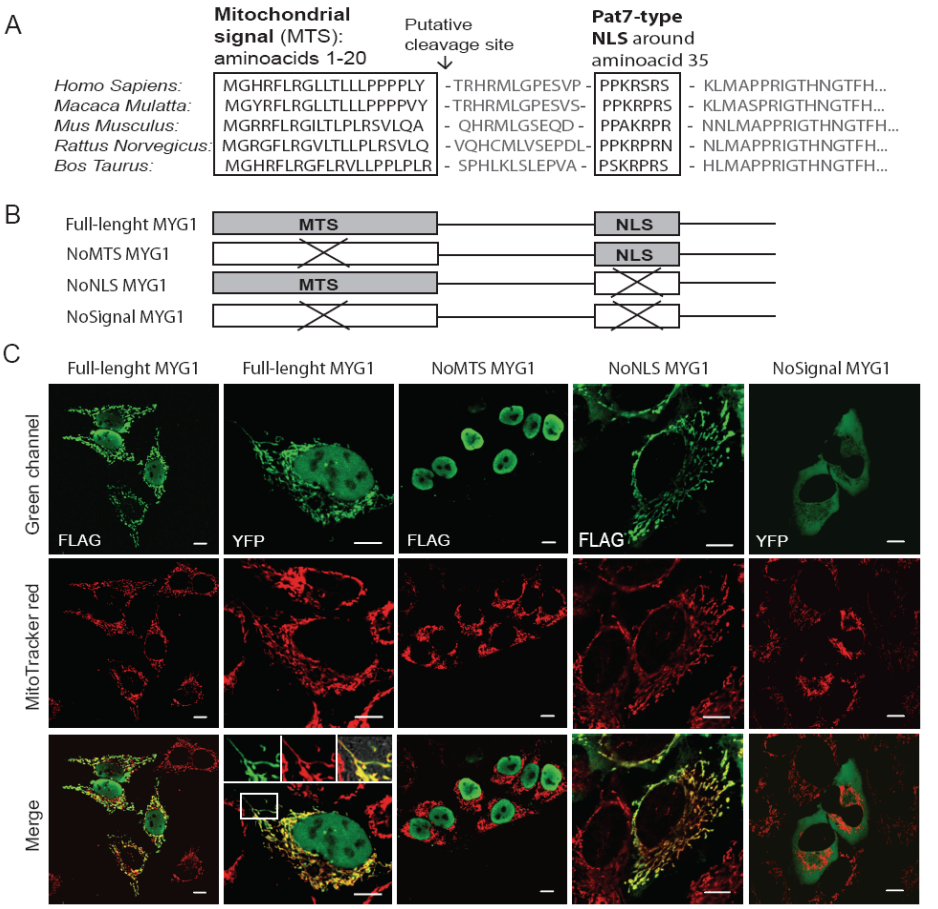

Figure 9. Subcellular targeting signal sequences in the N-terminus of Myg1 protein. (**A**) Location of signal sequences in Myg1 orthologues in different mammalian species. (**B**) Schematic design of mutant cDNA constructs with signal deletions. (**C**) Subcellular localization of YFP and FLAG fusion constructs of full-length Myg1 protein and cellular targeting signal deletion mutants. Scale bars represent 10 μm.

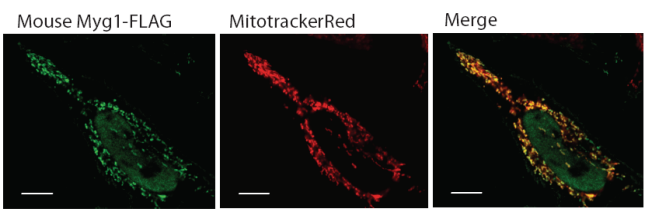

Figure 10. Subcellular localization of YFP-tagged mouse Myg1 protein.

The secondary structure prediction database SOSUI (Hirokawa *et al*, 1998) indicates that human Myg1 is a soluble protein with an average hydrophobicity of –0.4.

In order to examine the spatiotemporal dynamics of Myg1, a bleaching experiment was performed in living cells transformed with YFP-tagged Myg1 protein. A distinct area of fluorescence was photo-bleached both in the mitochondria and nucleus. The bleached area in the nucleus was directionally filled with fluorescence from the neighbouring unbleached areas indicating fast diffusion of Myg1 in the nucleus (Figure 11A). The recovery of fluorescence in mitochondria was not uniformly interpretable; therefore the precise properties of Myg1 in the mitochondria remain to be elucidated in future studies. We also investigated the possibility that there was active shuttling of Myg1 protein between the nucleus and mitochondria by bleaching only the nucleus or only the mitochondria in cells where protein synthesis had been blocked by cyclohexamide (Figure 11B: Before bleach). During the 40 min follow up period, no transposition of fluorescence from the unbleached nucleus to the bleached mitochondria or from the unbleached mitochondria to the bleached nucleus was observed (Figure 11B).

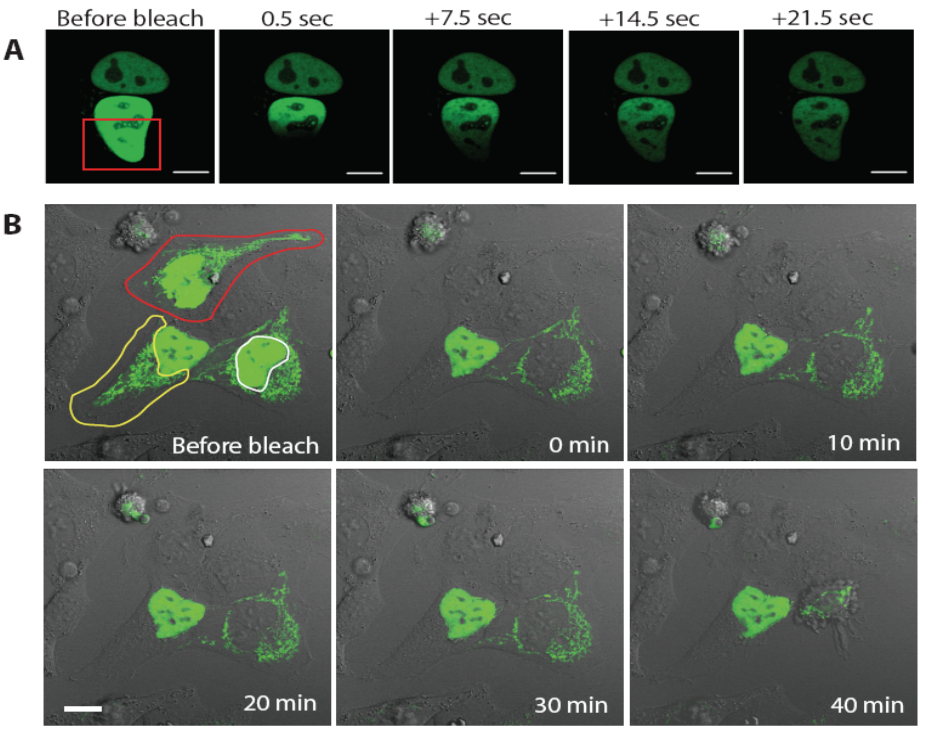

Figure 11. Photo-bleaching experiments to investigate dynamics of YFP-tagged Myg1 inside nucleus and between nucleus and mitochondria. (**A**) Photo-bleaching series of YFP-Myg1 in the nucleus. Red square depict area that was bleached thereafter; the cells were followed for 21.5 seconds. (**B**) Photo-bleaching series following possible shuttling of Myg1 between the nucleus and mitochondria in HeLA cells treated with the protein synthesis inhibitor cyclohexamide. Red, yellow and white lines depict areas that were bleached thereafter: the whole cell, only mitochondria or only nucleus, accordingly. The cells were followed for 40 minutes. Scale bars represent 10 µm.

2.2. Myg1 protein interactions

Previously, two independent studies have reported a physical interaction of Myg1 with Heat shock protein 90 (Hsp90) (Falsone *et al*, 2005; Millson *et al*, 2005). In order to confirm these results and to identify new potential interaction partners, we immunoprecipitated C-terminally FLAG-tagged Myg1 from HeLa cells. Silver staining revealed a strong band of approximately 42 kDa (Figure 12A) that corresponded to the predicted molecular weight of Myg1, but no unique protein bands compared with FLAG-Erg1 negative control (Figure 12A). Additionally, western blot analyses of the immunoprecipitated samples were negative for Hsp90 immunoreactivity (Figure 12B). Thus, we could not identify any Myg1 co-precipitated proteins. One of the many functions of Hsp90 is transportation of proteins into the mitochondria (Ellis, 2003). We therefore tested the possibility that the subcellular localization of Myg1 was dependent on Hsp90 activity by using Hsp90 inhibitor geldanamycine. At doses (1 µM in cell medium) that are known to inhibit Hsp90 activity (Picard, 2006), Myg1 protein was still transported both into the mitochondria and nucleus in HeLa cells (data not shown).

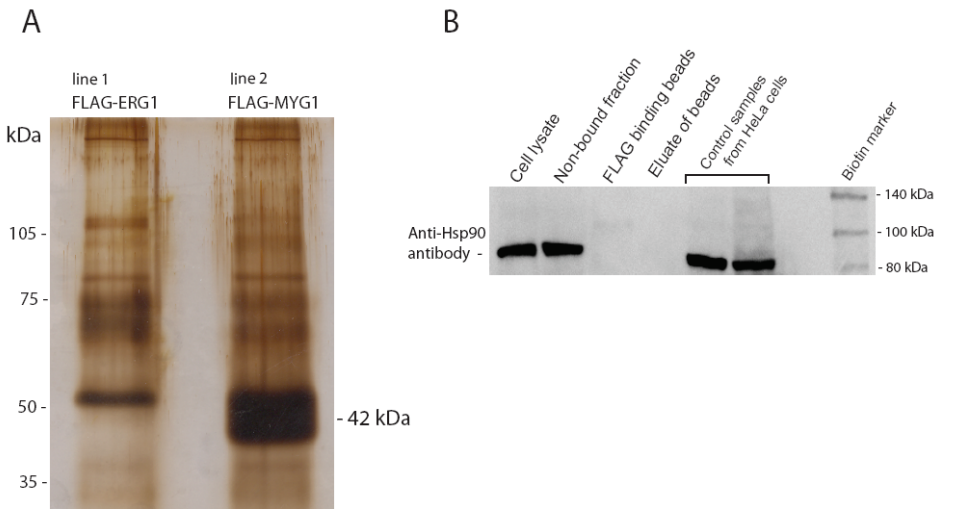

Figure 12. Immunoprecipitation experiment. (**A**) Immunoprecipitated samples on silver staining gel: FLAG-ERG (line 1) and FLAG-Myg1 (line 2). (**B**) Western blot analysis demonstrating Hsp90 immunoreactivity in different phases of immunoprecipitation experiment. Hsp90 immunoreactivity is present in cell lysate and in fraction that is not bound to anti-FLAG beads. Hsp90 signal is lost in the solution of FLAG1 binding beads and in the eluate of beads. Two additional control-samples that were included are positive for Hsp90 signal.

2.3. *MYG1* knockdown and global expression profiling

To identify molecular pathways related to Myg1 function, we performed a siRNA (short interfering RNAs) induced knockdown of *MYG1* mRNA in HeLa cells followed by global expression profiling with the Affymetrix GeneChip U133 Plus 2.0 Array, that covers most of the coding human trascriptome. We used two different siRNAs, both of which induced an approximately 10-fold reduction in *MYG1* mRNA relative to mock-treated or scrambled siRNA-treated cells, without producing any obvious changes in the appearance of the cells. The list of 39 probesets corresponding to 30 different transcripts with at least 1.5-fold significant ($p<0.01$) change in expression levels after treatment with both siRNAs is shown in Table 6. Functional clustering according to Gene Ontology (GO) database (www.geneontology.org) enabled us to divide 22 transcripts into 5 functional groups. The function of 8 transcripts is currently unknown. Functional clusters and their numerical GO references are: "1. Nucleus/ Nucleic acid binding (GO:0005634)"; "2. Immune response (GO:0006955)"; "3. Developmental process (GO:0032502)"; "4. Metabolic process (GO: 0008152)" and "5. Establishment of localization/ Transport (GO:0051234)".

Table 6. Significantly changed genes after *MYG1* knockdown. The list of 39 probesets corresponding to 30 different transcripts with at least 1.5-fold significant ($p<0.01$) up- or downregulation after treatment with both siRNAs. Titles that separate six gene groups present names of functional gene clusters according Gene Ontology (GO) database (www.geneontology.org); GO reference ID numbers are given in brackets.

		siRNA 1		siRNA 3		Combined	
Accession	**Gene**	**fold change**	**p-value**	**fold change**	**p-value**	**fold change**	**p-value**
1. Nucleus/Nucleic acid binding (GO:0005634)							
AI638279	Bromodomain and WD repeat domain containing 1	**–1.7**	0.001	**–2.12**	0.001	**–1.88**	0.000
AJ224167	SNHG4 Small nucleolar RNA host gene	**–2.13**	0.006	**–1.67**	0.009	**–1.88**	0.001
BG230758	Mediator of RNA polymerase II transcription, subunit 8 homolog	**1.66**	0.008	**1.64**	0.002	**1.65**	0.000
BG230758	Mediator of RNA polymerase II transcription, subunit 8 homolog	**1.52**	0.006	**1.5**	0.005	**1.51**	0.000
CA442932	POLR1B: polymerase (RNA) I polypeptide B, 128kDa	**–1.67**	0.000	**–1.65**	0.000	**–1.66**	0.000
AI754423	VGLL3: vestigial like 3 (Drosophila)	**–2.04**	0.003	**–1.62**	0.007	**–1.81**	0.002
2. Immune response (GO:0006955)							
BF983379	CD59 molecule, complement regulatory protein	**1.6**	0.003	**1.64**	0.001	**1.62**	0.000
X16447	CD59 molecule, complement regulatory protein	**1.76**	0.001	**1.58**	0.001	**1.67**	0.000
NM_000611	CD59 molecule, complement regulatory protein	**1.78**	0.003	**1.54**	0.001	**1.66**	0.000
BC002666	GBP1: guanylate binding protein 1, interferon-inducible, 67kDa	**3.48**	0.000	**2.34**	0.002	**2.91**	0.001

Accession	Gene	siRNA 1		siRNA 3		Combined	
		fold change	p-value	fold change	p-value	fold change	p-value
AW014593	GBP1: guanylate binding protein 1, interferon-inducible, 67kDa	**3.08**	0.004	**2.09**	0.000	**2.59**	0.001
NM_004120	GBP2: guanylate binding protein 2, interferon-inducible	**2.1**	0.002	**2.07**	0.001	**2.08**	0.002
NM_025217	ULBP2: UL16 binding protein 2	**1.86**	0.008	**1.85**	0.006	**1.85**	0.000
3. Developmental process (GO:0032502)							
AC004010	AMIGO2: adhesion molecule with Ig-like domain 2	**–1.71**	0.001	**–1.99**	0.000	**–1.84**	0.000
M73554	CCND1: cyclin D1	**–1.71**	0.006	**–1.56**	0.005	**–1.63**	0.006
AF138300	DCN: decorin	**2.06**	0.001	**2.42**	0.001	**2.24**	0.000
AF138303	DCN: decorin	**1.96**	0.001	**2.28**	0.008	**2.12**	0.000
AF138302	DCN: decorin	**1.91**	0.001	**2.38**	0.000	**2.15**	0.000
M27968	FGF2: fibroblast growth factor 2 (basic)	**–1.56**	0.005	**–1.55**	0.003	**–1.55**	0.000
AA634272	Signal transducer and activator of transcription 3	**1.61**	0.000	**1.77**	0.000	**1.69**	0.000
BC000627	Signal transducer and activator of transcription 3	**1.54**	0.007	**1.83**	0.000	**1.69**	0.000
4. Metabolic process (GO:0008152)							
AI922855	CPE: carboxypeptidase E	**1.5**	0.009	**1.77**	0.005	**1.63**	0.000
U84246	NEU1: sialidase 1 (lysosomal sialidase)	**2.46**	0.001	**1.92**	0.004	**2.19**	0.000
J05594	Prostaglandin dehydrogenase 1	**1.83**	0.006	**1.56**	0.005	**1.7**	0.000
AA722878	PRR6: proline rich 6	**–1.63**	0.008	**–1.61**	0.000	**–1.62**	0.000
5. Establishment of localization/ Transport (GO:0051234)							
BE502030	RAB27A: RAB27A, member RAS oncogene family	**1.61**	0.008	**1.71**	0.009	**1.66**	0.000
U38654	RAB27A: RAB27A, member RAS oncogene family	**2.03**	0.001	**1.77**	0.003	**1.9**	0.000
BE535746	REEP1: receptor accessory protein 1	**1.55**	0.003	**1.56**	0.000	**1.56**	0.000
AW235061	Solute carrier family 1 (glutamate transporter), member 1	**1.67**	0.001	**1.56**	0.002	**1.61**	0.001
AF047033	Solute carrier family 4, sodium bicarbonate cotransporter, member 7	**–1.61**	0.003	**–2.3**	0.003	**–1.9**	0.000
6. Unknown							
U90548	Butyrophilin, subfamily 3, member A3	**1.75**	0.005	**2.03**	0.000	**1.89**	0.000
BF002121	CDNA clone IMAGE:4816860	**–1.53**	0.008	**–2.15**	0.001	**–1.79**	0.000
AF070569	Chromosome 17 open reading frame 91	**1.66**	0.004	**1.65**	0.006	**1.66**	0.000
AI300571	Full-length cDNA clone CS0DJ002YF02 of T cells	**1.86**	0.002	**1.69**	0.009	**1.78**	0.001
AI709406	Homo sapiens, clone IMAGE:5547644, mRNA	**–1.61**	0.005	**–1.64**	0.003	**–1.63**	0.000
AI870473	LOC221710: Hypothetical protein LOC221710	**–2.05**	0.008	**–1.58**	0.010	**–1.78**	0.002
NM_007083	Nudix (nucleoside diphosphate linked moiety X)-type motif 6	**1.59**	0.004	**1.74**	0.006	**1.66**	0.000
AI580268	Nudix (nucleoside diphosphate linked moiety X)-type motif 6	**1.54**	0.007	**1.78**	0.008	**1.66**	0.000
BG288115	TMEM65: transmembrane protein 65	**–1.99**	0.000	**–2.19**	0.000	**–2.09**	0.000

3. Phenotyping *Myg1*-deficient mice

3.1. General characteristics of *Myg1*-deficient mice

Successful deletion of *Myg1* gene was confirmed by absence of *Myg1* mRNA specific signal in *Myg1*-deficient (-/-) embryos (Figure 3C) and in brain sections from *Myg1*-deficient adult mice (Figure 7). *In situ* RNA hybridization on whole mouse embryos *Gad1* RNA probe that was used as a positive control revealed similar patterning of the signal in both wild-type and *Myg1* mutant (-/-) mice (data not shown). We could not detect major aberrations during the embryonic development of *Myg1* mutant (-/-) mouse (Figure 3C). As a result of homologous recombination LacZ-NEO cassette was inserted immediately after the *Myg1* promoter and LacZ transgene replaced all seven exons of *Myg1* gene. Therefore we expected that *Myg1* promoter triggers promoter-specific β-galactosidase staining similarly with *Wfs1*-deficient mice described by Luuk *et al* (2008). However, X-Gal staining of *Myg1* (-/-) tissues was negative for β-galactosidase (data not shown). Sequencing genomic DNA around *Myg1* gene locus in *Myg1* (-/-) mouse revealed that insertion of BamHI restriction site (GGATCC) immediately after mouse *Myg1* promoter (ends with AT-nucleotides) introduced a new ATG-codon 20 bp before ATG for β-galactosidase. Therefore endogenous *Myg1* promoter triggers expression of a six-aminoacid peptide that is terminated by premature stop-codon TGA that is partly overlapping with non-functional ATG-codon for β-galactosidase. In conclusion, mouse *Myg1* promoter was completely invalidated after targeted disruption event and no *Myg1* or β-galactosidase transcripts could not be triggered. Additionally, sequencing genomic DNA around *Myg1* gene in *Myg1* (-/-) mouse confirmed that no mutations were unpurposely introduced inside coding regions of closest upstream neighbour gene *Pfdn5* (a gene that was overlapped with the 5' genomic arm) and closest downstream neighbour gene *Aaas* (a gene that was overlapped with the 3' genomic arm of *Myg1*-targeting construct).

3.2. First phenotyping battery

3.2.1. Elevated plus-maze test. Significant effect of genotype ($F(1,91)=6.76$ $p<0.05$) and genotype × sex interaction ($F(1,91)=4.50$ $p<0.05$) was observed in the stretched-attend postures. Significant effect of sex was observed in the % open entries ($F(1,91)=10.16$ $p<0.005$), % open arm time ($F(1,91)=6.54$ $p<0.05$), number of head-dippings ($F(1,91)=5.33$ $p<0.05$) and % unprotected head-dippings ($F(1,91)=5.10$ $p<0.05$). Although male mutant mice (-/-) were less anxious as indicated by the lower number of SAPs ($p<0.01$) and the higher % of unprotected head-dippings ($p<0.05$) when compared to their wild-type littermates (Figure 13D, 13F), the main behavioural difference was revealed between male and female wild-type (+/+) mice. Compared to their male counterparts female wild-type mice showed significantly higher % open entries ($p<0.05$), higher % open arm time ($p<0.05$), lower number of SAPs ($p<0.05$), higher num-

ber of head-dippings ($p<0.05$) as well as higher % unprotected head-dippings ($p<0.05$). Such difference suggests lower anxiety level in female wild-type (+/+) mice. A similar sex-related behavioural difference was absent in mice lacking *Myg1* gene (-/-).

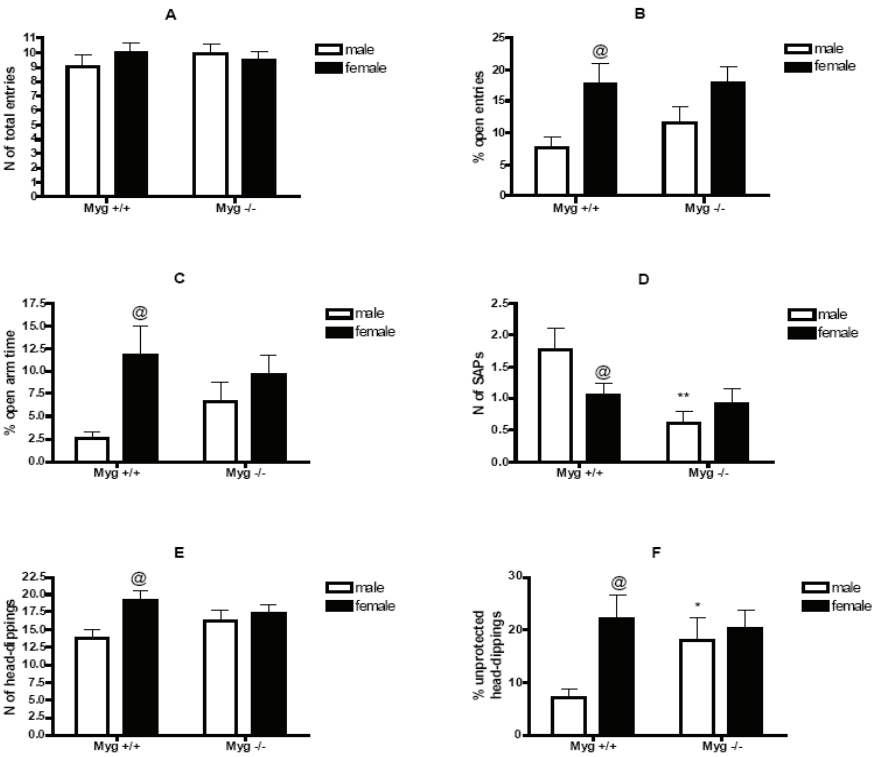

Figure 13. Elevated plus-maze test in mice lacking *Myg1* (-/-) and their wild-type (+/+) littermates. (**A**) total number of arm entries; (**B**) % open entries; (**C**) % open arm time; (**D**) number of stretched-attend postures (SAPs); (**E**) number of head-dippings; (**F**) % unprotected head-dippings. * $p<0.05$, ** $p<0.01$: mice lacking *Myg1* (-/-) compared to their wild-type littermates (+/+) of the same sex; $^{@}$ $p<0.05$: female mice compared to male mice of the same genotype.

3.2.2. Locomotor activity and habituation. Locomotor activity was significantly affected by both sex and genotype × sex interaction: distance (sex: ($F(1,92)=4.43$ $p<0.05$); genotype × sex interaction ($F(1,92)=7.52$ $p<0.01$)), number of rearings (sex: ($F(1,92)=4.01$ $p<0.05$); genotype × sex interaction ($F(1,92)=4.67$ $p<0.05$), number of corner entries (sex: ($F(1,92)=9.59$ $p<0.005$); genotype × sex interaction ($F(1,92)=4.87$ $p<0.05$)), % center distance (sex: ($F(1,92)=8.32$ $p<0.005$); genotype × sex interaction ($F(1,92)=5.85$ $p<0.05$). Exceptionally, % center distance was significantly affected by genotype only as

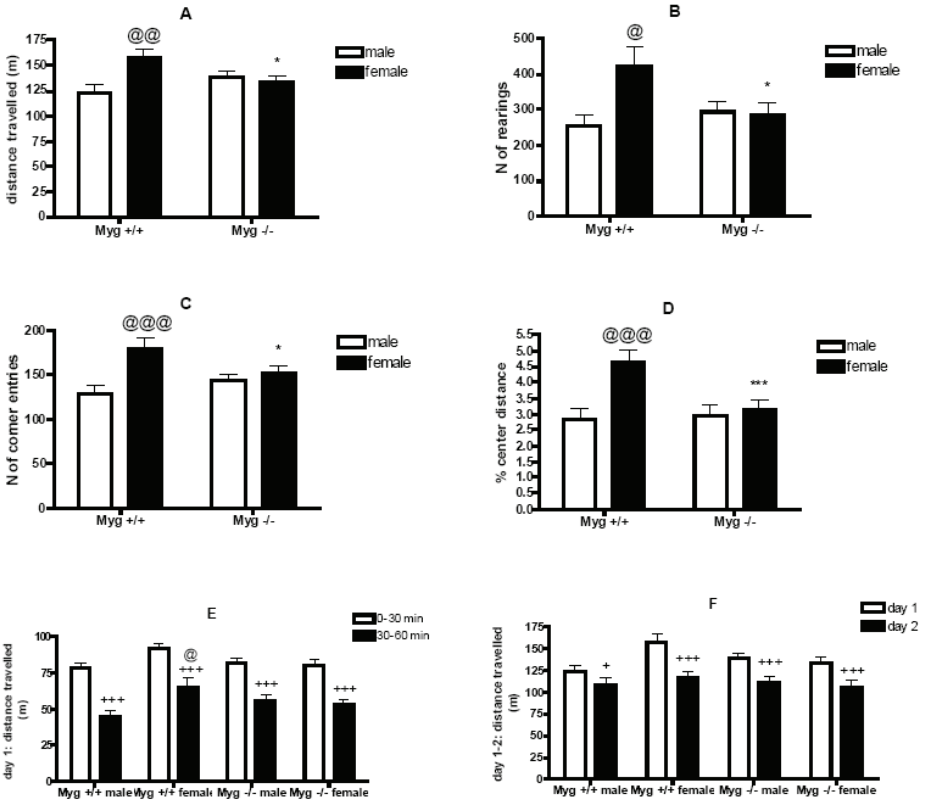

Figure 14. Locomotor activity test and habituation in mice lacking *Myg1* (-/-) and their wild-type (+/+) littermates. (**A**) distance travelled; (**B**) number of rearings; (**C**) number of corner entries; (**D**) % centre distance; (**E**) distance travelled during the first and the second 30 min period of testing on day 1 (within-trial habituation); (**F**) distance travelled during 60 min testing on two consecutive days (between-trial habituation). * $p<0.05$, *** $p<0.005$: mice lacking *Myg1* (-/-) compared to their wild-type littermates (+/+) of the same sex; $^{@}$ $p<0.05$, $^{@@}$ $p<0.01$, $^{@@@}$ $p<0.005$: female mice compared to male mice of the same genotype (and during the same period in panel **E**); $^{+}$ $p<0.05$, $^{+++}$ $p<0.005$: comparison between distances travelled during different periods (panel **E**) or days (panel **F**) of respective group.

well ($F(1,92)=4.48$ $p<0.05$). Female wild-type mice (+/+) were significantly more active than female mutant mice (-/-) in terms of distance travelled ($p<0.05$), number of rearings ($p<0.05$) and number of corner entries ($p<0.05$) (Figure 14A–C). Also, female wild-type mice travelled significantly larger proportion of distance in the center of the arena as compared to their female mutant littermates ($p<0.005$) (Figure 14D), suggesting higher level of trait anxiety in female mice lacking *Myg1* (-/-). It should be noted, that in wild-type (+/+), but not *Myg1*-deficient mice (-/-), significant sex-dependent behavioural differences were observed with females being significantly more active (distance: $p<0.01$; number of rearings: $p<0.05$; number of corner entries: $p<0.005$) and less anxious (% center distance: $p<0.005$). Within-trial habituation was significantly influenced by period of exposure ($F(1,92)=290.13$ $p<0.005$), sex ($F(1,92)=4.39$ $p<0.05$) and genotype × sex interaction ($F(1,92)=7.49$ $p<0.01$), whereas between-trial habituation was affected by day ($F(1,92)=99.06$ $p<0.05$), day × sex interaction ($F(1,92)=5.21$ $p<0.05$) and day × genotype × sex interaction ($F(1,92)=4.83$ $p<0.05$). Both within- and between-trial habituation, defined as a significant reduction in distance travelled over time, were evident in all groups (Figure 14E-F). However, in female wild-type mice (+/+) locomotor activity remained significantly higher during the second period of the first exposure on day 1 when compared to male wild-type mice ($p<0.05$) (Figure 14E). Such sex-specific difference was, again, not observed in mice lacking *Myg1* gene.

3.2.3. Hot plate test. No differences between genotypes or sexes were found in either latency to shake or lick hind paw, or latency to jump in the hot plate test (Figure 15A, 15B).

3.2.4. Social interaction test. Significant effects of sex ($F(1,60)=16.16$ $p<0.005$) and genotype × sex interaction ($F(1,60)=5.06$ $p<0.05$) were revealed. Male mutant (-/-) mice spent substantially more time in active social interaction than male wild-type (+/+) mice ($p<0.05$) and female mutant (-/-) mice ($P<0.005$) (Figure 15C). No behavioural difference was observed between male and female wild-type (+/+) mice.

3.2.5. Forced swim test. Immobility time in the forced swim test was influenced by neither genotype nor sex (Figure 15D).

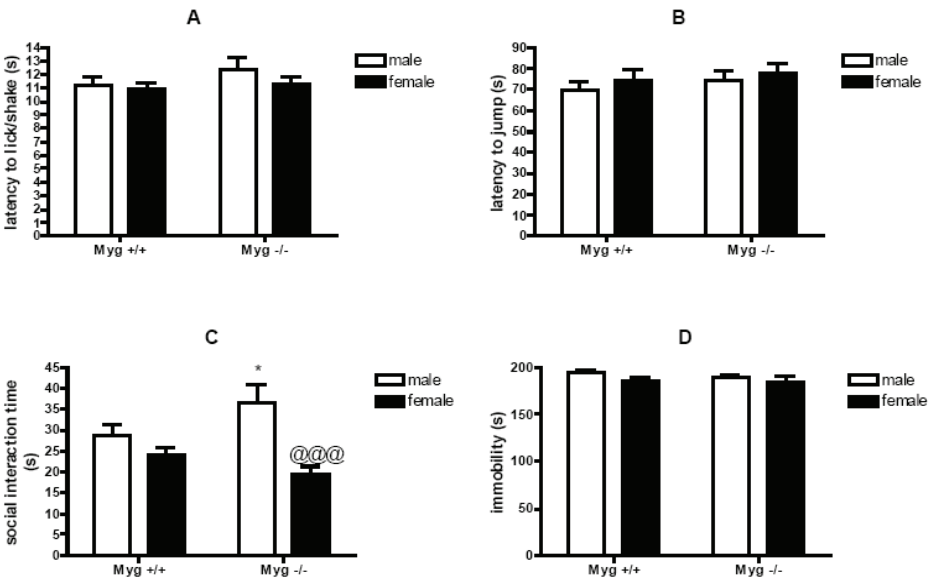

Figure 15. Hot plate test, social interaction and forced swim test. (**A**) hot plate test: latency to lick or shake hind paw; (**B**) hot plate test: latency to jump; (**C**) social interaction time; (**D**) forced swim test: immobility time. * $p<0.05$: mice lacking *Myg1* (-/-) compared to their wild-type littermates of the same sex; @@@ $p<0.005$: female mice compared to male mice of the same genotype.

3.2.6. Rota-rod. Both the latency to fall or revolve, and the number of falls or revolutions were significantly affected by trial ($F(2,184)=80.14$ $p<0.005$, and $F(2,184)=85.01$ $p<0.005$, respectively) and sex ($F(1,92)=5.58$ $p<0.05$, and $F(1,92)=7.55$ $p<0.01$, respectively). Rota-rod performance in mice lacking *Myg1* (-/-) was comparable to that of wild-type mice, and substantial improvement of performance across trials (procedural learning) was evident in all groups (Figure 16A, 16B).

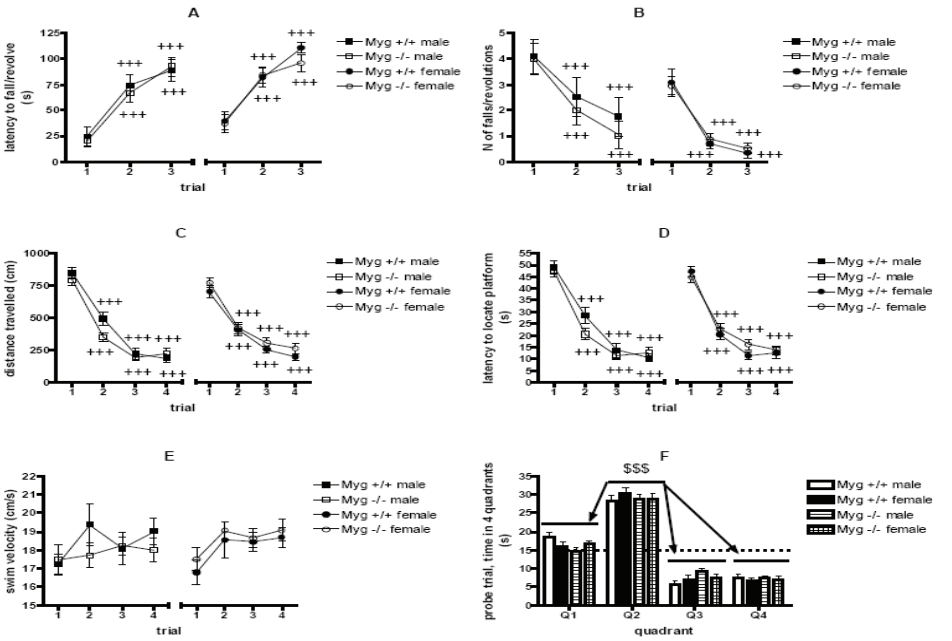

Figure 16. Rota-rod and water maze. (**A**) Rota-rod: latency to fall or revolve; (**B**) rota-rod: number of falls or revolutions; (**C**) water maze: distance travelled; (**D**) water maze: latency to locate platform; (**E**) water maze: swim velocity; (**F**) water maze: time in four quadrants (probe trial). Quadrant Q2 is target quadrant and dotted line denotes chance (15 s). $^{+++}$ $p<0.005$: performance on trial 1 compared to the following trials (rota-rod) or performance on day 1 compared to the following days (water maze) of respective group; $^{\$\$\$}$ $p<0.005$: time in target quadrant Q2 compared to time in any other quadrant of respective group.

3.2.7. Indirect calorimetry. The body weights of male and female mice were significantly different ($p<0.005$) in this experiment, whereas no differences were detected between the body weights of wild-type (+/+) and *Myg1*-deficient (-/-) mice (Figure 17A). Locomotor activity did not significantly differ between genotypes or sexes. Habituation occurred in all groups and more or less stable low values were achieved during last 45 min of the test (Figure 17B). RER was significantly affected by time ($F(7,644)=27.53$ $p<0.005$), but not by genotype or sex. O_2 consumption was significantly affected by sex ($F(1,92)=11.89$ $p<0.005$),

time ($F(7,644)=178.29$ $p<0.005$), time × sex interaction ($F(7,644)=4.08$ $p<0.005$) and time × genotype interaction ($F(7,644)=3.63$ $p<0.005$). Similarily, CO_2 production was affected by sex ($F(1,92)=12.31$ $p<0.005$), time ($F(7,644)=212.40$ $p<0.005$), time × sex interaction ($F(7,644)=2.60$ $p<0.05$) and time × genotype interaction ($F(7,644)=2.44$ $p<0.05$). Accordingly, significant effects of sex ($F(1,92)=12.11$ $p<0.005$), time ($F(7,644)=187.22$ $p<0.005$), time × sex interaction ($F(7,644)=3.82$ $p<0.005$) and time × genotype interaction ($F(7,644)=3.43$ $p<0.005$) on heat production were observed. Despite comparable levels of locomotor activity during the last 45 min of testing (Figure 17B), O_2 consumption, CO_2 production and heat production remained somewhat elevated in female mutant (-/-) mice (Figure 17D-F). However, this elevation was not statistically significant when compared to respective time point in female wild-type (+/+) mice.

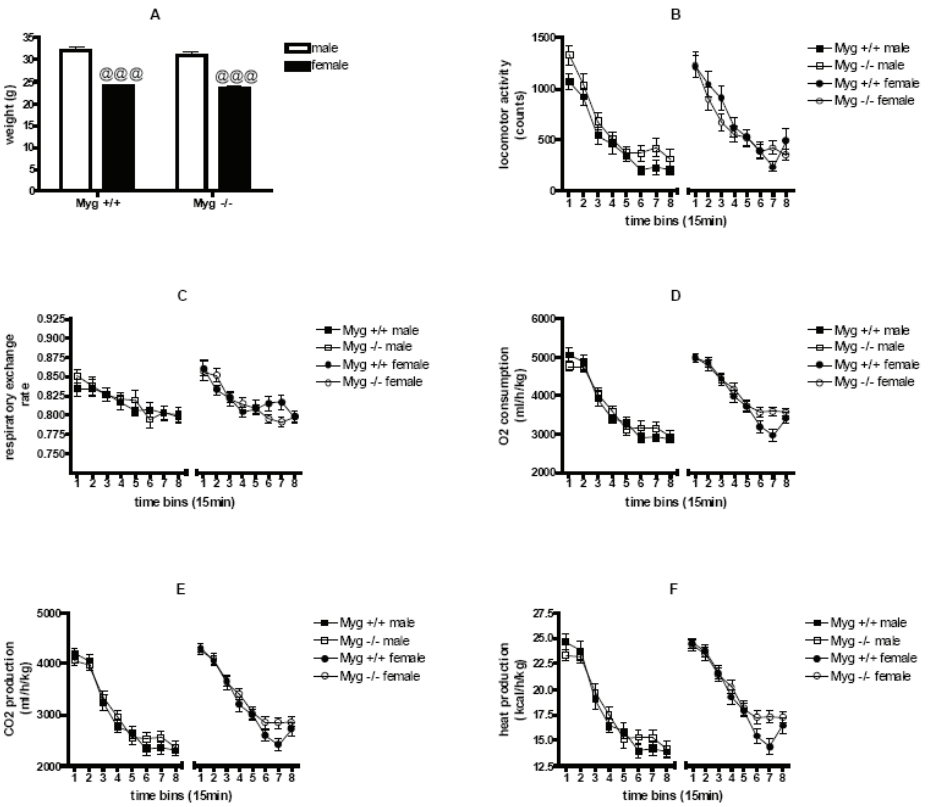

Figure 17. Indirect calorimetry in mice lacking *Myg1* (-/-) and their wild-type (+/+) littermates. (**A**) body weight (pre-test); (**B**) locomotor activity; (**C**) respiratory exchange rate; (**D**) oxygen O_2 consumption; (**E**) carbon dioxide CO_2 production; (**F**) heat production. $^{@@@}$ $p<0.005$: female mice compared to male mice of the same genotype.

3.2.8. Water maze. In the acquisition phase of the water maze, the distance travelled and latency to find the submerged platform were both affected by trial ($F(3,273)=233.81$ $p<0.005$, and $F(3,273)=277.12$ $p<0.005$, respectively) and sex × trial interaction ($F(3,273)=3.77$ $p<0.05$, and $F(3,273)=2.90$ $p<0.05$, respectively). Swim velocity was affected by trial only ($F(3,273)=7.44$ $p<0.005$). Spatial learning, defined as significant reduction of distance and latency to find the submerged platform across days, clearly occurred in all groups. Neither genotype nor sex significantly modified the acquisition phase of the water maze (Figure 16C-E). In the probe trial, significant effect of quadrant was established ($F(3,364)=321.11$ $p<0.005$). All groups clearly demonstrated preference for the target quadrant Q2 (Figure 16F). Again, the invalidation of *Myg1* gene failed to affect the performance of mice in the probe trial, indicating unaltered spatial learning and memory in *Myg1*-deficient (-/-) mice (Figure 16F).

3.2.9. Sensory-motor description. No significant sensory or motor anomalies were found in *Myg1* (-/-) mice (Table 7).

Table 7. Sensory-motor description in mice lacking *Myg1* (-/-) and their wild-type (+/+) littermates. No differences between groups were detected.

Parameter	*Myg1* +/+ male	*Myg1* +/+ female	*Myg1*-/- male	*Myg1*-/- female
Latency to find visible food pellet (s)	70 ± 9	102 ± 16	70 ± 11	67 ± 12
Latency to find hidden food pellet (s)	212 ± 30	235 ± 36	235 ± 25	295 ± 35
Forepaw reach (%)	100	96	96	100
Pupillary reflex (%)	100	100	100	100
Ear twitch (%)	100	96	100	100
Eye blink (%)	100	100	100	100
Facial reaction to tactile stimulus (%)	91	92	96	96
Righting reflex (%)	100	100	100	100
Wirehang (s)	58 ± 2	60 ± 0	60 ± 0	60 ± 0
Maximum vertical pole performance (%)	57	80	67	85

3.3. Second phenotyping battery

3.3.1.Light-dark exploration. No significant differences between genotypes or sexes were revealed in the light-dark exploration (Figure 18A, 18B).

3.3.2. Marble burying test. The number of marbles buried was not affected by either genotype or sex (Figure 18C). Although the main effect of sex was established in the distance travelled ($F(1,79)=7.94$ $p<0.01$), *post hoc* comparison did not reveal any significant differences between the groups (data not shown).

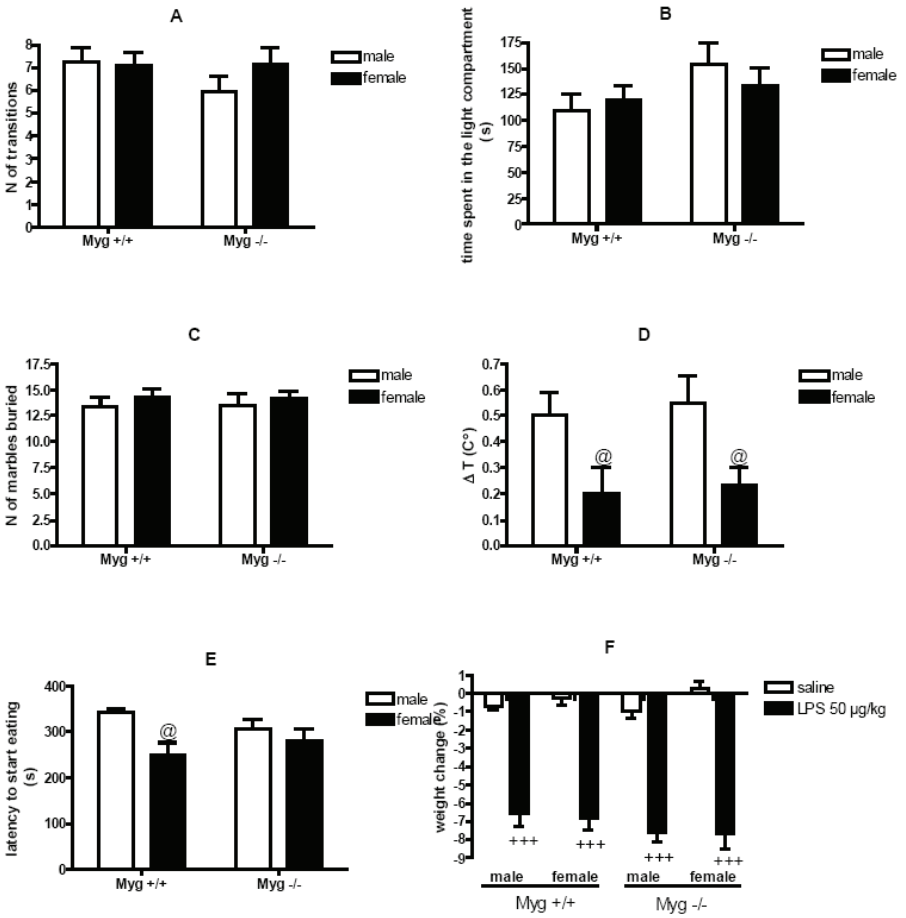

Figure 18. Light-dark exploration, marble burying test, stress-induced hyperthermia, hyponeophagia test and LPS-induced weight loss. (**A**) light-dark exploration: number of transitions; (**B**) light-dark exploration: time spent in the light compartment; (**C**) marble burying test: number of marbles buried; (**D**) stress-induced hyperthermia: change in temperature (ΔT); (**E**) hyponeophagia test: latency to start eating; (**F**) LPS (50 µg/kg) induced weight loss. $^{@}$ $p<0.05$: female mice compared to male mice of the same genotype; $^{+++}$ $p<0.005$: LPS-treated group compared to saline-treated group of respective genotype and sex.

3.3.3. Stress-induced hyperthermia. Significant effect of sex was observed ($F(1,79)=11.19$ $p<0.005$). Repeated measurement of rectal temperature produced significantly stronger hyperthermia in male mice compared to their female counterparts ($p<0.05$), and this difference was not modified by genotype (Figure 18D).

3.3.4. Hyponeophagia test. The latency to start eating was significantly affected by sex ($F(1,79)=7.51$ $p<0.01$). Female wild-type (+/+) mice demonstrated significantly shorter latencies than male wild-type (+/+) mice. However, no such difference was found between male and female mice lacking *Myg1* (-/-) (Figure 18E).

3.3.5. Restraint-induced analgesia. Significant effect of restraint ($F(1,74)=36.30$ $p<0.005$) was established. When compared to their unstressed controls, restraint produced significantly longer tail-flick latencies (analgesia) in female wild-type (+/+) mice ($p<0.05$), male mutant (-/-) mice ($p<0.05$) and female mutant (-/-) mice ($p<0.01$). In male wild-type (+/+) mice, a tendency to increased tail-flick latency was observed in the restraint-group ($p<0.10$) (Figure 19A). No genotype- or sex-dependent differences were established.

3.3.6. LPS-induced weight loss. LPS administration induced a highly significant weight loss in all groups ($F(1,74)=323.72$ $p<0.005$), but this effect was not modified by either genotype or sex (Figure 18F).

3.4. Additional tests

3.4.1. Body weight, rectal temperature and blood glucose. Body weights at 2 months of age were significantly affected by sex ($F(1,63)=135.63$ $p<0.005$). Female mice weighed significantly less than their male counterparts ($p<0.005$). Body weight was not altered by the invalidation of *Myg1*. Rectal temperatures did not differ between groups. Blood glucose concentrations were significantly affected by sex ($F(1,63)=38.09$ $p<0.005$), with female mice showing significantly lower values than male mice ($p<0.005$), independent of genotype. Data are summarised in Table 8.

Table 8. Body weight, rectal temperature and blood glucose concentration at 2 months. $^{@@@}$ $p<0.005$: a significant difference between male and female mice of the same genotype.

Parameter	*Myg1* male	+/+*Myg1* +/+ female	*Myg1* -/- male	*Myg1* -/- female
Body weight (g)	29.1 ± 0.6	20.8 ± 0.7 $^{@@@}$	29.3 ± 0.8	21.0 ± 0.7 $^{@@@}$
Rectal temperature (C°)	37.8 ± 0.2	37.8 ± 0.1	37.7 ± 0.2	38.2 ± 0.2
Blood glucose (mmol/l)	7.75 ± 0.2	6.70 ± 0.2 $^{@@@}$	8.09 ± 0.2	6.57 ± 0.2 $^{@@@}$

3.4.2. Restraint-induced corticosterone elevation. Significant effects of sex ($F(1,55)=12.69$ $p<0.005$), stress ($F(1,55)=285.25$ $p<0.005$) and genotype × stress interaction ($F(1,55)=7.27$ $p<0.01$) were revealed. Corticosterone values in unstressed animals were not affected by genotype or sex. Restraint produced a robust increase in plasma corticosterone concentrations in all groups ($p<0.005$). However, in female wild-type (+/+) mice restraint-induced corticosterone elevation was significantly higher than in male wild-type (+/+) mice ($p<0.005$) and female *Myg1*-deficient (-/-) mice ($p<0.005$) (Figure 19B). The sex-specific difference observed in restrained wild-type (+/+) mice was not found in restrained mutant (-/-) mice.

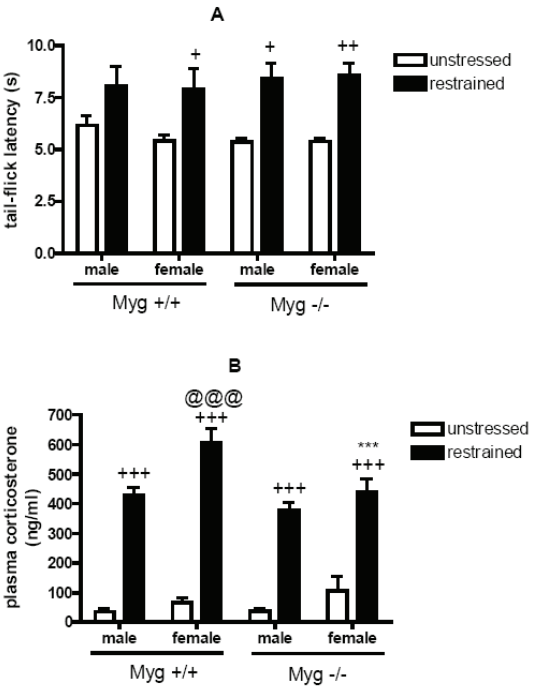

Figure 19. Restraint-induced analgesia and plasma corticosterone elevation. (**A**) restraint-induced analgesia: tail-flick latency; (**B**) restraint-induced plasma corticosterone elevation. *** $p<0.005$: mice lacking *Myg1* (-/-) compared to their wild-type littermates (+/+) of the same sex and treatment condition; @@@ $p<0.005$: female mice compared to male mice of the same genotype and treatment condition; + $p<0.05$, ++ $p<0.01$, +++ $p<0.005$: restrained group compared to unstressed group of respective genotype and sex.

3.4.3. Restraint-induced *Myg1* expression in brain structures of wild-type (+/+) mice. In the prefrontal cortex a significant effect of restraint on *Myg1* expression was established ($F(1,27)=11.17$ $p<0.005$). *Post hoc* comparison showed that restraint reduced *Myg1* expression in female mice ($p<0.05$), and a similar tendency was observed in male mice (Figure 20A). Neither sex nor

restraint had any effect on *Myg1* expression in the mesolimbic area or temporal lobe (Figures 20B, 20C).

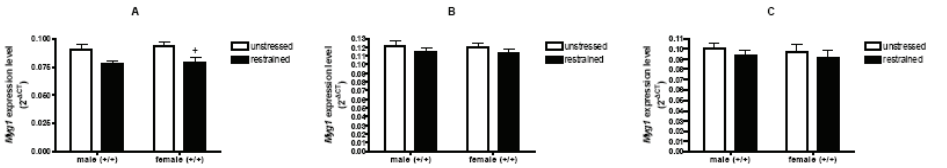

Figure 20. Changes in *Myg1* gene expression in restrained wild-type (+/+) mice. (**A**) prefrontal cortex; (**B**) mesolimbic area; (**C**) temporal lobe. $^{+}$ $p<0.05$: restrained group compared to unstressed group of respective sex.

4. Implication of *MYG1* in vitiligo and functional polymorphisms in human *MYG1*

4.1. *MYG1* genotypes in vitiligo patients and normal controls

From the initial set of SNPs, we failed to genotype rs1534284 and rs4759054 with SNPlex platform. Moreover, four SNPs (rs2694861, rs4325348, rs2279025, and 4759281) were monogenic in Estonian population with only major alleles being present. Sequencing genomic DNA of 54 subjects (30 controls and 24 vitiligo patients) revealed that rs1534284/rs1534283 double-polymorphism is likewise prevalently monogenic in Estonian population with only Myg1 4Arg allele being present. The polymorphic SNPs in our study were rs1465073 in *MYG1* promoter (-119C/G) and rs1545650 (C/T) located in short 281 bp intergenic area between *MYG1* and *AAAS* (accession: NM_015665) gene. Direct sequencing of rs1465073 polymorphism in 40 incidental subjects completely overlapped with SNPlex results. The minor allele (G) of the rs1465073 was more frequent in the vitiligo group compared to the control group (47.1% versus 39.3%, p=0.0385; OR 1.37, 95%CI 1.02–1.85) consistent with a susceptibility effect. Analysis based on the stage of progression of the vitiligo revealed that the increased frequency of the minor allele (G) of rs1465073 occurred prevalently in the group of patients with active vitiligo (n=86) compared to the control group (48.2% *versus* 39.3%, p=0.0398; OR 1.44, 95%CI 1.02–2.03). There was no statistically significant effect in the distribution of the minor allele of rs1465073 between patients with stable vitiligo (n=38) and control group (44.6% *versus* 39.3%, p=0.378; OR 1.24, 95%CI 0.76–2.02). The average age, mean onset and duration of vitiligo did not differ between patients with active *versus* stable vitiligo. Although minor allele (T) of rs1545650 was more prevalent in patients than in control individuals (3.3% *versus* 1.6%, respectively), the difference remained not significant (p=0.172; OR 2.08; 95% CI 0.71–6.07). LD analysis (solid spine algorithm) indicated that the rs1465073 polymorphism, which is located in the promoter of

the *MYG1* gene, was not in strong LD with the *MYG1* rs1545650 polymorphism located 7.7 kb downstream (|D'| 0.23). No significant effects in the distribution of the *MYG1* gene allele frequencies were found when patients with different clinical subtypes of vitiligo were analysed separately or when analysis was performed regarding the extent of the skin lesion.

4.2. *MYG1* expression in the skin of vitiligo patients compared with healthy controls

A statistically significant increase in *MYG1* expression was observed in both lesional ($2^{-\Delta CT}$=4.3, $p<0.01$) and nonlesional ($2^{-\Delta CT}$= 4.5, $p<0.001$) skin of vitiligo patients compared to the skin of healthy control subjects ($2^{-\Delta CT}$=3.2) (Figure 21A). No significant difference was detected in lesional and nonlesional skin between male and female vitiligo patients (data not shown). mRNA expression of tyrosinase, an essential marker for melanogenesis, was determined in the skin samples of the same patients to ensure that the samples faithfully represent melanocyte specific differences between lesional and nonlesional skin. Down-regulation of tyrosinase mRNA expression has been documented in lesional skin of vitiligo patients (Machado Filho *et al*, 2005). Accordingly, a statistically significant decrease in tyrosinase expression was observed in lesional skin of vitiligo patients ($2^{-\Delta CT}$=0.2) compared to nonlesional skin of vitiligo patients ($2^{-\Delta CT}$=2.8) and healthy control subjects ($2^{-\Delta CT}$=1.7, both $p<0.0001$). *MYG1* expression level was lower in healthy male ($2^{-\Delta CT}$=2.2) than female subjects ($2^{-\Delta CT}$= 3.7, $p<0.01$) (Figure 21B). In male patients, *MYG1* expression level was higher both in nonlesional ($2^{-\Delta CT}$=4.8, $p<0.0001$) and lesional skin ($2^{-\Delta CT}$=4.2, $p<0.0001$) (Figure 21C). In female patients the increase in *MYG1* expression was also evident (unaffected skin $2^{-\Delta CT}$=4.3, p=0.19; affected skin $2^{-\Delta CT}$=4.3, p=0.18), although it did not strictly meet the requirements of statistical significance (Figure 21D). No differences in the expression of *MYG1* were detected between different subgroups of vitiligo based on the extent of involvement of the disease. In general, *MYG1* mRNA expression was increased in each subgroup of vitiligo and was not dependent on whether the biopsy had been taken from lesional or unaffected skin. Exceptionally, we observed no difference in *MYG1* expression between nonlesional skin of nonactive subtype of vitiligo (n=9; 3 males and 6 females) and healthy control subjects.

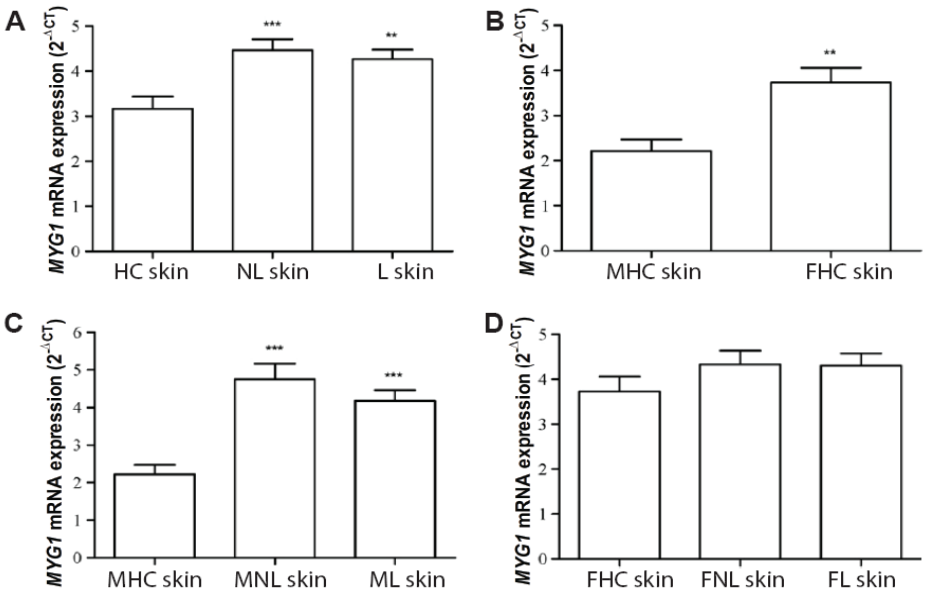

Figure 21. *MYG1* mRNA expression in vitiligo patients and healthy controls. (**A**) *MYG1* mRNA expression level in nonlesional (NL)vitiligo skin, lesional (L) vitiligo skin and non sun-exposed skin of healthy control (HC) subjects; *** $p < 0.001$, ** $p<0.01$. (**B**) *MYG1* mRNA expression level in the skin of healthy female (FHC) and male (MHC) subjects; ** $p<0.01$. (**C**) *MYG1* mRNA expression level in nonlesional (MNL) and lesional (ML) skin of male vitiligo patients compared with healthy male (MHC) subjects (*** $p<0.0001$) and (**D**) *MYG1* mRNA expression level in nonlesional (FNL) and lesional (FL) skin of female vitiligo patients and in the skin of healthy female (FHC) subjects. Data are expressed as mean $2^{-\Delta CT}$ value relative to *HPRT*.

4.3. The impact of promoter genotype on *MYG1* expression in healthy controls

MYG1 mRNA levels in the skin of healthy controls correlated with -119C/G polymorphism (Figure 22A, healthy controls). *MYG1* mRNA expression of G homozygous subjects ($2^{-\Delta CT}$=3.87±0.67) was significantly (p=0.01) higher than in subjects who had homozygous C in the same position ($2^{-\Delta CT}$=2.64±0.39). The expression value of heterozygous subjects remained in between ($2^{-\Delta CT}$=3.43± 1.29), but due to relatively high deviation, it was not statistically different from either homozygous groups. In vitiligo patients we could not detect a similar difference and there were no statistically significant differences in *MYG1* mRNA levels between the groups divided according to -119C/G genotypes (Figure 22A, vitiligo patients).

Our finding that *MYG1* expression level in control subjects is dependent on -119C/G promoter polymorphism was independent from the sex effect (See Table 5 for distribution of male and female controls divided according to

promoter genotype). Higher expression of *MYG1* in the skin biopsies of controls with G/G genotype was not derived from generally higher *MYG1* expression of female controls because mostly males represented this group. Similarly, lower expression of *MYG1* with C/C genotype was not derived from generally lower *MYG1* expression of male controls because only females represented this group.

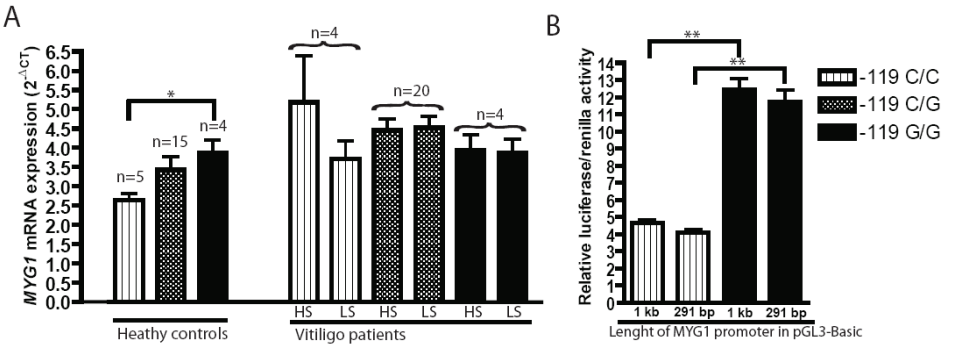

Figure 22. Impact of *MYG1* promoter SNP (-119C/G) on *MYG1* mRNA expression. (**A**) *MYG1* mRNA expression levels in the skin biopsies of healthy subjects and vitiligo patients; n indicates number of subjects in each group; the error bars present standard deviation of the mean. Abbreviations: HS – healthy skin; LS – lesioned skin. (**B**) *MYG1* promoter activity in luciferase assay. Data is shown relative to the activity of empty pGL3-Basic. Pattern codes corresponding to three genotypes for both (**A**) and (**B**) are shown on the right.* $p<0.05$; ** $p<0.01$

4.4. Promoter genotype in cell culture

Additionally we performed luciferase reporter assay in the cell culture to measure the influence of -119C/G polymorphism in the *in vitro* system with minimum interacting factors. In luciferase assay both short and long promoter fragment with -119G allele had more than 2.5 fold higher activity than -119C allele (Figure 22B). Comparison of 291 bp promoter fragments showed that -119G allele had 2.66 times higher activity ($p<0.01$) and comparison of 1 kb promoter fragments revealed that -119G allele had 2.89 times higher activity ($p<0.01$). Additionally our results demonstrate that 291 bp *MYG1* promoter fragment is sufficient to trigger maximum activity of *MYG1* gene. The CMV promoter that we used as a positive control induces high-level constitutive expression in a variety of mammalian cell lines (Fitzsimons *et al*, 2002). In general *MYG1* promoter was 4–8 times less active than CMV promoter depending on the promoter allele (data not shown).

4.5. Arg4Gln polymorphism

As we found in study I, amino-acid four is a part of a mitochondrial targeting signal. Because Myg1 Arg4Gln polymorphism changes basic amino acid (Arg) into polar and uncharged (Gln), we studied if Arg4Gln has an influence on subcellular localization of Myg1. We have previously shown that full-length Myg1 4Arg genotype that is common among Caucasians localizes into the nucleus and mitochondria. The same localization was confirmed in the current study (Figure 23A). Myg1 4Gln variant was completely unable to enter mitochondria. We could detect YFP signal in the nucleus and slight homogenous signal in the cytoplasm, but there were no cells where Myg1 4Gln-YFP signal would be overlapped with MitoTracker (Figure 23B).

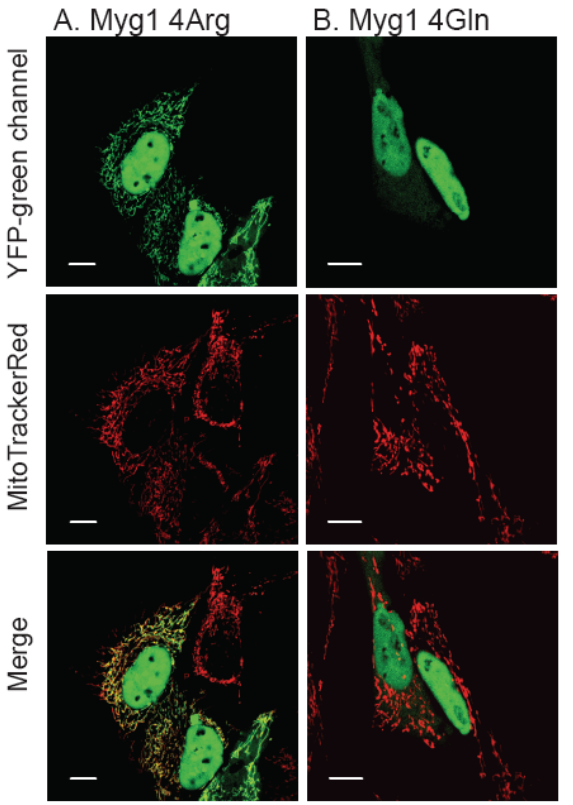

Figure 23. **Subcellular localization of human *MYG1* cDNA with both variants for Myg1 Arg4Gln polymorphism.** Mitochondrial localization YFP tagged *MYG1* cDNA with arginine in the position amino acid four (**A**) is completely eliminated if arginine is replaced with glutamine (**B**). Scale bars represent 10μm.

DISCUSSION

1. Highly conserved ubiquitous gene with mild phenotype in knockdown and knockout studies

Myg1 gene was initially found to be highly expressed in freely proliferating melanocytes (Smicun, 2000). We came to be interested in *Myg1* after it was identified as a most up-regulated gene in response to cat odour exposure in the amygdaloid area of rats (Kõks *et al*, 2004). Comparing sequences from different species revealed that *Myg1* is a highly conserved gene, but there were no other publications available about this gene. Therefore, the current study was designed to investigate Myg1 comprehensively in mRNA, protein, cell culture and organism level. We found that *MYG1* is ubiquitously expressed and localizes to the nucleus and mitochondria. siRNA mediated 90% knockdown of *MYG1* mRNA did not cause any visible changes in HeLa cells. However, expression of immune system related genes were up-regulated and several transcripts encoding developmental factors were significantly altered after *MYG1* knockdown in cell culture. Data about effects of *Myg1*-deficiency in yeast and *Caenorhabditis elegans* is available from genome-wide studies that have been established in these species. Deletion of the *MYG1* orthologue in yeast or suppression of its expression in *Caenorhabditis elegans* (Kamath *et al*, 2003) has not revealed an obvious phenotype although their fitness is reduced in some conditions. In *Saccharomyces cerevisiae*, the organism remains viable after deletion of the *MYG1* orthologue, but fitness is reduced in rich medium (YPD) (Deutschbauer *et al*, 2005) and growth defect can be detected if ethanol (YPE) is used as the carbon source (Steinmetz *et al*, 2002). Nevertheless, we expected that deletion of conserved factor such as Myg1 in more complex organism as mouse could produce remarkable phenotype. Surprisingly, the initial phenotyping of *Myg1*-deficent mice have revealed that despite ubiquitous and developmentally regulated expression of *Myg1* transcript; *Myg1*-deficient mice are vital, fertile and display no gross abnormalities. *Myg1* deficiency caused only moderate alterations in anxiety related behaviour and stress-reactions in mice but also remarkable reduction of sex-dependent behavioural variations.

2. Expression and characteristics of *Myg1* promoter and transcript

The full length transcript of *Myg1* is 1.3 kb long and it is expressed in all organs and major brain structures in adult mouse and human tissues. In agreement with the widespread expression, the short intervening promoter region is GC rich and lacks a TATA box similar to many other constitutive promoters (Yang *et al*, 2007). Only 291 bp promoter fragment that also included short 5'-UTR of

MYG1 gene was needed to trigger maximum activity of luciferase expression in our *in vitro* assay. 291 bp fragment has been used, because this is the maximum of *MYG1* unique promoter area that is not overlapped with 3'-UTR of closest upstream neighbour gene *Prefoldin 5*. In this study we found several isoforms of *Myg1* mRNA and protein that appeared to be either ubiquitous, tissue specific or specific to cellular localization. We identified ubiquitous but scantly expressed short alternative splice form of mouse *Myg1* transcript. Another alternative mRNA variant was found in human testis: besides 1.3 kb mRNA that is present in all other tissues, there is additional strongly expressed 1.5 kb fragment in the testis. As our northern probe covered full length of *MYG1* mRNA, it is not clear whether this additional 200 bp could be an extra exon, an alternative poly-A tail or anything else. We also detected two variants of wild-type Myg1 in protein gel and excluded the possibility that smaller variant is resulted from cleavage of mitochondrial targeting signal indicating that smaller variant is most likely caused by another post-translational proteolytic cleavage. Therefore Myg1 expression seems to be regulated by various alternative splicing and post-translational modifications.

3. Dynamic expression of *Myg1* transcript during development

Growing data suggest that Myg1 is involved in developmental processes. At first *Myg1* tends to be up-regulated in pluripotent cells (Sharov *et al*, 2003; Golan-Mashiach *et al*, 2005) compared with differentiated cells, furthermore, *Myg1* expression is dynamic during embryonic (Mathavan *et al*, 2005; Weng *et al*, 2006) and postnatal development (Dorrell *et al*, 2004). We detected dynamic expression of *Myg1* during embryogenesis and also in the post-natal brain of mouse. During embryogenesis a strong up-regulation was observed from embryonic days E7 and E11. At E11.75 expression was particularly prominent in developing brain, limb buds and tail region and in the eye. During the early stages from E8.5 to E10.5 *Myg1* expression appeared to be remarkably more uniform, but in E11.75 embryo *Myg1* expression was strongest in ectoderm-derived areas including developing neuro-epithelium and eye. Pre-natal strong expression level of *Myg1* is retained until birth, when the major part of neurogenesis and neuronal migration has occurred in mice. These results suggest for specific requirement of Myg1 in the course of brain maturation, however not specifically in cell proliferation and migration since no anatomical abnormalities were detected in *Myg1* mutant (-/-) mice.

Experimental data suggest putative protein interactions of Myg1 that can explain developmentally regulated expression of Myg1 transcript. Myg1 is down-regulated in Oct4 (Pou5f1) knockdown embryos (Foygel *et al*, 2008) and also down-regulated after conditional knockout of TLX (Nr2e1) (Zhang *et al*, 2008). Oct4 is an embryonic stem cell (ESC) pluripotency regulator and TLX regulates proliferation of adult neural stem cells. As *Myg1* expression is reduced

after knockdown of regulatory proteins in stem cells, it could be possible that Myg1 is induced by factors that regulate pluripotency. This hypothesis is even more supported by the finding that *Myg1* has a putative Oct4 binding site suggesting that *Myg1* is a candidate target gene of Oct4 (Zhou *et al*, 2007; Foygel *et al*, 2008). Remarkable similarities can be noted between cellular effects of Myg1 and Oct4: overexpression of *Oct4* mRNA induces developmental arrest in a dose dependent manner (Foygel *et al*, 2008). Interestingly, according to our preliminary experimental data, over-expression of Myg1 also induces arrest in cell division. We noticed it unexpectedly when trying to make photo-series of Myg1-transfected cells that were about to divide (unpublished data). Despite numerous trials we could not follow cell-division in *Myg1* transfected cells that was not the case in the cells transfected with other expression constructs. However this initial notion needs further quantitative studies. Myg1 involvement in the cellular pathways related with Oct4 and TLX can explain dynamic expression of *Myg1* during prenatal and postnatal development. The expression levels of Oct4 or TLX were not changed in response to Myg1 knockdown in cell culture, but there were several developmental factors that showed remarkable change: the most upregulated transcript in this group, *Decorin*, is a member of the small leucine-rich proteoglycan superfamily and plays important biological roles through its ability to bind other extracellular matrix proteins and certain growth factors (Grant *et al*, 2002). *Basic fibroblast growth factor* (*FGF2*), that is downregulated after *MYG1* knockdown is a wide-spectrum mitogenic, angiogenic, and neurotrophic factor that has been implicated in a multitude of physiological and pathological processes, including limb development, angiogenesis, wound healing, and tumor growth (Ortega *et al*, 1998). Therefore, the developmental impact of Myg1 may be mediated in conjuction of factors like *Decorin* and *FGF2*. The factors that are related with growth and development are also related with cell division and deviations in growth factor pathways may lead to cancer. Therefore it is not suprising that Myg1 has been found to have altered expression in cancer tissues (Baris *et al*, 2004; Chandran *et al*, 2007; Foltz *et al*, 2009). It is remarkable that global array data that Myg1 tends to be upregulated in pluripotent cells (Sharov *et al*, 2003; Golan-Mashiach *et al*, 2005) together with data that Myg1 is rather down-regulated in malignant tumors (Chandran *et al*, 2007; Foltz *et al*, 2009) lends further support to our preliminary experimental data that Myg1 can establish inhibitory effect on cell division. Taken together, Myg1 seems to be a cellular factor implicated in pluripotency, development and possibly differentiation. However, Myg1 properties in cell cycle regulation are object for further research in order to get more insight of how Myg1 is involved in cell pluripotency and malignancy.

4. *Myg1* is ubiquitously expressed in adult brain

Our quantitative RT-PCR and *in situ* analysis of *Myg1* mRNA confirm that *Myg1* is a ubiquitously expressed gene in the adult brain and other tissues. Our *in situ* analysis of *Myg1* transcript in adult mouse brain is similar with *Myg1 in situ* data from Allen Brain Atlas (http://mouse.brain-map.org/welcome.do). Additionally, *Myg1 in situ* staining in Allen Brain Atlas is highly similar with that of a ubiquitous gene *Hprt1* that we also use as a housekeeper gene. *Myg1* specific *in situ* staining is also remarkably similar with Nissl staining that can be found in Mouse Brain Atlas (Paxinos & Watson, 2000). Therefore, in most cases, the extensively stained areas specific to *Myg1 in situ* probe most probably reflect adult mouse brain areas with denser cell groups (such as medial habenular nucleus, hippocampus, several hypothalamic nuclei *etc*). Co-staining with known ubiquitous gene specific probe is needed to tell if there are areas in adult mouse brain where basal *Myg1* expression is more or less extensive. However, there are distinct cells that have intensive *Myg1* specific staining, for example in the ependymal layer of the ventricular system, in the CA3 region of hippocampus and in the Purkinje cell layer of cerebellum (Figure 8). Distinct extensively stained single cells can be seen also in cerebral cortex and other brain areas (data not shown) and it would be interesting to study what is specific about these cells by co-stainings with different cellular markers.

Remarkable evidence indicates that despite ubiquitous expression in the brain and other tissues, *Myg1* is obviously not a housekeeper gene and its expression can extensively change in response to intercellular or environmental stimuli. Besides our initial finding that *Myg1* is a most up-regulated gene in the amygdaloid area of rats exposed to predator (cat) odour (Kõks *et al*, 2004), other studies have indicated that *Myg1* is relevant in the brain or even harbours specific functions in the brain: *MYG1* is down-regulated in the entorhinal cortex and hippocampus of Alzheimer's patients (Liang *et al*, 2008); furthermore, *Myg1* mRNA expression has been shown to increase in the mouse cerebral cortex in response to chronic administration of simvastatin that has been reported to prevent Alzheimer's disease (Johnson-Anuna *et al*, 2005). In primary cortical neuron culture *Myg1* mRNA is increasing with expression peak three hours after glutamatergic NMDA receptor activation; therefore *Myg1* can be involved in long-lasting synaptic changes (Hong *et al*, 2004). Finally, *Myg1* expression in the rat's cingulate cortex is more than 3-fold up-regulated specifically 9 hours after experimental ischemic stroke (middle cerebral artery occlusion) (Rickhag *et al*, 2006).

The ubiquitous maintenance of *Myg1* expression throughout mouse lifespan suggests its requirement in functioning of differentiated neurons and other adult tissues. Nevertheless, we report that mutant mice lacking *Myg1* (-/-) are vital and fertile, and they do not display any gross anatomical, sensory or motor abnormalities. Moreover, contrary to what could be expected, the behavioural and physiological alterations in these mice are quite modest. *Myg1* (-/-) mice perform normally in the water maze (spatial learning and memory) and rota-rod

(procedural learning), and their habituation to locomotor activity test (non-associative learning) is not altered. Since we first identified *Myg1* in a screen for anxiety-related genes (Kõks *et al*, 2004), we were most interested in anxiety- and stress-related phenotype in mice lacking *Myg1*. The plus-maze test revealed that male mutant mice (-/-) were significantly less anxious than their wild-type (+/+) littermates as indicated by the higher % unprotected head-dippings and lower number of stretched-attend postures. Additionally, increased social exploration in male mice is indicative of reduced anxiety. However, this alteration was not reproduced in other anxiety-related tests (i.e. spatial distribution of locomotor activity, light-dark exploration, marble burying test, stress-induced hyperthermia and hyponeophagia test). Moreover, the proportion of the distance travelled in the center of the locomotor activity arena, which is an indicator of trait anxiety, revealed increased anxiety in female mutant (-/-) mice. Again, this difference between genotypes was not reproduced in other tests of anxiety. Taken together, *Myg1* is ubiquitously expressed in the adult brain and the expression of *Myg1* transcript is changed in reaction to various stimuli in the brain. Nevertheless, *Myg1*-deficent mice have no deviations in their cognitive abilities and their behaviour is only mildly altered in anxiety-related tests.

5. Myg1 and stress in cellular and organism level

As discussed above, *Myg1* expression in healthy adult tissues is rather homogenous and ubiquitous and seems to be regulated mainly in various stress/illness conditions. On cellular level the stress response comprises an evolutionarily highly conserved mechanism that protects cells from sudden environmental change or frequent fluctuations in environmental factors (Kültz, 2003). The evidence that Myg1 is altered in reaction to basic cellular stress comes from yeast: the expression of *Myg1* orthologue in yeast declines in response to oxidative stress, heavy metal stress, heat shock, osmotic stress and DNA damage (Chen *et al*, 2003). Heat shock proteins are highly conserved in many organisms and make up one of the most abundant gene group that is induced during many types of stress (Kültz, 2003). There are two reports suggesting that Myg1 interacts with Hsp90 that is one of most prevalent HSP protein. Co-immunoprecipitation with endogenous Hsp90 identified Myg1 among 39 protein interaction partners in human HEK293 cells (Falsone *et al*, 2005). In yeast two-hybrid screen, Myg1 orthologue *YER156C* was identified as a putative interaction partner of yeast Hsp90 (Millson *et al*, 2005). In the current study we could not confirm the physical interaction between Myg1 and Hsp90 in a direct Myg1 pull-down and the putative interaction between the factors needs further experimental support. After *MYG1* knock-down in cell culture, however, we detected a mild down-regulation of Hsp90 alpha (AF028832) and beta subunits (BG612458) (1.2- and 1.17-fold reduction, respectively; $p<0.02$). Additionally, another HSP, mitochondrial chaperon Hsp60 (BF965447) was one

of the most down-regulated gene after *MYG1* knockdown. Both siRNAs induced an approximately 2.5-fold decrease in Hsp60 mRNA, however, with moderate statistical power considering genome-wide chip analysis ($p<0.02$). Decreased expression was also found for Hsp70 subunits 1B (NM_005346) and 4 (BC002526) (1.49 and 1.27-fold, respectively; $p<0.03$), and *Prohibitin* (NM_002634) (1.25-fold decrease, $p<0.01$), a chaperon known to be located, similarly to Myg1, in both the nucleus and mitochondria (Mishra *et al*, 2005).

The tendency of expression change of *Myg1* transcript in stress/illness conditions, however, tends to correlate with metabolic activity of the cell: namely; *Myg1* expression is declining during cell starvation (Kristensen *et al*, 2008) or degeneration for example in human age-related cataract lenses (Hawse *et al*, 2003) or in the entorhinal cortex and hippocampus of Alzheimer patients (Liang *et al*, 2008). On the contrary, an increase in *Myg1* transcript can be noted in activated cells: *Myg1* mRNA is increasing after glutamatergic NMDA receptor activation in primary cortical neuron culture (Hong *et al*, 2004). Additionally, *Myg1* expression in rat's cingulate cortex is more than 3-fold up-regulated specifically 9 hours after experimental ischemic stroke, whereas late expressed genes are related to stress, cellular proliferation, and events associated with inflammation and regenerative processes (Rickhag *et al*, 2006). *Myg1* was initially found as an upregulated gene in the amygdaloid area of rats after exposure to cat odour (Kõks *et al*, 2004). In the current study we additionally showed that *Myg1* gene expression was significantly reduced by restraint stress in the prefrontal cortex of female wild-type (+/+) mice. In male mice this effect was not statistically significant. The expression of *Myg1* was not affected in other brain areas (mesolimbic area or temporal cortex including amygdaloid area). Both cat odour and restraint stress induce strong anxiety/ stress reaction in rodents, therefore we expected similar changes in the transcriptomes of relevant brain areas. Current evidence suggest that *Myg1* expression is not consistent in two anxiety conditions that we have studied; furthermore, *Myg1* expression in anxiety is also not correlating with neuronal activity that couple anxiety reaction: according to a recent study, c-fos mRNA, that is considered to be a marker of neuronal activity, is induced in prefrontal area of rat already after 15 minutes of restraint stress application (Trnecková *et al*, 2006). Therefore, if *Myg1* expression was correlated with brain activity, it could be expected that if *Myg1* mRNA is similarily increased. Since we detected mild but significant decrease of *Myg1* mRNA, it seems that the activity of the cell does not completely explain expressional activity of *Myg1*. Interestingly, we also found that in addition to diverse changes in anxiety-like behaviour in mice lacking *Myg1* (-/-), female mutant mice showed significantly weaker corticosterone response to restraint stress. Therefore, *Myg1*-deficiency can also interrupt stress reaction in the hormonal level. This effect could be related to the high expression signal of *Myg1* mRNA in the paraventricular nucleus of hypothalamus, playing a role in the regulation of the hypothalamic-pituitary-adrenal stress axis. Again, a co-staining of *Myg1* probe with known markers for hypothalamic nuclei is needed to elucidate whether *Myg1*

expression is specific in hypothalamus. Our finding suggests that besides cellular level, Myg1 can be implicated in stress reactions in the hormonal level.

6. Mitochondrially localized Myg1 and metabolism

There is numerous evidence that Myg1 expression is changing during cellular activation, specifically, it tends to be down-regulated in restricted energy conditions. However, in activated cells Myg1 expression does not always correlate with the activity of the cell and this is, therefore, most likely dependent on the precise nature of cellular activity. Our experiments demonstrated the existence of nuclear and mitochondrial targeting signals in the N-terminal region of human and mouse Myg1 proteins. Mitochondrial localization is in accordance with predictions that were made by comparing human proteins with yeast mitochondrial homologues (Cameron *et al*, 2005). Moreover, the Myg1 orthologue GAMM1 protein-like (AT5G41970; Accession: NM_123562) has been found in gel-based separations of the mitochondrial proteome in *Arabidopsis thaliana* (Heazlewood *et al*, 2004) and *YER156C;* Myg1 orthologue in yeast has been associated with mitochondrial-enriched proteins that tend to be down-regulated after copper starvation (van Bakel *et al*, 2005). Functional conservation of sub-cellular signal sequences of Myg1 was reinforced by the existence of similar sub-cellular distribution of mouse and human Myg1 in HeLa cells. We could not detect active shuttling of Myg1 between the nucleus and mitochondria, neither in steady state nor during the S-phase, indicating that Myg1 performs simultaneous tasks in the two compartments. Obviously, we can not exclude that Myg1 could, under particular conditions not employed in this study, move from the nucleus to the mitochondria or *vice versa*, but the apparent lack of common nuclear export signals indicates that a shuttling needs to be facilitated by additional factors. The secondary structure analysis, photobleaching and immunoprecipitation experiments support the notion that Myg1 is a soluble non-membrane-bound protein.

The expression level of *Myg1* transcript is fluctuating during embryonic development and fades remarkably in the post-natal brain maturation, therefore it tends to be up-regulated in actively proliferating and differentiating neural precursors. But our *in vivo* knock-out model confirms that *Myg1* is not essential for proper development. Therefore one possible explanation could be that the expression level of mitochondrially localized *Myg1* correlates with metabolic activity in the cell and differential expression of *Myg1* during development may at least partially be related with increased activity of cells that are dividing and differentiating. We also anticipated that the *Myg1* knock-out *in vivo* would lead to alterations in metabolic activity. However, no alterations were observed in the body weight, rectal temperature or blood glucose concentrations in mice lacking *Myg1* (-/-). Furthermore, indirect calorimetry indicated metabolic rate comparable to wild-type (+/+) mice. It should be noted still, that during the last 30 min of the test, the oxygen consumption, carbon dioxide production and heat

production remained somewhat elevated in female mutant (-/-) mice indicating increased metabolism. Male mice showed slight tendency in same direction. The shortened protocol that we used in this study has been validated in our laboratory by pharmacological means and may have been relatively insensitive as a part of a larger screening battery to detect subtle differences in genetically manipulated animals, therefore we are currently developing more sensitive protocol to estimate metabolic rates of *Myg1*-deficent mice in more detail.

Intrestingly, the expression pattern of *Myg1* correlates with that of a single mitochondrial gene coding a subunit of mitochondrial H+ transporting ATP synthase (Atp5g2). According to the WebQTL database (http://www.genenetwork.org/) *Myg1* probe (1424088_at) correlates negatively with Atp5g2 probe (1456128_at) in several mouse brain tissues. The correlation values are -0.77 in the nucleus accumbens (Oct 07, RMA); -0.693 in the striatum (Apr05, RMA); -0.689 in the prefrontal cortex (Dec06, RMA); -0.6116 in the eye (Sep08, RMA) and -0.607 in the cerebellum (May05, RMA). Atp5g2 transcript encodes a subunit of a protein that is essentially involved in cellular metabolism. The mitochondrial F1F0 ATP synthase is a critical enzyme that works by coupling the proton motive force generated by the electron transport chain via proton transfer through the F0 or proton-pore forming domain of this enzyme to release ATP from the catalytic F1 domain (Grover *et al*, 2008). Atp5g2 is coding a single subunit c from F0 complex (ATP synthase, H+ transporting, mitochondrial, subunit c (subunit 9), isoform 2). The consistent negative correlation between probes representing mRNAs of Myg1 and Atp5g2 is remarkable. However, no transcripts related with mitochondrial metabolism were significantly changed after *MYG1* siRNA knockdown and as we now know, Myg1 is also located in the cell nucleus indicating that the functional relevance on Myg1 is probably not limited to metabolism. Nevertheless, there is evidence suggesting that Myg1 might have a role related with metabolic activity; therefore our next studies will be focused on *Myg1*-deficient mice to elucidate possible metabolic alterations in these mutants more specifically.

7. Arg4Gln polymorphism affects mitochondrial entrance of Myg1 protein

Expression of YFP-tagged Myg1 fusion proteins in HeLa cells revealed that glutamine in fourth position (Myg1 4Gln allele) completely eliminated mitochondrial entrance of YFP-tagged Myg1 protein. Our analysis of human ESTs and genomic sequences in NCBI and UCSC (http://genome.ucsc.edu/) databases confirm that Myg1 Arg4Gln polymorphism is present in human populations (Table 4). According to currently available data, there can be either arginine or glutamine in the fourth position of Myg1 in humans and in the current experiment we showed that only positively charged arginine in the fourth position enables mitochondrial entrance. It is likely that acidic glutamine

disturbs a common property of mitochondrial targeting sequence to form an amphiphilic helical structure that is essential for the effective transport of a mitochondrial protein (Shimoda-Matsubayashi *et al*, 1996). It has been described earlier that single amino acid substitution can completely eliminate the functionality of MTS: single substitution glycine 12 to glutamic acid in a mitochondrial targeting sequence disturbs mitochondrial localization of the human wild-type 8-oxoguanine DNA glycosylase (hOGG1) (Audebert *et al*, 2008). Our results provide another example of a single amino acid substitution in mitochondrial signal that eliminates mitochondrial entrance of a protein.

We sequenced 54 Caucasian subjects for Myg1 Arg4Gln and confirmed that they were all homozygous for Myg1 4Arg allele that corresponds to previous HapMap data for 60 Caucasian subjects (Utah residents with ancestry from Northern and Western Europe). According to HapMap database heterozygosity for Myg1 Arg4Gln polymorphism (rs1534284) has been currently detected only in YRI (Yoruba in Ibadan) population from Nigeria. Among 57 subjects from YRI population who were genotyped for HapMap project 20 subjects (35.1%) were heterozygous for Myg1 Arg4Gln polymorphism but there are no subjects who are homozygous for Myg1 4Gln allele. According to currently available data, Myg1 4Gln allele that disturbs mitochondrial entrance of Myg1 has never been detected in the homozygous state. We propose that persons with Myg1 4Gln variant do not survive or have health condition that keeps them out from the study groups. High frequency of general heterozygosity (0.175) of Myg1 Arg4Gln can also be a target of natural selection, similarly with 9-amino acid deletion in SLC4A1 gene that is completely lethal in homozygous state (Wilder *et al*, 2009), but heterozygosity persists with a maximum frequency of 0.175 due to protective effect with respect to cerebral malaria in Southeast Asia. The frequency of heterozygosity (Myg1 Arg4Gln) in Nigeria is similar with 9-amino acid deletion in SLC4A1 gene in Asia (0.175). Therefore it is likely that Myg1 Arg4Gln is a target of similar selection. Considering our present subjects, we cannot explain the relevance of our finding, but we propose that Myg1 has important functions inside mitochondria. However, our *Myg1*-deficient mouse model shows that the deletion of *Myg1* has no major effect on any crucial life function. We also showed that mouse Myg1 protein that in amino-acid level has 85.6% similarity with human Myg1, is also located inside mitochondria and nucleus. However, it has been shown in several cases that mouse knockout models do not always reflect what happens in case of human mutations. For example, deletion of the closest down-stream neighbour of *Myg1*, *Aaas*, in mice did not produce any symptoms that are typical for triple A syndrome that will develop in humans with mutations in *AAAS* gene (Huebner *et al*, 2006). Therefore it would still be interesting to study the distribution and effects of Myg1 Arg4Gln polymorphism in several human populations.

8. Implication of Myg1 in immune response

Several global expression profiling reports support Myg1 involvement in immune response (Cao *et al*, 2004; Taylor *et al*, 2004; Axelsson *et al*, 2007; Zarate-Blades *et al*, 2009). However, it seems that Myg1 can be upregulated or downregulated in the context of immune response: *MYG1* expression is 2.78-fold decreased 24 hours after infection of human endothelial cell culture with *Trypanosoma cruzi* parasite (Costales *et al*, 2009). At the same time *Myg1* is up-regulated in the skin of patients with atopic eczema that is chronic inflammatory skin disease and characterized by abundant up-regulation of inflammatory genes (Sääf *et al*, 2008). Therefore, the alteration of Myg1 in immune response is most likely dependent on specificity of the immune reaction: whether it is chronic *vs* acute or whether it involves innate or adaptive immune system. Immune reaction-related genes were consistently up-regulated after siRNA mediated *MYG1* knockdown in HeLa cells. Two genes, guanylate binding protein 1, interferon-inducible, 67kDa (GBP1, NM_002053) and guanylate binding protein 2, interferon-inducible (GBP2, NM_004120) were more than two-fold up-regulated after *MYG1* knockdown. GBP1 and GBP2 are among the most abundant antiviral proteins induced by interferon-gamma that induces the expression of many genes to orchestrate a cellular response and establish the antiviral state of the cell (Prakash *et al*, 2000). Other immune response-related genes that are up-regulated after *MYG1* knockdown are CD59 molecule, complement regulatory protein (NM_000611) and UL16 binding protein 2 (ULBP2, NM_025217). ULBP2 is part of MHC class I-related cell surface protein family (ULBPs) (Cosman *et al*, 2001). ULBPs are human ligands for NKG2D (natural killer group 2D) that is one of the major triggering receptors of natural killer (NK) cells (Sutherland *et al*, 2006). Additionally, almost the whole family of MHC-I genes (major histocompatibility complex, class I, A, B, C, E, F and G) was significantly up-regulated after knockdown of *MYG1* transcript. However, two siRNAs induced a remarkably different increase in MHC-I genes: siRNA1 induced on average 1.3-fold increase ($p<0.05$) whereas siRNA3 induced much more extensive 1.9-fold increase in MHC-I transcripts ($p<0.01$, data not shown). We could not explain the different effect of two siRNAs as with both the *Myg1* knockdown effect was detected to be equally 90%. However, the notion that the activation of immune response related genes is specific for *MYG1* siRNA treatment is supported by previous knockdown experiments where no such changes were seen for unrelated siRNAs (Vikeså *et al*, 2006).

Because our siRNA knockdown of *MYG1 in vitro* produced a robust up-regulation of several immune reaction-related genes, we anticipated that the *Myg1* knockout *in vivo* could lead to alterations in the response to immune challenge. In the current study we could not get statistically significant effects in immune reaction in *Myg1*-deficient mice, however, considering the simple design of our preliminary experiment, we saw promising tendencies: both male and female *Myg1*-defficent mice lost more weight in response to administration

of LPS (50 ug/ul) than wild-type males and females. These tendencies have encouraged us to design more specific tests to detect subtle differences in mice lacking *Myg1* (-/-) and further studies employing more sophisticated methods are currently on their way.

9. Myg1 in the skin: elevated expression of *MYG1* gene in vitiligo and promoter genotype

Besides brain, *Myg1* expression can be altered in disease processes in the skin. As cited above, *Myg1* gene was initially found to be highly expressed in freely proliferating mouse melanocytes compared with melanoma cells (Smicun, 2000). The initial naming of *Myg1* was somewhat misleading, because the main finding in the initial study was actually down-regulation of *Myg1* transcript in melanoma cells compared with control cells (normal melanocytes). According to Su *et al* (2004), the expression level of *MYG1* transcript in human skin is rather under average, compared with other human tissues. However, another study indicates the relevance of *MYG1* in the skin: *MYG1* is up-regulated in the skin of patients with atopic eczema that is a chronic inflammatory skin disease, characterized by abundant up-regulation of inflammatory genes (Sääf *et al*, 2008).

In the present study we showed that *MYG1* mRNA expression is elevated in the skin of vitiligo patients (Kingo *et al*, 2006). Furthermore, *MYG1* mRNA levels in the skin samples of healthy controls correlate with *MYG1* promoter polymorphism -119C/G and subjects with homozygous -119G allele have significantly higher *MYG1* mRNA levels than subjects with homozygous -119C allele. Higher activity of -119G promoter was confirmed by using *in vitro* luciferase reporter assay. -119G promoter was on average more than 2.5 fold more active regardless of the length of the promoter fragment. Single marker association analysis showed that the active -119G allele was more frequent in vitiligo patients compared to controls. Further analysis based on the stage of progression of vitiligo revealed that the increased frequency of more active -119G allele occurred prevalently in the group of patients with active vitiligo compared to the control group. This finding is in line with our data of *MYG1* expression in the skin of vitiligo patients, where no difference in *MYG1* expression between nonlesional skin of stable subtype of vitiligo and healthy control subjects was detected. At the same time a statistically significant increase in *MYG1* expression in both lesional and nonlesional skin of patients with active vitiligo and in lesional skin of patients with stable vitiligo was found, raising the possibility that *MYG1* is least reactive in the stable stage unaffected vitiligo skin. According to growing evidence, the *MYG1* gene is predominantly implicated in actively progressing vitiligo.

Minor allele -119G was related to higher *MYG1* mRNA levels only in the control group, but not in the vitiligo group. In general, *MYG1* mRNA is elevated in both involved and uninvolved skin of vitiligo patients despite active

or less active promoter genotype. This finding suggests that increased *MYG1* mRNA level in the skin of vitiligo patients is only partially dependent on endogenous promoter activity and there are other factors besides -119C/G polymorphism that mediate *MYG1* expression levels in the skin of vitiligo patients. It is likely that part of the effect of increased *MYG1* expression in vitiligo comes from higher prevalence of naturally more active -119G promoter carriers in the vitiligo group. We propose that the elevation of *MYG1* expression in vitiligo can be both cause and effect, depending on the case. Vitiligo patients with -119G promoter have genetic inclination for higher expression and patients with less active promoter genotype harbour other genetic susceptibility loci, but *MYG1* expression in their skin is still increased as a consequence of cellular changes that characterize vitiligo skin. Alteration of p300 (E1A-associated 300 kDa protein) binding site is a potential reason why *MYG1* -119G promoter allele is more active in normal control subjects and *in vitro* luciferase assay. The analysis of binding sites in the -119 promoter region was performed by using TRANSFAC software Consensus DNA binding sequence for p300 is 5'-GGGAGTG-3' (Rikitake & Moran, 1992) that corresponds 100% to the bases from -125 to -119 of *MYG1*-119G allele. *MYG1*-119C alters the last position of this site (5'-GGGAGTC-3'), p300 that is mostly known as histone deacetylase can also act as a bridge or scaffold between transcription factors and the basal transcription machinery to enhance the transcription activation (Chan & La Thangue, 2001). However, besides p300 there can be other transcriptional or epigenetic factors that are sensitive to *MYG1*-119C/G substitution.

10. Possible mechanisms that link Myg1 with vitiligo

The expression pattern of Myg1 is ubiquitous, but there is evidence that Myg1 function in the skin can be differential; for example, during embryonic development, *Myg1* is predominantly expressed in the ectoderm derived tissues, including epidermis, indicating that Myg1 is involved in the development of skin, therefore Myg1 function in the skin can be specific at least in some phases of development. Our association analysis and expression studies suggest that *MYG1* is one of the genes that, in interaction with other genetic and environmental factors, are responsible for the development of vitiligo. However, *MYG1* expression in the skin seems to be not specific to melanocytes: according to our preliminary results, *MYG1* expression in cultured melanocytes is lower than expression in full skin biopsy and comparable or equal with *MYG1* expression in cultured fibroblasts derived from the same skin (data not shown). Therefore the precise function of *MYG1* in the development of vitiligo is still unclear, but we have two major speculations: up-regulation of several immune system-related genes after *MYG1* siRNA knockdown in cell culture suggests that Myg1 can act as a mediator in the immune processes that are disturbed in vitiligo patients. Several theories have been proposed about the mechanism of vitiligo pathogenesis, but autoimmune hypothesis is the most popular at present

(Westerhof & d'Ischia, 2007) and a recent comprehensive review about vitiligo genetics (Spritz, 2007) emphasizes that genetic factors underlying autoimmune diseases and vitiligo are often overlapping. Besides immunological approach, the study of the metabolic deregulations leading to toxic damage of the melanocytes appears to be more and more relevant (Dell'Anna & Piqardo, 2006). Therefore, alternatively: mitochondrially localized Myg1 can be involved in the regulation of altered metabolism and imbalance of antioxidants in vitiligo. Growing amount of data provides further evidence for an altered mitochondrial functionality of vitiligo patients (Dell'Anna *et al*, 2003; Prignano *et al*, 2009). Different authors suggest that oxidative stress plays a central role in the process of melanocyte degradation (Dell'Anna *et al*, 2003; Dell'Anna & Piqardo, 2006; Maresca *et al*, 1997; Jimbow *et al*, 2001). The fact that *MYG1* expression is elevated in both uninvolved and involved skin in case of vitiligo is in line with findings that melanocytes from normally pigmented skin of vitiligo patients also exhibit high *in vitro* susceptibility to chemical and physical oxidative stress (Dell'Anna & Piqardo, 2006). Further studies will be needed to explain the mechanisms of vitiligo pathogenesis and to understand the precise function of Myg1 in vitiligo.

11. Sex specific regulation and expression of Myg1

During our studies we found several unexpected sex-specific differences in *Myg1* knockout effects and *MYG1* expression levels. *Myg1* (-/-) mice indicate an absence of several sex-dependent behavioural differences that are evident in wild-type (+/+) mice. Compared to male (+/+) mice female wild-type (+/+) mice were significantly less anxious (plus-maze test, % center distance in the locomotor activity test, stress-induced hyperthermia, hyponeophagia test), more active (locomotor activity test), and showed a more intense endocrine response to restraint (corticosterone elevation). By contrast, in *Myg1* (-/-) mice no sex-dependent differences were found in the plus-maze test, locomotor activity test, hyponeophagia test and restraint-induced corticosterone elevation. Yet, in the stress-induced hyperthermia test sex-dependent differences were obvious in both genotypes, whereas in the social interaction test a difference between male and female mice observed in *Myg1* (-/-) mice was not noted in wild-type (+/+) mice. Sex-dependent differences across various physiological functions in rodents are well established. It has been found that the prevalence of sex-specific differences is dependent on mouse strain (Rodgers & Cole, 1993). It is possible, according to our present data, that *Myg1* is another gene that contributes to the expression of sex-dependent behavioural differences in mice.

We also detected sex-specific differences in the skin of normal control subjects. In our study male controls had significantly lower *MYG1* expression than female controls. There are reports that vitiligo occurs twice as often in female than in male (Westerhof & d'Ischia, 2007). Our finding that in case of vitiligo *MYG1* expression is increasing is in line with naturally higher *MYG1*

expression in women. For a long time, it has been suggested that estrogens may be involved in the depigmentation process of vitiligo, because the initiation/ progression of the disease is observed at pregnancy, postpartum, in the menopause or after the use of oral contraceptives/hormonal substitution (Schallreuter *et al*, 2006). Cheng *et al* (2006) identified *MYG1* as a putative estrogen receptor alpha target gene. Therefore it is possible that Myg1 can regulate hormonal balance directly through estrogen receptor. However, most studies report no difference in occurrence of vitiligo between males and females (Alkhateeb *et al*, 2003); still, sex-specific findings in our study provide interesting data that should be considered during planning or interpreting further experiments.

12. Concluding remarks and future prospects

Myg1 is widely expressed and highly conserved factor that localizes to the nucleus and the mitochondria. *Myg1* expression in normal adult tissues is ubiquitous and homogenous but can be changed as a response to several environmental stimuli affecting the cellular activity. In different embryonic phases *Myg1* expression is characterized by dynamic expression intensity and specific pattern indicating developmental impact of Myg1.

In the current study we have linked Myg1 with various cellular functions. However, these cellular processes are not completely distinctive, but intertwined with each other: alterations in immune response are tightly related with cellular malignancy; cell cycle related pathways are directly implicated in pluripotency, differentiation and development. Finally, cellular metabolism is related with cellular activity in every level: increased metabolism is coupled with cell activation during immune reaction or cell division. Our suggestion is that the function of Myg1 is essentially basic because it has been crucial to maintain *Myg1* gene from protozoans to humans.

To elucidate the more specific function of Myg1, it would be critical to study Myg1 in functional assays. The hypothesis that Myg1 is a putative phosphoesterase comes from sequence homology studies. The next goal would be to target the real substrates for Myg1. Several potential candidates have been suggested in this study (Oct4, TLX, FGF2, Decorin, Atp5g2, Hsp90, Hsp60, GBP1, GBP2, MHC-I related proteins, *etc*). Also, it would be informative to measure the expression level of *Myg1* transcript in different cell types in the skin and testis.

One of our most promising tools in the study of Myg1 function *in vivo* will be *Myg1*-deficient mice. Tissue samples of *Myg1*-defficent mice could be used as a knockout tissue model. The compensatory mechanisms will always remain a significant problem in knockout studies (Clifton *et al*, 2003), however, it would be informative to study mild gene effects, such as *Myg1*-deficiency, in another genetical background (Crawley, 2008). Based on the experiments we still hypothesize that Myg1 is needed in critical stress situations, therefore, one of the next experiments would be to induce more severe immunological

challenge to *Myg1* knockout mice than we did during the current experiments. Additionally, we are planning to screen metabolic processes of these mice in more detail.

If we are able to gain more information about Myg1 in the cell, it could hopefully help to explain the mechanism why *MYG1* has elevated expression in the skin of vitiligo patients, how big is the implication of *MYG1* promoter activity in elevated levels of the transcript and what is the specific function of Myg1 in actively progressing vitigo. Our data is currently correlative and we have only some suggestions concerning the cellular pathways linking Myg1 with vitiligo. Finally, it would be extremely informative to solve the question what happens with subjects who carry homozygous Myg1 4Gln genotype: a mutation that disturbs mitochondrial entrance of Myg1 in the population of Nigeria. So far we know that HapMap only includes data from Myg1 Arg4Gln heterozygous and Myg1 4Arg homozygous subjects. There is currently no information why Myg1 4Gln homozygous subjects are not present in HapMap database.

CONCLUSIONS

1. Myg1 protein is a ubiquitously expressed and highly conserved factor. In adult tissues *Myg1* mRNA expression is ubiquitous and homogenous; in different embryonic phases *Myg1* expression is characterized by specific pattern and dynamic intensity, indicating developmental impact of Myg1.
2. Myg1 localizes in the nucleus and mitochondria and we also demonstrated the existence of nuclear and mitochondrial targeting signals in the N-terminal region of human and mouse Myg1 proteins. We showed that Myg1 4Gln allele that has remarkable prevalence in the Nigerian population disturbs mitochondrial entrance of Myg1. Because our subjects from the Estonian population were consistently homozygous for Myg1 4Arg allele, we cannot confirm the relevance of Myg1 Arg4Gln, but our current results suggest that Myg1 has important functions in the mitochondria. According to our studies it is most likely that Myg1 is involved in cellular pathways implicated in cellular stress, immune response, development and metabolism.
3. Phenotyping of *Myg1*-deficient mice revealed that *Myg1* (-/-) mice are vital, fertile and display no gross abnormalities. *Myg1*-deficiency caused moderate alterations in anxiety-related behaviour and stress-reactions in mice, but also remarkable reduction of sex-dependent behavioural differences. In our primary screen, *Myg1*-deficient mice displayed no significant alterations in immune response or metabolic activity, but several mild tendencies encourage us to study these functions further in *Myg1* (-/-) mice.
4. Both *MYG1* promoter polymorphism -119C/G and Arg4Gln polymorphism in the mitochondrial signal of Myg1 have an impact on the function of the *MYG1* gene and protein. Our *in vivo* and *in vitro* promoter activity analysis together with association analysis confirms that -119C/G polymorphism influences *MYG1* mRNA levels. Our results suggest that more active -119G is the risk-allele for the development of vitiligo and more specifically risk-allele for the maintenance of the active progression stage of the disease.

REFERENCES

[1] Abramov U, Raud S, Innos J, Lasner H, Kurrikoff K, Türna T, Puussaar T, Õkva K, Matsui T, Vasar E (2008). Different housing conditions alter the behavioral phenotype of CCK_2 receptor deficient mice. *Behav Brain Res* **193**(1):108–16.

[2] Alkhateeb A, Fain PR, Thody A, Bennett DC, Spritz RA (2003). Epidemiology of vitiligo and associated autoimmune diseases in Caucasian probands and their families. *Pigment Cell Res* **16**(3):208–14.

[3] Aravind L & Koonin EV (1998). A novel family of predicted phosphoesterases includes Drosophila prune protein and bacterial RecJ exonuclease. *Trends Biochem Sci* **23**:17–9.

[4] Areda T, Raud S, Philips MA, Innos J, Matsui T, Kõks S, Vasar E, Karis A, Asser T (2006). Cat odour exposure decreases exploratory activity and alters neuropeptide gene expression in CCK(2) receptor deficient mice, but not in their wild-type littermates. *Behav Brain Res* **169**(2):212–9.

[5] Audebert M, Charbonnier JB, Boiteux S, Radicella JP (2002). Mitochondrial targeting of human 8-oxoguanine DNA glycosylase hOGG1 is impaired by a somatic mutation found in kidney cancer. *DNA Repair* **1**:497–505.

[6] Axelsson H, Lönnroth C, Andersson,M, Wang W, Lundholm, K (2007). Global Tumor RNA Expression in Early Establishment of Experimental Tumor Growth and Related Angiogenesis following Cox-Inhibition Evaluated by Microarray Analysis. *Cancer Informatics* **2**:199–213.

[7] Bakewell MA, Shi P, Zhang J (2007). More genes underwent positive selection in chimpanzee evolution than in human evolution. *Proc Natl Acad Sci U S A* **104**:7489–94.

[8] Baris O, Savagner F, Nasser V, Loriod B, Granjeaud S, Guyetant S, Franc B, Rodien P, Rohmer V, Bertucci F, Birnbaum D, Malthièry Y, Reynier P, Houlgatte R (2004). Transcriptional profiling reveals coordinated up-regulation of oxidative metabolism genes in thyroid oncocytic tumors. *J Clin Endocrinol Metab* **89**(2):994–1005.

[9] Barrett JC, Fry B, Maller J, Daly MJ (2005). Haploview: analysis and visualization of LD and haplotype maps. *Bioinformatics* **21**:263–5.

[10] Braissant O & Wahli W (1998). A simplified in situ hybridization protocol using non-radioactively labelled probes to detect abundant and rare mRNAs on tissue sections. *Biochemica* **1**:10–6.

[11] Cameron JM, Hurd T, Robinson BH (2005). Computational identification of human mitochondrial proteins based on homology to yeast mitochondrially targeted proteins. *Bioinformatics* **21**:1825–30.

[12] Cantile M, Cindolo L, Napodano G, Altieri V, Cillo C (2003). Hyperexpression of locus C genes in the *HOX* network is strongly associated *in vivo* with human bladder transitional cell carcinomas *Oncogene* **22**(41):6462–8.

[13] Canton I, Akhtar S, Gavalas NG, Gawkrodger DJ, Blomhoff A, Watson PF, Weetman AP, Kemp EH (2005). A single-nucleotide polymorphism in the gene encoding lymphoid protein tyrosine phosphatase (PTPN22) confers susceptibility to generalised vitiligo. *Genes Immun* **6**:584–7.

[14] Cao S, Xiang Z, Ma X (2004). Global gene expression profiling in interleukin-12-induced activation of CD8(+) cytotoxic T lymphocytes against mouse mammary Carcinoma. *Cell Mol Immunol* **1**:357–66.

[15] Chan HM & La Thangue NB (2001). p300/CBP proteins: HATs for transcriptional bridges and scaffolds. *J Cell Sci* **14**:2363–73.
[16] Chan WY, Lee TL, Wu SM, Ruszczyk L, Alba D, Baxendale V, Rennert OM (2006). Transcriptome analyses of male germ cells with serial analysis of gene expression (SAGE). *Mol Cell Endocrinol* **250**:8–19.
[17] Chandran UR, Ma C, Dhir R, Bisceglia M, Lyons-Weiler M, Liang W, Michalopoulos G, Becich M, Monzon FA (2007). Gene expression profiles of prostate cancer reveal involvement of multiple molecular pathways in the metastatic process. *BMC Cancer* **7**:64.
[18] Chen D, Toone WM, Mata J, Lyne R, Burns G, Kivinen K, Brazma A, Jones N, Bähler J (2003). Global transcriptional responses of fission yeast to environmental stress. *Mol Biol Cell* **14**(1):214–29.
[19] Chen JJ, Huang W, Gui JP, Yang S, Zhou FS, Xiong QG, Wu HB, Cui Y, Gao M, Li W, Li JX, Yan KL, Yuan WT, Xu SJ, Liu JJ, Zhang XJ (2005). A novel linkage to generalized vitiligo on 4q13-q21 identified in a genome-wide linkage analysis of Chinese families. *Am J Hum Genet* **76**(6):1057–65.
[20] Cheng AS, Jin VX, Fan M, Smith LT, Liyanarachchi S, Yan PS, Leu YW, Chan MW, Plass C, Nephew KP, Davuluri RV, Huang TH (2006). Combinatorial analysis of transcription factor partners reveals recruitment of c-MYC to estrogen receptor-alpha responsive promoters. *Mol Cell* **21**(3):393–404.
[21] Clifton PG, Lee MD, Somerville EM, Kennett GA, Dourish CT (2003). 5-HT1B receptor knockout mice show a compensatory reduction in 5-HT2C receptor function. *Eur J Neurosci* **17**(1):185–90.
[22] Cosman D, Müllberg J, Sutherland CL, Chin W, Armitage R, Fanslow W, Kubin M, Chalupny NJ (2001). ULBPs, novel MHC class I-related molecules, bind to CMV glycoprotein UL16 and stimulate NK cytotoxicity through the NKG2D receptor. *Immunity* **14**(2):123–33.
[23] Costales JA, Daily JP, Burleigh BA (2009). Cytokine-dependent and-independent gene expression changes and cell cycle block revealed in Trypanosoma cruzi-infected host cells by comparative mRNA profiling. *BMC Genomics* **10**:252.
[24] Crawley JN (2007). What's wrong with my mouse?: Behavioral phenotyping of transgenic and knock-out mice, 2nd edition. John Wiley & Sons, Inc., Hoboken, NJ.
[25] Crawley JN (2008). Behavioral phenotyping strategies for mutant mice. *Neuron* **57**, 809–18.
[26] De La Vega FM, Gordon D, Su X, Scafe C, Isaac H, Gilbert DA, Spier EG (2005). Power and sample size calculations for genetic case/control studies using gene-centric SNP maps: application to human chromosomes 6, 21, and 22 in three populations. *Hum Hered* **60**(1):43–60.
[27] Dell'Anna ML, Urbanelli S, Mastrofrancesco A, Camera E, Iacovelli P, Leone G, Manini P, D'Ischia M, Picardo M (2003). Alterations of mitochondria in peripheral blood mononulcear cells of vitiligo patients. *Pigment Cell Res* **16**:553–9.
[28] Dell'Anna ML & Picardo M (2006). A review and a new hypothesis for non-immunological pathogenetic mechanisms in vitiligo. *Pigment Cell Res* **19**(5):406–11.
[29] Deutschbauer AM, Jaramillo DF, Proctor M, Kumm J, Hillenmeyer ME, Davis RW, Nislow C, Giaever G (2005). Mechanisms of haploinsufficiency revealed by genome-wide profiling in yeast. *Genetics* **169**:1915–25.
[30] Dorrell MI, Aguilar E, Weber C, Friedlander M (2004). Global Gene Expression Analysis of the Developing Postnatal Mouse Retina. *Invest Ophthalmol Vis Sci* **45**:1009–19.

[31] Ellis RJ (2003). Molecular chaperones: Plugging the transport gap. *Nature* **421**:801–2.
[32] Falsone SF, Gesslbauer B, Tirk F, Piccinini AM, Kungl AJ (2005). A proteomic snapshot of the human heat shock protein 90 interactome. *FEBS Lett* **579**:6350–4.
[33] Fitzsimons HL, Bland RJ, During MJ (2002). Promoters and regulatory elements that improve adeno-associated virus transgene expression in the brain. *Methods* **28**:227–36.
[34] Foltz G, Yoon JG, Lee H, Ryken TC, Sibenaller Z, Ehrich M, Hood L, Madan A (2009). DNA methyltransferase-mediated transcriptional silencing in malignant glioma: a combined whole-genome microarray and promoter array analysis. *Oncogene* **28**(29):2667–77.
[35] Foygel K, Choi B, Jun S, Leong DE, Lee A, Wong CC, Zuo E, Eckart M, Reijo Pera RA, Wong WH, Yao MW (2008). A novel and critical role for Oct4 as a regulator of the maternal-embryonic transition. *PLoS One* **3**(12):e4109.
[36] Golan-Mashiach M, Dazard JE, Gerecht-Nir S, Amariglio N, Fisher T, Jacob-Hirsch J, Bielorai B, Osenberg S, Barad O, Getz G, Toren A, Rechavi G, Itskovitz-Eldor J, Domany E, Givol D (2005). Design principle of gene expression used by human stem cells: implication for pluripotency. *Faseb J* **19**(1):147–9.
[37] Grant DS, Yenisey C, Rose RW, Tootell M, Santra M, Iozzo RV (2002). Decorin suppresses tumor cell-mediated angiogenesis. *Oncogene* **21**(31):4765–77.
[38] Grover GJ, Marone PA, Koetzner L, Seto-Young D (2008). Energetic signalling in the control of mitochondrial F_1F_0 ATP synthase activity in health and disease. *Int J Biochem Cell Biol* **40**(12):2698–701.
[39] Hackl H, Burkard TR, Sturn A, Rubio R, Schleiffer A, Tian S, Quackenbush J, Eisenhaber F, Trajanoski Z (2005). Molecular processes during fat cell development revealed by gene expression profiling and functional annotation. *Genome Biol* **6**:R108.
[40] Hawse JR, Hejtmancik JF, Huang Q, Sheets NL, Hosack DA, Lempicki RA, Horwitz J, Kantorow M (2003). Identification and functional clustering of global gene expression differences between human age-related cataract and clear lenses. *Mol Vis* **9**:515–37.
[41] Heazlewood JL, Tonti-Filippini JS, Gout AM, Day DA, Whelan J, Millar AH (2004). Experimental analysis of the Arabidopsis mitochondrial proteome highlights signaling and regulatory components, provides assessment of targeting prediction programs, and indicates plant-specific mitochondrial proteins. *Plant Cell* **16**:241–56.
[42] Hirokawa T, Boon-Chieng S, Mitaku S (1998). SOSUI: classification and secondary structure prediction system for membrane proteins. *Bioinformatics* **14**(4): 378–9.
[43] Hong SJ, Li H, Becker KG, Dawson TM (2004). Identification and analysis of plasticity-induced late response genes. *Proc Natl Acad Sci U S A* **101**(7):2145–50.
[44] Huebner A, Mann P, Rohde E, Kaindl AM, Witt M, Verkade P, Jakubiczka S, Menschikowski M, Stoltenburg-Didinger G, Koehler K (2006). Mice lacking the nuclear pore complex protein ALADIN show female infertility but fail to develop a phenotype resembling human triple A syndrome. *Mol Cell Biol* **26**(5):1879–87.
[45] Jimbow K, Chen H, Park JS, Thomas PD (2001). Increased sensitivity of melanocytes to oxidative stress and abnormal expression of tyrosinase-related protein in vitiligo. *Brit J Dermatol* **144**(1):55–65.

[46] Jin Y, Mailloux CM, Gowan K, Riccardi SL, LaBerge G, Bennett DC Fain PR, Spritz RA (2007). *NALP1* in Vitiligo-Associated Multiple Autoimmune Disease. *N Engl J Med* **356**(12):1216–25.
[47] Johnson-Anuna LN, Eckert GP, Keller JH, Igbavboa U, Franke C, Fechner T, Schubert-Zsilavecz M, Karas M, Müller WE, Wood WG (2005). Chronic administration of statins alters multiple gene expression patterns in mouse cerebral cortex. *J Pharmacol Exp Ther* **312**(2):786–93.
[48] Jønson L, Vikeså J, Krogh A, Nielsen LK, Hansen T, Borup R, Johnsen AH, Christiansen J, Nielsen FC (2007). Molecular composition of IMP1 ribonucleoprotein granules. *Mol Cell Proteomics* **6**(5):798–811.
[49] Kamath RS, Fraser AG, Dong Y, Poulin G, Durbin R, Gotta M, Kanapin A, Le Bot N, Moreno S, Sohrmann M, Welchman DP, Zipperle P, Ahringer J (2003). Systematic functional analysis of the Caenorhabditis elegans genome using RNAi. *Nature* **421**(6920):231–7.
[50] Kaufman MH (1995). The Atlas of Mouse Development. Academic Press Ltd., London.
[51] Kimura Y, Nagao A, Fujioka Y, Satou A, Taira T, Iguchi-Ariga SM, Ariga H (2007). MM-1 facilitates degradation of c-Myc by recruiting proteasome and a novel ubiquitin E3 ligase. *Int J Oncol* **31**(4):829–36.
[52] Kingo K, Philips MA, Aunin E, Luuk H, Karelson M, Rätsep R, Silm H, Vasar E, Kõks S (2006). *MYG1*, novel melanocyte related gene, has elevated expression in vitiligo. *J Dermatol Sci* **44**(2):119–22.
[53] Kingo K, Aunin E, Karelson M, Rätsep R, Silm H, Vasar E, Kõks S (2008). Expressional changes in the intracellular melanogenesis pathways and their possible role the pathogenesis of vitiligo. *J Dermatol Sci* **52**(1):39–46.
[54] Koehler K, Brockmann K, Krumbholz M, Kind B, Bönnemann C, Gärtner J, Huebner A (2008). Axonal neuropathy with unusual pattern of amyotrophy and alacrima associated with a novel *AAAS* mutation p.Leu430Phe. *Eur J Hum Genet* **16**(12):1499–506.
[55] Kõks S, Luuk H, Nelovkov A, Areda T, Vasar E (2004). A screen for genes induced in the amygdaloid area during cat odor exposure. *Genes Brain Behav* **3**:80–9.
[56] Kristensen AR, Schandorff S, Høyer-Hansen M, Nielsen MO, Jäättelä M, Dengjel J, Andersen JS (2008). Ordered organelle degradation during starvation-induced autophagy. *Mol Cell Proteomics* **7**(12):2419–28.
[57] Kültz D (2003). Evolution of the cellular stress proteome: from monophyletic origin to ubiquitous function. *J Exp Biol* **206**:3119–24.
[58] Lee SA, Chan CH, Tsai CH, Lai JM, Wang FS, Kao CY, Huang CY (2008). Ortholog-based protein-protein interaction prediction and its application to inter-species interactions. *BMC Bioinformatics* 9(Suppl 12):S11.
[59] Lehtonen A, Lund R, Lahesmaa R, Julkunen I, Sareneva T, Matikainen S (2003). IFN-alpha and IL-12 activate IFN regulatory factor 1 (IRF-1), IRF-4, and IRF-8 gene expression in human NK and T cells. *Cytokine* **24**(3):81–90.
[60] Liang WS, Dunckley T, Beach TG, Grover A, Mastroeni D, Ramsey K, Caselli RJ, Kukull WA, McKeel D, Morris JC, Hulette CM, Schmechel D, Reiman EM, Rogers J, Stephan DA (2008). Altered neuronal gene expression in brain regions differentially affected by Alzheimer's disease: a reference data set. *Physiol Genomics* **33**(2):240–56.
[61] Little PFR (2005). Structure and function of the human genome. *Genome Res* **15**:1759–66.

[62] Loh YH, Wu Q, Chew JL, Vega VB, Zhang W, Chen X, Bourque G, George J, Leong B, Liu J, Wong KY, Sung KW, Lee CW, Zhao XD, Chiu KP, Lipovich L, Kuznetsov VA, Robson P, Stanton LW, Wei CL, Ruan Y, Lim B, Ng HH (2006). The Oct4 and Nanog transcription network regulates pluripotency in mouse embryonic stem cells. *Nat Genet* **38**(4):431–40.

[63] Luuk H, Kõks S, Plaas M, Hannibal J, Rehfeld JF, Vasar E (2008). Distribution of Wfs1 protein in the central nervous system of the mouse and its relation to clinical symptoms of the Wolfram syndrome. *J Comp Neurol* **509**(6):642–60.

[64] Luuk H, Plaas M, Raud S, Innos J, Sütt S, Lasner H, Abramov U, Kurrikoff K, Kõks S, Vasar E (2009). Wfs1-deficient mice display impaired behavioural adaptation in stressful environment. *Behav Brain Res* **198**:334–45.

[65] Lü X, Bao X, Huang Y, Qu Y, Lu H, Lu Z (2009). Mechanisms of cytotoxicity of nickel ions based on gene expression profiles. *Biomaterials* **30**:141–8.

[66] Machado Filho CD, Almeida FA, Proto RS, Landman G (2005). Vitiligo: analysis of grafting versus curettage alone, using melanocyte morphology and reverse transcriptase polymerase chain reaction for tyrosinase mRNA. *Sao PauloMed J* **123**(4):187–91.

[67] Maresca V, Roccella M, Roccella F, Camera E, Del Porto G, Passi S, Grammatico P, Picardo M (1997). Increased sensitivity to peroxidative agents as possible pathogenic factor of melanocyte damage in vitiligo. *J Invest Dermatol* **109**(3):310–3.

[68] Mathavan S, Lee SG, Mak A, Miller LD, Murthy KR, Govindarajan KR, Tong Y, Wu YL, Lam SH, Yang H, Ruan Y, Korzh V, Gong Z, Liu ET, Lufkin T (2005). Transcriptome Analysis of Zebrafish Embryogenesis Using Microarrays. *PLoS Genet* **1**(2):260–76.

[69] McIlwain KL, Merriweather MY, Yuva-Paylor LA, Paylor R (2001). The use of behavioral test batteries: effects of training history. *Physiol Behav* **73**:705–17.

[70] Millson SH, Truman AW, King V, Prodromou C, Pearl LH, Piper PW (2005). A two-hybrid screen of the yeast proteome for Hsp90 interactors uncovers a novel Hsp90 chaperone requirement in the activity of a stress-activated mitogen-activated protein kinase, Slt2p (Mpk1p). *Eukaryot Cell* **4**(5):849–60.

[71] Mishra S, Murphy LC, Nyomba BL, Murphy LJ (2005). Prohibitin: a potential target for new therapeutics. *Trends Mol Med* **11**(4):192–7.

[72] Nakai K & Horton P (1999). PSORT: a program for detecting sorting signals in proteins and predicting their subcellular localization. *Trends Biochem Sci* **24**:34–6.

[73] Nepomuceno-Silva JL, De Melo LD, Mendonça SM, Paixão JC, Lopes UG (2004). Characterization of Trypanosoma cruzi TcRjl locus and analysis of its transcript. *Parasitology* **129**(3):325–33.

[74] Njung'e K & Handley SL (1991). Evaluation of marble burying behavior as a model of anxiety. *Pharmacol Biochem Behav* **38**:63–7.

[75] Ortega S, Ittmann M, Tsang SH, Ehrlich M, Basilico C (1998). Neuronal defects and delayed wound healing in mice lacking fibroblast growth factor 2. *Proc Natl Acad Sci U S A* **95**(10):5672–7.

[76] Paxinos G & Watson C (2000). The Mouse Brain in Stereotaxic Coordinates. Academic Press, San Diego.

[77] Picard D (2006). Intracellular dynamics of the Hsp90 co-chaperone p23 is dictated by Hsp90. *Exp Cell Res* **312**:198–204.

[78] Prakash B, Praefcke GJ, Renault L, Wittinghofer A, Herrmann C (2000). Structure of human guanylate-binding protein 1 representing a unique class of GTP-binding proteins. *Nature* **403**:567–71.

[79] Prignano F, Pescitelli L, Becatti M, Di Gennaro P, Fiorillo C, Taddei N, Lotti T (2009). Ultrastructural and functional alterations of mitochondria in perilesional vitiligo skin. *J Dermatol Sci* **54**:157–67.

[80] Rickhag M, Wieloch T, Gidö G, Elmér E, Krogh M, Murray J, Lohr S, Bitter H, Chin DJ, von Schack D, Shamloo M, Nikolich K (2006). Comprehensive regional and temporal gene expression profiling of the rat brain during the first 24 h after experimental stroke identifies dynamic ischemia-induced gene expression patterns, and reveals a biphasic activation of genes in surviving tissue. *J Neurochem* **96**(1):14–29.

[81] Rikitake Y & Moran E (1992). DNA-binding properties of the E1A-associated 300-kilodalton protein. *Mol Cell Biol* **2**:2826–36.

[82] Rodgers RJ & Cole JC (1993). Influence of social isolation, gender, strain, and prior novelty on plus-maze behaviour in mice. *Physiol Behav* **54**:729–36.

[83] Rogers MA, Edler L, Winter H, Langbein L, Beckmann I, Schweizer J (2005). Characterization of New Members of the Human Type II Keratin Gene Family and a General Evaluation of the Keratin Gene Domain on Chromosome 12q13.13. *J Invest Dermatol* **124**:536–44.

[84] Rustici G, Mata J, Kivinen K, Lió P, Penkett CJ, Burns G, Hayles J, Brazma A, Nurse P, Bähler J (2004). Periodic gene expression program of the fission yeast cell cycle. Nat Genet **36**(8):809–17.

[85] Sääf AM, Tengvall-Linder M, Chang HY, Adler AS, Wahlgren CF, Scheynius A, Nordenskjöld M, Bradley M (2008). Global Expression Profiling in Atopic Eczema Reveals Reciprocal Expression of Inflammatory and Lipid Genes. *PloS One* **3**(12):e4017.

[86] Sato S, Roberts K, Gambino G, Cook A, Kouzarides T, Goding CR (1997). CBP/p300 as a co-factor for the Microphthalmia transcription factor. *Oncogene* **14**:3083–92.

[87] Schallreuter KU, Chiuchiarelli G, Cemeli E, Elwary SM, Gillbro JM, Spencer JD, Rokos H, Panske A, Chavan B, Wood JM, Anderson D (2006). Estrogens can contribute to hydrogen peroxide generation and quinone-mediated DNA damage in peripheral blood lymphocytes from patients with vitiligo. *J Invest Dermatol* **126**(5):1036–42.

[88] Schallreuter KU, Bahadoran P, Picardo M, Slominski A, Elassiuty YE, Kemp EH, Giachino C, Liu JB, Luiten RM, Lambe T, Le Poole IC, Dammak I, Onay H, Zmijewski MA, Dell'Anna ML, Zeegers MP, Cornall RJ, Paus R, Ortonne JP, Westerhof W (2008). Vitiligo pathogenesis: autoimmune disease, genetic defect, excessive reactive oxygen species, calcium imbalance, or what else? *Exp Dermatol* **17**(2):139–40.

[89] Sharov AA, Piao Y, Matoba R, Dudekula DB, Qian Y, VanBuren V, Falco G, Martin PR, Stagg CA, Bassey UC, Wang Y, Carter MG, Hamatani T, Aiba K, Akutsu H, Sharova L, Tanaka TS, Kimber WL, Yoshikawa T, Jaradat SA, Pantano S, Nagaraja R, Boheler KR, Taub D, Hodes RJ, Longo DL, Schlessinger D, Keller J, Klotz E, Kelsoe G, Umezawa A, Vescovi AL, Rossant J, Kunath T, Hogan BL, Curci A, D'Urso M, Kelso J, Hide W, Ko MS (2003). Transcriptome analysis of mouse stem cells and early embryos. *PLoS Biol* **1**(3):410–9.

[90] Shi L, Fateimi H, Sidwell RW, Patterson PH (2003). Maternal influenza infection causes marked behavioral and pharmacological changes in the offspring. *J Neurosci* **23**:297–302.

[91] Shimoda-Matsubayashi S, Matsumine H, Kobayashi T, Nakagawa-Hattori Y, Shimizu Y, Mizuno Y (1996). Structural Dimorphism in the Mitochondrial Targeting Sequence in the Human Manganese Superoxide Dismutase Gene A Predictive Evidence for Conformational Change to Influence Mitochondrial Transport and a Study of Allelic Association in Parkinson's Disease. *Biochem Biophys Res Commun* **226**:561–5.

[92] Smicun Y (2000). The human homologue of *MYG1* the highly conserved gene from autonomously proliferating mouse melanocytes: *Swiss Institute of Bioinformatics*.

[93] Spritz RA, Gowan K, Bennett DC, Fain PR (2004). Novel vitiligo susceptibility loci on chromosomes 7 (AIS2) and 8 (AIS3), confirmation of SLEV1 on chromosome 17, and their roles in an autoimmune diathesis. *Am J Hum Genet* **74**:188–91.

[94] Spritz RA (2007). The genetics of generalized vitiligo and associated autoimmune diseases. *Pigment Cell Res* **20**:271–8.

[95] Steinmetz LM, Scharfe C, Deutschbauer AM, Mokranjac D, Herman ZS, Jones T, Chu AM, Giaever G, Prokisch H, Oefner PJ, Davis RW (2002). Systematic screen for human disease genes in yeast. *Nat Genet* **31**(4):400–4.

[96] Su AI, Wiltshire T, Batalov S, Lapp H, Ching KA, Block D, Zhang J, Soden R, Hayakawa M, Kreiman G, Cooke MP, Walker JR, Hogenesch JB (2004). A gene atlas of the mouse and human protein-encoding transcriptomes. *Proc Natl Acad Sci USA* **101**:6062–7.

[97] Sutherland CL, Rabinovich B, Chalupny NJ, Brawand P, Miller R, Cosman D (2006). ULBPs, human ligands of the NKG2D receptor, stimulate tumor immunity with enhancement by IL-15. *Blood* **108**(4):1313–9.

[98] Tanaka TS, Kunath T, Kimber WL, Jaradat SA, Stagg CA, Usuda M, Yokota T, Niwa H, Rossant J, Ko MS (2002). Gene Expression Profiling of Embryo-Derived Stem Cells Reveals Candidate Genes Associated With Pluripotency and Lineage Specificity. *Genome Res* **12**(12):1921–8.

[99] Tasan RO, Lin S, Hetzenauer A, Singewald N, Herzog H, Sperk G (2009). Increased novelty-induced motor activity and reduced depression-like behavior in neuropeptide Y (NPY)-Y4 receptor knockout mice. *Neuroscience* **158**:1717–30.

[100] Taylor MW, Grosse WM, Schaley JE, Sanda C, Wu X, Chien SC, Smith F, Wu TG, Stephens M, Ferris MW, McClintick JN, Jerome RE, Edenberg HJ (2004). Global effect of PEG-IFN-alpha and ribavirin on gene expression in PBMC in vitro. *J Interferon Cytokine Res* **24**(2):107–18.

[101] Tomczak KK, Marinescu VD, Ramoni MF, Sanoudou D, Montanaro F, Han M, Kunkel LM, Kohane IS, Beggs AH (2004). Expression profiling and identification of novel genes involved in myogenic differentiation *Faseb J* 18(2):403–5.

[102] Traherne JA (2008). Human MHC architecture and evolution: implications for disease association studies. *Int J Immunogenet* **35**(3):179–92.

[103] Trnecková L, Armario A, Hynie S, Sída P, Klenerová V (2006). Differences in the brain expression of c-fos mRNA after restraint stress in Lewis compared to Sprague-Dawley rats. *Brain Res* **1077**(1):7–15.

[104] Vainberg IE, Lewis SA, Rommelaere H, Ampe C, Vandekerckhove J, Klein HL, Cowan NJ (1998). Prefoldin, a chaperone that delivers unfolded proteins to cytosolic chaperonin. *Cell* **93**(5):863–73.

[105] van Bakel H, Strengman E, Wijmenga C, Holstege FC (2005). Gene expression profiling and phenotype analyses of S. cerevisiae in response to changing copper reveals six genes with new roles in copper and iron metabolism. Physiol. *Genomics* **22**:356–67.
[106] Vikesaa J, Hansen TV, Jønson L, Borup R, Wewer UM, Christiansen J, Nielsen FC (2006). RNA-binding IMPs promote cell adhesion and invadopodia formation. *EMBO J* **25**(7):1456–68.
[107] Võikar V, Polus A, Vasar E, Rauvala H (2005). Long-term individual housing in C57BL/6J and DBA/2 mice: assessment of behavioral consequences. *Genes Brain Behav* **4**:240–52.
[108] Võikar V, Vasar E, Rauvala H (2004). Behavioral alterations induced by repeated testing in C57BL/6J and 129S2/Sv mice: implications for phenotyping screens. *Genes Brain Behav* **3**:27–38.
[109] Weng T, Chen Z, Jin N, Gao L, Liu L (2006). Gene Expression Profiling Identifies Regulatory Pathways Involved in the Late Stage of Rat Fetal Lung Development. *Am J Physiol Lung Cell Mol Physiol* **291**:L1027–37.
[110] Westerhof W & d'Ischia M (2007). Vitiligo puzzle: the pieces fall in place. *Pigment Cell Res* **20**:345–59.
[111] Wilder JA, Stone JA, Preston EG, Finn LE, Ratcliffe HL, Sudoyo H (2009). Molecular population genetics of *SLC4A1* and Southeast Asian Ovalocytosis. *J Hum Genet* **54**:182–7.
[112] Wilkinson DG (1993). Whole-mount in situ hybridization of vertebrate embryos. In *In situ* Hybridization: A Practical Approach (Wilkinson, D.G. ed.):75–83, IRL Press, Oxford.
[113] Wren JD (2009). A global meta-analysis of microarray expression data to predict unknown gene functions and estimate the literature-data divide. *Bioinformatics* **25**:1694–701.
[114] Yang C, Bolotin E, Jiang T, Sladek FM, Martinez E (2007). Prevalence of the Initiator over the TATA box in human and yeast genes and identification of DNA motifs enriched in human TATAless core promoters. *Gene* **389**:52–65
[115] Zárate-Bladés CR, Bonato VL, da Silveira EL, Oliveira e Paula M, Junta CM, Sandrin-Garcia P, Fachin AL, Mello SS, Cardoso RS, Galetti FC, Coelho-Castelo AA, Ramos SG, Donadi EA, Sakamoto-Hojo ET, Passos GA, Silva CL (2009). Comprehensive gene expression profiling in lungs of mice infected with Mycobacterium tuberculosis following DNAhsp65 immunotherapy. *J Gene Med* **11**(1):66–78.
[116] Zhang XJ, Chen JJ, Liu JB (2005). The genetic concept of vitiligo. *J Dermatol Sci* **39**:137–46.
[117] Zhang CL, Zou Y, He W, Gage FH, Evans RM (2008). A role for adult TLX-positive neural stem cells in learning and behaviour. *Nature* **451**(7181):1004–7.
[118] Zhou Q, Chipperfield H, Melton DA, Wong WH (2007). A gene regulatory network in mouse embryonic stem cells. *Proc Natl Acad Sci U S A* **104**(42): 16438–43.

SUMMARY IN ESTONIAN

Myg1 geeni ja valgu iseloomustamine: ekspressioonimuster, rakusisene lokalisatsioon, geeni puudulikkusega hiir ja funktsionaalsed polümorfismid inimesel

Sissejuhatus

Myg1 geen tuvastati algselt hiirte melanotsüütidest (Smicun, 2000), ning sellest tuleneb ka geeni nimi: "*Melanotsüüte prolifereeriv geen 1*" (*Melanocyte proliferating gene 1*, *Myg1*). Meie laboris tuvastati *Myg1* esmalt geenina, mille ekspressioon rottide amügdalas märkimisväärselt tõusis (1,8 kordne mRNA taseme tõus) pärast seda, kui rotid puutusid 30 minuti jooksul kokku stressitekitava kassilõhnaga (Kõks *et al*, 2004). Järjestuse homoloogia alusel peetakse Myg1 valku oletatavalt fosfoesteraasiks ning lisaks võib andmebaasidest leida informatsiooni, et tegemist on väga konserveerunud geeniga: Myg1 on evolutsiooni käigus säilinud kõikides eukarüootides alates pärmist inimeseni, ent esineb ka mõnedes ainuraksetes algloomades (Nepomuceno-Silva *et al*, 2004). Kuna spetsiifilisemad uurimused Myg1 valgu kohta puudusid, siis viidi käesolevas töös läbi katsed eesmärgiga iseloomustada Myg1 geeni ja valku igakülgselt, alates ekspressioonimustrist ja rakulisest paiknemisest, geeni puudlikkusega hiire fenotüübi iseärasustest ning samuti kirjeldada algselt melanotsüütidest tuvastatud geeni võimalikku osalust pigmentatsioonihäire vitiliigo kujunemisel.

Eesmärgid

Käesoleva töö üldeesmärgiks oli koguda igakülgset informatsiooni *Myg1* geeni ja valgu kohta. Selle uurimistöö spetsiifilised eesmärgid olid järgmised:

1. Iseloomustada *MYG1*/*Myg1* geeni ekspressioonimustrit areneva ning täisealise hiire ja inimese erinevates kudedes ja koelõikudel.
2. Kirjeldada Myg1 valgu rakusisest paiknemist, leida võimalikke interaktsioonipartnereid ning tuvastada rakufunktsioone, milles Myg1 valk osaleb.
3. Luua *Myg1*-puudulikkusega hiiremudel ja iseloomustada selle hiire kognitiivseid ja motoorseid võimeid ning käitumist ja füsioloogilisi reaktsioone ärevuse ja stressimudelites.
4. Uurida algselt melanotsüütidest tuvastatud *MYG1* geeni seotust pigmentatsioonihäire vitiliigoga ning iseloomustada inimese potentsiaalselt funktsionaalseid polümorfisme *MYG1* geenis (-119C/G polümorfism promootoris ja Arg4Gln mitokondriaalses signaalis).

Meetodid

Myg1/*MYG1* geeni ekspressiooni määramiseks inimesel ja hiirel kasutati kvantitatiivset reaalaja-PCR meetodit, transkripti pikkuse määramiseks kasutati Northern analüüsi inimese kudedest ning ekpressioonimustri täpsemaks selgitamiseks kasutati *in situ* hübridisatsiooni hiire täisembrüo- ning täisealise hiire

ajulõikudel. Kõik rakukultuuri eksperimendid viidi läbi HeLa rakukultuuris. Myg1 valgu rakusisese lokalisatsiooni määramiseks viidi normaalne ning ilma oletatavate signaaljärjestusteta *MYG1* geeni cDNA YFP (pEYFP-N1) ning FLAG (pQM-FLAGCTag) markereid sisaldavatesse vektoritesse. *MYG1* promootori aktiivsuse määramiseks viidi 1 kb ja 300 bp suurused *MYG1* promootori fragmendid lutsiferaasi geeni sisaldavasse vektorisse (pGL3-basic). *MYG1* mRNA 90% allasurumise (*knock-down*) indutseerimiseks rakukultuuris kasutati kahte siRNA-d (Qiagen), millest üks seondus eksonite 3 ja 4 ühenduskohta ning teine ekonile 7. *MYG1* transkripti *knock-down* efekt kinnitati kvantitatiivse reaalaja-PCR meetodil ning globaalse rakusisese geenikspressiooni muutuse hindamiseks koguti rakud 72 tundi pärast siRNA-de transfekteerimist ja viidi läbi geenikspressiooni analüüs kasutades Affymetrixi geenikiipe (HG-U133plus2 arrays). Myg1 immuno-pretsipitatsioonil kasutati FLAG-markeriga seotud FLAG-Myg1 liitvalku. *Myg1*-puudulikkusega hiire loomiseks loodi DNA konstrukt, mis sisaldas genoomset järjestust mõlemalt poolt hiire *Myg1* geeni ning viidi see tüvirakkudesse, kus homoloogilise rekombinatsiooni tulemusena asendati markergeeniga (LacZ-NEO) kõik hiire *Myg1* geeni 7 eksonit. Käitumiskatseteks kasutati F2 põlvkonna homosügootseid *Myg1* $^{(+/+)}$ ja *Myg1* $^{(-/-)}$ isaseid ja emaseid pesakonnakaaslasi segataustal. Mutantse hiire fenotüübi määramine viidi läbi kahe erineva testipatareina. Esimeses patareis (hiirte arv igas grupis 21–26) testiti erinevaid käitumuslikke ja füsioloogilisi funktsioone (plusspuur, lokomotoorne aktiivsus, kuuma plaadi test, sotsiaalne interaktsioon, sundujumine, rota-rod, kalorimeeter, Morrise vesipuur ning üldine sensomotoorne kirjeldamine). Teine testipatarei (hiirte arv igas grupis 20–21) hindas spetsiifilisemalt ärevuse ning stressiga seotud reaktsioone (hele-tume puur, kuuli matmine, stressist indutseeritud hüpertermia, hüponeofaagia, saba jõnksatuse test immobiliseerimisest tingitud analgeesia hindamiseks ning LPS-ist indutseeritud kaalukaotus). Lisaks mõõdeti eraldi hiirtel (hiirte arv igas grupis 14–17) immobiliseerimise stressist tingitud kortikosterooni taseme muutust ning *Myg1* ekspressioonitaseme muutust kolmes ajukoes (temporaalsagar, frontaalkoor, mesolimbiline piirkond). *MYG1* geeni osaluse määramiseks vitiligo puhul võrreldi kvantitatiivse real-aja PCR meetodil määratud *MYG1* geeni ekspressiooni taset vitiligopatsientide (n=32) terves ning haiges nahas *MYG1* ekspressioonitasemega tervete kontrollindiviidide nahas (n=27). Samuti võrreldi *MYG1* geeni polümorfismide esinemist vitiligopatsientide (n=124) ja kontrollgrupi (n=325) vahel. Polümorfisme inimese *MYG1* geenis määrati SNPlex genotüpeerimisplatvormil (Applied Biosystems) *MYG1* promootori polümorfismi -119C/G mõju *MYG1* ekspressioonile uuriti lisaks katseisikutele, kelle puhul oli kättesaadav nii genotüübi kui ekspressiooni info (n=52), ka rakukultuuris lutsiferaasi reporteranalüüsil.

Peamised tulemused

Myg1/*MYG1* geeni ekspressioon esines kõikides uuritud inimese ning hiire kudedes, mis viitab geeni väga laialdasele esinemisele organismis. Tuvastasime *Myg1* mRNA tugeva arengulise kõikumise embrüonaalses eas ning *Myg1*

transkripti järk-järgulise vähenemise postnataalselt hiire ajus. Täisealises organismis on *Myg1*/*MYG1* geeni ekspressioon stabiilne ning teistest kudedest märkimisväärselt kõrgem ekspressioon tuvastati vaid testises. Rakusiseselt paikneb Myg1 rakutuumas ning mitokondrites. Oletatavate signaaljärjestuste kustutamisel tegime kindlaks, et esimesed 20 aminohapet on vajalikud Myg1 transportimiseks mitokondritesse ning aminohapped 33–39 toimivad tuuma lokalisatsiooni signaalina. Mõlema signaaljärjestuse kustutamisel lokaliseerus Myg1 valk difuusselt tsütoplasmas. Samuti tuvastasime, et inimestel esinev Arg4Gln polümorfism mõjutab Myg1 valgu transportimist mitokondritesse ning Myg1 4Gln varianti mitokondritesse ei viida. siRNAde poolt indutseeritud *MYG1* mRNA allasurumise järgselt tõusis mitmete immuunsüsteemiga seotud ning arengus oluliste faktorite transkriptide ekspressioonitase. *Myg1*-puudulikkusega hiirtel ei esine nähtavaid arengulisi ja anatoomilisi kõrvalekalded ning tuvastasime vaid mõõdukaid kõrvalekaldeid ärevuse ning stressiga seotud käitumuslikes ja füsioloogilistes reaktsioonides. Märkimisväärne on aga see, et *Myg1*-puudulikkusega emaste ja isaste hiirte vahel ei esine mitmeid soolised erinevused, mis on tavalised metsiktüüpi hiirtele. *MYG1* geeni ekspressioon on tõusnud vitiliigohaigete patsientide kahjustatud nahas. Aktiivse vitiliigo puhul on *MYG1* tase tõusnud ka vitiliigopatsientide terves nahas. Need tulemused on kooskõlas meie assotsiatsiooniuuringutega, kus leidsime, et –119C/G promootori polümorfismi (rs1465073) aktiivsem alleel (G) on vitiliigo puhul riskialleeliks, ning seda just aktiivselt progresseeruva vitiliigoga haigete grupis.

Järeldused

1. *Myg1*/*MYG1* geen kodeerib laialdase ekspressioonimustriga transkripti, millel on dünaamiline ekspressioonitase nii embrüonaalse kui postnataalse arengu käigus. Täiskasvanueas muutub *Myg1*/*MYG1* geeni ekspressioon reaktsioonina erinevatele haigus- või keskkonna seisunditele.
2. Myg1 valk paikneb raku mitokondrites ning tuumas, kuhu valk suunatakse N-terminuses asuvate signaaljärjestuste põhjal. Arg4Gln mutatsioon mõjutab Myg1 valgu transporti mitokondritesse ning Myg1 4 Gln mitokondritesse ei viida. Meie tulemuste kokkuvõttes osaleb Myg1 valk kõige tõenäolisemalt raku stressi, immuunvastuse, arengu ja metabolismiga seotud radades.
3. Ärevuse ja stressiga seotud testides ilmnenud mõõdukad kõrvalekalded *Myg1*-puudulikkusega hiirtel kinnitavad, et Myg1 on vajalik stressiolukordades. Vähenenud soospetsiifilised erinevused *Myg1*-puudulikkusega emaste ja isaste hiirte vahel aga viitavad, et tegemist võib olla faktoriga, mis reguleerib soospetsiifilist käitumist ja füsioloogilisi reaktsioone.
4. -119C/G promootori polümorfismi aktiivsem alleel (G) on vitiliigo puhul riskialleeliks eelkõige aktiivelt progresseeruva vitiliigo haigete grupis. Tõenäoliselt on aktiivsema alleeli sagedasem esinemine seotud kõrgenenud *MYG1* geeni ekspressioonitasemega vitiliigohaigete patsientide kahjustatud nahas ning aktiivse vitiliigo puhul ka vitiliigopatsientide terves nahas.

ACKNOWLEDGEMENTS

The present study was financed by University of Tartu research grant PARFS 07915, Estonian Ministry of Education grants No. SF0180148s08 and SF0180043s07, Estonian Science Foundation Grants 6576 and 7479, the European Union through the European Regional Development Fund and by the Archimedes Foundation.

My sincere gratitude to everyone who contributed to this work directly or indirectly:

- Professor **Eero Vasar** for support and for understanding that my most creative working hours are not from nine to five and from Monday to Friday.
- Professor **Sulev Kõks** for encouragement and the idea to study Myg1 in the first place and for his quick reaction when I decided to make fire on my lab-desk during first autumn in the department.
- People from the Department of Dermatology and Venerology, University of Tartu, especially **Külli Kingo**, for fruitful collaboration.
- Professor **Finn Cilius Nielsen** and professor **Jens Rehfeld** from the Department of Clinical Biochemistry, Rigshospitalet, Copenhagen, Denmark for encouragement, trust and all the resources needed for performing my experiments.
- Labmates from Rigshospitalet: **Susanne**, **Joan**, **Jonas**, **Lars** and **Lis**. Thank you for the good time we had, for sharing the lab space and for discussing many technical issues. I also want to thank my guesthouse friends, especially **Chandra**, **Florence** and **Yohei**, for the nice international dinners we had.
- Labmates from the Department of Physiology: **Kersti**, **Paula**, **Silva**, **Hendrik**, **Urho**, **Mario**, **Kristi**, **Ene**, **Este**, **Indrek**, **Kaido**, **Kati**, **Sirli**, **Tarmo**, **Aleksei**, **Anne**, **Maarja**, **Kertu**, **Anton**, **Ruth**, **Ülle** and **Ranno** for the nice time in the lab we have shared together. It has been a real pleasure to work and have fun with all of you.
- My parents **Ilme** and **Eerik** for constant encouragement and not losing the faith that I will have PhD one day, brother **Jaanus** for teaching me how to fight with boys, aunts **Liia**, **Aili** and **Mare** and cousins **Dr Irene, Dr Margit**, **Dr Pille**, **Dr Kaisa** and **Dr Kaia** for being good examples.
- Dear friends **Malle & Eku**, **Merileid**, **Liis**, **Eda**, **Monika**, **Aire** and **Maret** for reminding me that there is also life outside the lab.
- My sincerest gratitude to **Jürgen** for being next to me through all my mood swings, understanding, caring and supporting. Thank you, **Lennart**, for finally arriving and lending your helping hands in the most crucial part of the dissertation! And finally I should not forget to mention the contribution of our furry friends **Udo** and **Donna** for cheering us up and for giving the best lectures of animal behaviour.

ORIGINAL PUBLICATIONS

CURRICULUM VITAE

Mari-Anne Philips

Date and place of birth	15.03.1979, Pärnu, Estonia
Citizenship	Estonian
Family status	open marriage, son (19.03.2010)
Address	19th Ravila St, Department of Physiology, University of Tartu (UT), Tartu 50411, Estonia
Telephone	+372 737 4335
E-mail	mari-anne.philips@ut.ee

Education

1994–1997	Pärnu Sütevaka Private High School of Humanities
1997–2002	BSc (2002) Psychology, UT
2002–2004	MSc (2004) Molecular and Cell Biology, UT
2004–2009	PhD Student (Neurosciences), UT

Working experience

2000–2001	Librarian, Department of Social Sciences, UT
2002–2003	School Psychologist, Tartu Raatuse High School
2005–2008	Research Fellow (0.5) Institute of Physiology, UT
2008–	Research Fellow, Institute of Physiology, UT

Awards

2005 Hilda and Harri Mägi Scholarship

2006 (3 months), **2007** (5 months) ja **2008** (4 months): Kristjan-Jaak Travel Scholarship for conducting experimental work for PhD studies in the Department of Clinical Biochemistry, University of Copenhagen, Denmark.

Professional training

2005, 9.06–17.06	Light Microscopy in Living Cells, EMBO Practical Course, Oeiras, Portugal
2006, 8.07–12.07	FENS Forum 2006 (5th Forum of European Neuroscience), Vienna, Austria (poster presentation)

2007, 31.05–2.06	2nd Neurizons Conference. Max Planck Institute for Experimental Medicine, Göttingen, Germany (poster presentation)
2009, 13.05–16.05	3rd Neurizons Conference. Max Planck Institute for Experimental Medicine, Göttingen, Germany (poster presentation)
2009, 20.09–25.09	ESF Research Conference: Gene Expression to Neurobiology and Behaviour: Human Brain Development and Developmental Disorders, Sant Feliu de Guixols, Spain (poster presentation)

Publications

1. **Philips MA,** Kingo K, Karelson M, Rätsep R, Aunin E, Reimann E, Reemann P, Porosaar O, Vikeså J, Nielsen FC, Vasar E, Silm H, Kõks S (2010). Promoter polymorphism –119C/G in *MYG1* (C12orf10) gene is related to vitiligo susceptibility and Arg4Gln affects mitochondrial entrance of Myg1. *BMC Med Genet*, **11**(1):56.
2. **Philips MA**, Abramov U, Lilleväli K, Luuk H, Kurrikoff K, Raud S, Plaas M, Innos J, Puussaar T, Kõks S, Vasar E (2010). *Myg1*-deficient mice display alterations in stress-induced responses and reduction of sex-dependent behavioural differences. *Behav Brain Res* **207**(1):182–95.
3. **Philips MA**, Vikeså J, Luuk H, Jønson L, Lilleväli K, Rehfeld JF, Vasar E, Kõks S, Nielsen FC (2009). Characterization of *MYG1* gene and protein: subcellular distribution and function. *Biol Cell* **101**(6):361–73.
4. Raud S, Sütt S, Plaas M, Luuk H, Innos J, **Philips MA**, Vasar E, Kõks S (2007). Cat odor exposure induces distinct changes in the exploratory behavior and Wfs1 gene expression in C57Bl/6 and 129Sv mice. *Neurosci Lett* **426**(2):87–90.
5. Kingo K, Aunin E, Karelson M, **Philips MA,** Rätsep R, Silm H, Vasar E, Soomets U, Kõks S (2007). Gene expression analysis of melanocortin system in vitiligo. *J Dermatol Sci* **48**(2):113–22.
6. Kingo K, **Philips MA**, Aunin E, Luuk H, Karelson M, Rätsep R, Silm H, Vasar E, Kõks S (2006). *MYG1*, novel melanocyte related gene, has elevated expression in vitiligo. *J Dermatol Sci* **44**(2):119–22.
7. Areda T, Raud S, Philips MA, Innos J, Matsui T, Kõks S, Vasar E, Karis A, Asser T (2006). Cat odour exposure decreases exploratory activity and alters neuropeptide gene expression in CCK(2) receptor deficient mice, but not in their wild-type littermates. *Behav Brain Res* **169**(2):212–9.
8. Areda T, Kõks S, **Philips MA**, Vasar E, Karis A, Asser T (2005). Alterations in opioid system of the rat brain after cat odor exposure. *Neurosci Lett* **377**(2):136–9.

9. Tõnissaar M, **Philips MA**, Eller M, Harro J (2004). Sociability trait and serotonin metabolism in the rat social interaction test. *Neurosci Lett* **367**(3):309–12.
10. Nelovkov A, **Philips MA**, Kõks S, Vasar E (2003). Rats with low exploratory activity in the elevated plus-maze have the increased expression of limbic system-associated membrane protein gene in the periaqueductal grey. *Neurosci Lett* **352**(3):179–82.

ELULOOKIRJELDUS

Mari-Anne Philips

Sünniaeg ja -koht	15.03.1979, Pärnu, Eesti
Kodakondsus	Eesti
Perekonnaseis	vabaabielus, poeg (19.03.2010)
Aadress	Ravila 19, TÜ Füsioloogia Instituut, Tartu 50411
Telefon	+372 737 4335
E-post	mari-anne.philips@ut.ee

Haridus

1994–1997	Pärnu Sütevaka Humanitaargümnaasium
1997–2002	TÜ Sotsiaalteaduskond, psühholoogia eriala, BSc (2002)
2002–2004	TÜ Bioloogia ja Geograafia teaduskond, molekulaar- ja rakubioloogia eriala, MSc (2004)
2004–2009	TÜ Arstiteaduskond, neuroteaduste doktoriõpe, doktorant

Teenistuskäik

2000–2001	TÜ Sotsiaalteaduskonna raamatukoguhoidja
2002–2003	Tartu Raatuse Gümnaasium, koolipsühholoog
2005–2008	TÜ Füsioloogia instituut, erakorraline teadur (0,5)
2008–	TÜ Füsioloogia instituut, teadur

Tunnustused ja stipendiumid

2005 Hilda ja Harri Mägi stipendium

2006 (3 kuud), **2007** (5 kuud) ja **2008** (4 kuud): Kristjan-Jaagu osalise õppe stipendium doktoritööks vajalike katsete läbi viimiseks Kopenhaageni Ülikooli Kliinilise Biokeemia instituudis Taanis

Erialane enesetäiendus

2005, 9.–17. juuni	*Light Microscopy in Living Cells*, EMBO kursus; Oeiras, Portugal
2006, 8.–12. juuli	FENS Forum 2006 (*5th Forum of European Neuroscience*), Viin, Austria (posterettekanne)

2007, 31.mai–2.juuni	*2nd Neurizons Conference*. *Max Planck Institute for Experimental Medicine*, Göttingen, Saksamaa (posterettekanne)
2009, 13.–16.mai	*3rd Neurizons Conference*. *Max Planck Institute for Experimental Medicine*, Göttingen, Saksamaa (posterettekanne)
2009, 20.–25. sept	ESF Research Conference: *Gene Expression to Neurobiology and Behaviour: Human Brain Development and Developmental Disorders*, Sant Feliu de Guixols, Hispaania (posterettekanne)

Publikatsioonid

1. **Philips MA,** Kingo K, Karelson M, Rätsep R, Aunin E, Reimann E, Reemann P, Porosaar O, Vikeså J, Nielsen FC, Vasar E, Silm H, Kõks S (2010). Promoter polymorphism -119C/G in *MYG1* (C12orf10) gene is related to vitiligo susceptibility and Arg4Gln affects mitochondrial entrance of Myg1. *BMC Med Genet*, **11**(1):56.
2. **Philips MA**, Abramov U, Lilleväli K, Luuk H, Kurrikoff K, Raud S, Plaas M, Innos J, Puussaar T, Kõks S, Vasar E (2010). *Myg1*-deficient mice display alterations in stress-induced responses and reduction of sex-dependent behavioural differences. *Behav Brain Res* **207**(1):182–95.
3. **Philips MA**, Vikeså J, Luuk H, Jønson L, Lilleväli K, Rehfeld JF, Vasar E, Kõks S, Nielsen FC (2009). Characterization of *MYG1* gene and protein: subcellular distribution and function. *Biol Cell* **101**(6):361–73.
4. Raud S, Sütt S, Plaas M, Luuk H, Innos J, **Philips MA**, Vasar E, Kõks S (2007). Cat odor exposure induces distinct changes in the exploratory behavior and Wfs1 gene expression in C57Bl/6 and 129Sv mice. *Neurosci Lett* **426**(2):87–90.
5. Kingo K, Aunin E, Karelson M, **Philips MA,** Rätsep R, Silm H, Vasar E, Soomets U, Kõks S (2007). Gene expression analysis of melanocortin system in vitiligo. *J Dermatol Sci* **48**(2):113–22.
6. Kingo K, **Philips MA**, Aunin E, Luuk H, Karelson M, Rätsep R, Silm H, Vasar E, Kõks S (2006). *MYG1*, novel melanocyte related gene, has elevated expression in vitiligo. *J Dermatol Sci* **44**(2):119–22.
7. Areda T, Raud S, Philips MA, Innos J, Matsui T, Kõks S, Vasar E, Karis A, Asser T (2006). Cat odour exposure decreases exploratory activity and alters neuropeptide gene expression in CCK(2) receptor deficient mice, but not in their wild-type littermates. *Behav Brain Res* **169**(2):212–9.
8. Areda T, Kõks S, **Philips MA**, Vasar E, Karis A, Asser T (2005). Alterations in opioid system of the rat brain after cat odor exposure. *Neurosci Lett* **377**(2):136–39.

9. Tõnissaar M, **Philips MA**, Eller M, Harro J (2004). Sociability trait and serotonin metabolism in the rat social interaction test. *Neurosci Lett* **367**(3):309–12.
10. Nelovkov A, **Philips MA**, Kõks S, Vasar E (2003). Rats with low exploratory activity in the elevated plus-maze have the increased expression of limbic system-associated membrane protein gene in the periaqueductal grey. *Neurosci Lett* **352**(3):179–82.

DISSERTATIONES NEUROSCIENTIAE UNIVERSITATIS TARTUENSIS

1. **Sirli Raud.** Cholecystokinin$_2$ receptor deficient mice: changes in function of GABA-ergic system. Tartu, 2005.
2. **Kati Koido.** Single-nucleotide polymorphism profiling of 22 candidate genes in mood and anxiety disorders. Tartu, 2005.
3. **Dzhamilja Safiulina.** The studies of mitochondria in cultured cerebellar granule neurons: characterization of mitochondrial function, volume homeostasis and interaction with neurosteroids. Tartu, 2006.
4. **Tarmo Areda.** Behavioural and neurogenetic study of mechanisms related to cat odour induced anxiety in rodents. Tartu, 2006.
5. **Aleksei Nelovkov.** Behavioural and neurogenetic study of molecular mechanisms involved in regulation of exploratory behaviour in rodents. Tartu, 2006.
6. **Annika Vaarmann**. The studies on cystatin B deficient mice: neurochemical and behavioural alterations in animal model of progressive myoclonus epilepsy of Unverricht-Lundborg type. Tartu, 2007.
7. **Urho Abramov.** Sex and environmental factors determine the behavioural phenotype of mice lacking CCK_2 receptors: implications for the behavioural studies in transgenic lines. Tartu, 2008.
8. **Hendrik Luuk.** Distribution and behavioral effects of WFS1 protein in the central nervous system. Tartu, 2009.
9. **Anne Must.** Studies on molecular genetics of male completed suicide in Estonian population. Tartu, 2009.
10. **Kaido Kurrikoff**. Involvement of cholecystokinin in chronic pain mechanisms and endogenous antinociception. Tartu, 2009.
11. **Anu Aonurm-Helm.** Depression-like phenotype and altered intracellular signalling in neural cell adhesion molecule (NCAM)-deficient mice. Tartu, 2010.
12. **Silva Sütt.** Role of endocannabinoid system and *Wfs1* in regulation of emotional behaviour: behavioural, pharmacological and genetic studies. Tartu, 2010.